HEINRICH HEINE
UNIVERSITÄT DÜSSELDORF

Immunoglobulin dependent modulation of Schwann cell differentiation: Implications for peripheral nerve damage and disease.

Inaugural-Dissertation

zur Erlangung des Doktorgrades
der Mathematisch-Naturwissenschaftlichen Fakultät
der Heinrich-Heine-Universität Düsseldorf

vorgelegt von

Nevena Tzekova
aus Sofia, Bulgarien

Düsseldorf, Dezember 2015

Aus dem Labor Translationale Gliazellforschung
der Neurologischen Klinik
der Heinrich-Heine-Universität Düsseldorf

Gedruckt mit der Genehmigung der
Mathematisch-Naturwissenschaftlichen Fakultät der
Heinrich-Heine-Universität Düsseldorf

Referent: Prof. Dr. Patrick Küry

Korreferent: Prof. Dr. Thomas Klein

Tag der mündlichen Prüfung: 15. Februar 2016

To my family

1 SUMMARY / ZUSAMMENFASSUNG

1.1 Summary

Schwann cells are the myelinating glial cells of the peripheral nervous system (PNS). They provide electric insulation of large caliber axons and play a crucial role in the function and maintenance of peripheral nerves. Schwann cells are also key players in nerve regeneration processes as they adapt to pathological situations by dedifferentiating, dividing, and subsequent promotion of axonal regeneration followed by redifferentiation and axonal myelination. In the case of nerve injury, they phagocytose extracellular myelin, attract macrophages for further debris clearance, and generate an attractive environment for axonal regrowth. The plastic differentiation potential of Schwann cells provides the PNS with a prominent regeneration capacity and indicates that these glial cells are central components of many nerve pathologies. Nevertheless, nerve regeneration in the PNS faces limitations, as evidenced in inherited neuropathies or in peripheral nerve pathologies induced by toxins, drugs, or diabetes, where nerve repair is currently an unmet therapeutic goal. Intravenous immunoglobulins (IVIG) have been used for more than two decades in the treatment of demyelinating immune system disorders, and are now considered first-choice medication in a number of acute and chronic inflammatory neuropathies. IVIG consist of polyclonal human immunoglobulins G (IgG), purified from large pools of human plasma donors, and their exact mode of action in demyelinating autoimmune diseases still needs to be defined. Currently, it believed that the underlying mode of action relates to multiple interactions with cells or components of the immune system. In the central nervous system (CNS), immunoglobulins were previously shown to influence oligodendroglial cells and to enhance remyelination activities. Furthermore, in the PNS indirect therapeutic effects of IVIG were demonstrated in demyelinating immune-related disease models and recent data point to a role of endogenous antibodies in rapid myelin clearance and axon regeneration after nerve injury. However, no direct effects of pooled immunoglobulins on Schwann cells, consequently no potential role in modulating the regeneration potential of these cells, has yet been described.

The aim of this thesis was to determine whether immunoglobulins, in particular IVIG, can directly interact with Schwann cells, influence cell homeostasis, gene expression and maturation processes and could thus be used to promote nerve regeneration.

In the present study a specific binding of human IVIG on the primary rat Schwann cell surface could be demonstrated. It was also revealed that this surface recognition might occur via variable $F(ab')_2$ domains of the antibody preparation. On the other hand, expression of the high affinity Fc receptor for immunoglobulin binding, CD64, was detected on the cells surface suggesting additional Fc mediated interactions to occur. Stimulation with IVIG led to

reduced cellular proliferation rates without affecting cell survival. In addition, accelerated growth of cellular processes resembling early stages of cellular maturation was observed. Notably, immature Schwann cells responded to IVIG binding by induction of myelin gene expression and upregulation of signaling cascades positively affecting the myelination process. Furthermore, IVIG treatment resulted in increase of myelin protein expression in differentiating and in myelination competent Schwann cells, as demonstrated by myelinating neuron/glia cocultures. Differential transcriptome analysis revealed the upregulation of some novel Schwann cell lineage factors, including the cytokine IL-18, the melanocyte marker Tyrp1 and the oligodendroglial transcription factor Olig1 upon IVIG stimulation. It could be then demonstrated for the first time that Schwann cells secrete IL-18 upon IVIG treatment and that the secretion of this cytokine self-instructs Schwann cells to support axonal growth.

Taken together, the present thesis has shown that IVIG positively affect the Schwann cell differentiation process. Our data reveals that immunoglobulins can directly influence Schwann cell plasticity by induction of maturation related signals. This is considered important regarding a potential promotion of nerve regeneration processes by IVIG.

1.2 Zusammenfassung

Die Schwannzellen sind die myelinisierenden Gliazellen des peripheren Nervensystems (PNS). Sie lagern sich an großkalibrigen Axonen einer Nervenzelle an und bilden zusammen mit Fetten und Eiweißen eine schützende Myelinhülle. Diese bewirkt eine elektrische Isolierung der Axone und die Verbesserung der Leitfähigkeit.

Schwannzellen haben damit wesentlichen Anteil an der Funktion und Aufrechterhaltung peripherer Nerven. Sie sind wichtig für die Nervenregeneration, weil sie sich durch Dedifferenzierung und Zellteilung schnell pathologischen Situationen anpassen können und durch ihre Fähigkeit zur anschließenden Redifferenzierung und Myelinisierung die axonale Regeneration fördern. Bei einer Nervenverletzung ist dies von zentraler Bedeutung: Schwannzellen phagozytieren extrazelluläres Myelin, locken für das weitere Aufräumen zellulärer Debis Makrophagen an und erzeugen eine attraktive Umgebung für das axonale Wachstum. Das plastische Differenzierungspotenzial von Schwannzellen verleiht dem PNS eine außergewöhnliche Regenerationsfähigkeit. Dennoch sind der Nervenregeneration des PNS Grenzen gesetzt, etwa bei erblichen Neuropathien oder Erkrankungen peripherer Nerven, verursacht durch toxische Substanzen, Medikamente oder Diabetes. Für diese Indikationen besteht derzeit noch keine Therapiemöglichkeit. Intravenöse Immunglobuline (IVIG) wurden seit mehr als zwanzig Jahren in der Behandlung von demyelinisierenden Autoimmunkrankheiten eingesetzt und werden heute bei einer Reihe von akuten und chronischen inflammatorischen Neuropathien verabreicht. IVIG bestehen aus polyklonalem humanem Immunglobulin G (IgG), das aus einem großen Donorpool menschlichen Blutplasmas aufgereinigt wird. Die genaue Wirkungsweise bei demyelinisierenden Autoimmunerkrankungen ist noch nicht abschließend erforscht. Derzeit wird angenommen, dass einer der zugrunde liegenden Wirkungsmechanismen aus Wechselwirkungen mit Zellen oder Komponenten des Immunsystems unterschiedlicher Art besteht. Im zentralen Nervensystem (ZNS) konnte schon nachgewiesen werden, dass Immunglobuline einen Einfluss auf Oligodendrogliazellen haben und deren Remyelinisierung fördern können. Ferner konnte indirekt über Tiermodelle eine therapeutische Wirkung von IVIG gegen demyelinisierende immunbezogene Erkrankungen im PNS erforscht werden. Jüngste Studien deuten auf eine Rolle von endogenen Antikörpern bei Nervenverletzungen hin: sie scheinen die Beseitigung des Myelins zu fördern und dadurch die axonale Regeneration anzuregen. Eine direkte Wirkung von gepoolten Immunglobulinen auf Schwannzellen konnte hingegen noch nicht nachgewiesen werden – es liegen keine Erkenntnisse vor, dass IVIG das Regenerationspotenzial von Schwannzellen modulieren.

Das Ziel dieser Arbeit war es festzustellen, ob Immunglobuline, insbesondere IVIG, einen direkten Einfluss auf die Homöostase, Genexpression und auf Differenzierungsprozesse der Schwannzellen haben und somit zur Förderung der Nervenregeneration beitragen können.
In der vorliegenden Studie konnte eine spezifische Bindung von humanen IVIG auf der Zelloberfläche primärer Ratten-Schwannzellen nachgewiesen werden. Es wurde weiter gezeigt, dass diese Oberflächenerkennung in den variablen $F(ab')_2$-Domänen der Antikörper begründet sein könnte. Darüber hinaus konnte die Expression des hochaffinen Fc-Rezeptors für Immunglobulin-Bindung, CD64, auf der Zelloberfläche nachgewiesen werden, was auf weitere Fc-vermittelte Wechselwirkungen zwischen der Schwannzelle und IVIG hinweist. IVIG-Stimulation führte zu reduzierten Zellproliferationsraten, ohne das Überleben der Zellen zu beeinflussen. Es wurde ein schnelleres Wachstum von zellulären Fortsätzen beobachtet, ähnlich wie in frühen Stadien der Zellreifung. Die Reaktion von nicht differenzierten Schwannzellen auf die IVIG-Bindung zeigte sich durch Hochregulation von Myelingenen und Induktion von Signalkaskaden, die den Myelinisierungsprozess positiv beeinflussen. Zusätzlich führte IVIG Behandlung von differenzierungs- und myelinisierungskompetenten Schwannzellen zu einer Erhöhung von Myelinproteinexpression, was unter anderem bei myelinisierenden, neuroglialen Cokulturen demonstriert werden konnte. Differentielle Transkriptomanalyse nach IVIG-Stimulation ergab eine Hochregulation einiger, neu mit Schwannzellen in Verbindung gebrachter Faktoren, etwa dem Botenstoff IL-18, dem Melanozyten-Marker Tyrp1 und dem oligodendroglialen Transkriptionsfaktor Olig1. Es konnte erstmals gezeigt werden, dass Schwannzellen nach IVIG Behandlung IL-18 sezernieren und dass die Sekretion dieses Zytokins die Schwannzellen dazu instruiert, das axonale Wachstum zu fördern.
Zusammenfassend hat die vorliegende Arbeit belegt, dass IVIG einen positiven Effekt auf den Schwannzell-Differenzierungsprozess aufweisen. Unsere Forschungsergebnisse belegen, dass Immunglobuline die Plastizität der Schwannzellen durch Induktion von reifungsbezogenen Signalen direkt beeinflussen. Dies ist relevant für eine mögliche Förderung der Nervenregenerationsprozesse durch IVIG.

2 INTRODUCTION

2.1 The nervous system and its cell types

The vertebrate nervous system is divided anatomically into central (CNS) and peripheral nervous system (PNS). The CNS is composed of the brain and spinal cord. The PNS is defined by the spinal and cranial nerves arising from the spinal cord as well as nerve ganglia. The vertebrate nervous system comprises multiple interacting cell types, which process specific types of information. Signals coming from the surrounding environment or the organism itself are served by cells of the sensory circuits. On the other hand, the resulting or occurred actions are represented by cells of the motor circuits. These sensory and motor components are well connected with each other with the help of associating cellular elements and make up together the base of higher behavior (Dale Purves, 2008).

The major cellular components of the nervous tissue are neurons and supporting cells, also referred to as glial cells (glia meaning “glue” in Greek). Neurons communicate via electrical signaling and have thus a specialized morphology for this signal transmission. Incoming and integrated information is transferred via electrical signals by the axon, a unique outgrowth from the neuronal soma. Arborized cell processes, the so-called dendrites, are responsible for synaptic input from other neuronal cells (Dale Purves, 2008). Glial cells are more numerous than neurons, exhibit diverse functions, and are subdivided into micro- and macroglia. Macroglia start their embryological development from ectodermal precursors within the nervous system and encompass oligodendrocytes, Schwann cells, and astrocytes. Schwann cells and oligodendrocytes form the lipid-rich, insulating sheaths around axons in the PNS and CNS, respectively. These so-called myelin sheaths enable a faster and proper conduction of electrical signals by means of a salutatory signal transduction. Oligodendrocytes possess multiple processes and are able to myelinate multiple axons at a time, whereas Schwann cells form myelin sheaths around a single axon, only. Astrocytes are restricted to the CNS and are responsible for trophic support, clearing of cellular debris in disease and injury, or scar formation. They further interact with endothelial cells and provide the cellular link to neurons in the blood-brain barrier (BBB). Microglia originate from hematopoietic monocyte precursors and are therefore the CNS equivalent of macrophages. Their role involves clearance of cellular debris at the site of injury, secretion of immunomodulatory molecules and thus modulation of the inflammation process in the brain (Dale Purves, 2008) (Fields and Stevens-Graham, 2002, Abbott et al., 2006). The following chapters will focus on the myelinating glial cells of the PNS, the Schwann cells, as they represent the main cell type on which the current work was focused on.

2.2 The Schwann cell

2.2.1 Origin, lineage development, plasticity, and subtypes

Schwann cells evolve from the neural crest (Fig. 1). These multipotent cells originate from the dorsal site of the embryonic neural tube and give rise to peripheral neurons and glia, melanocytes, endocrine cells, smooth muscle, craniofacial cartilage and bone (Le Douarin et al., 1991, Jessen and Mirsky, 1999, Motohashi and Kunisada, 2015). Schwann cells undergo several major stages of development until they reach their mature state (Fig. 1). The first step is the formation of Schwann cell precursors (SCPs) from the migrating neural crest cells (at embryonic day 14-15 for rat, 12-13 for mouse). SCPs are an immediate source for Schwann cells, but they also have a role in trophic support for sensory and motor neurons and have been shown to generate endoneural fibroblasts (Joseph et al., 2004, Jessen and Mirsky, 2005). As a next step the SCPs transform into immature Schwann cells at embryonic day 15-17 for rat and 13-15 for mouse. Immature Schwann cells then give rise to promyelinating Schwann cells, which later - around birth - become either myelinating or non-myelinating cells (Fig. 1). The postnatal formation of myelinating or non-myelinating Schwann cells depends on the diameter of the axon they ensheath, large (>1 μm) or small diameter axons (<1 μm), respectively (Jessen and Mirsky, 2005). It is important to note that mature Schwann cells and their precursors exhibit high plasticity throughout their existence in the peripheral nerve. In injured nerves myelinating and non-myelinating Schwann cells can dedifferentiate into immature-like state. In this way they promote efficient peripheral nerve regeneration (Glenn and Talbot, 2013) (Mirsky et al., 2008). SCPs that have migrated to their target tissue show the potential to differentiate into other cell types such as melanocytes and endoneural fibroblasts (Joseph et al., 2004, Adameyko et al., 2009) (Motohashi and Kunisada, 2015, Newbern, 2015). Transection of adult mouse sciatic nerve revealed formation of pigmented cells around the nerve fascicles and transplantation of labeled Schwann cells into the injured nerves demonstrated that these melanocytes arose from the grafted Schwann cells (Rizvi et al., 2002). More recent studies have even shown that SCPs give rise to parasympathetic neurons during development (Dyachuk et al., 2014, Espinosa-Medina et al., 2014).

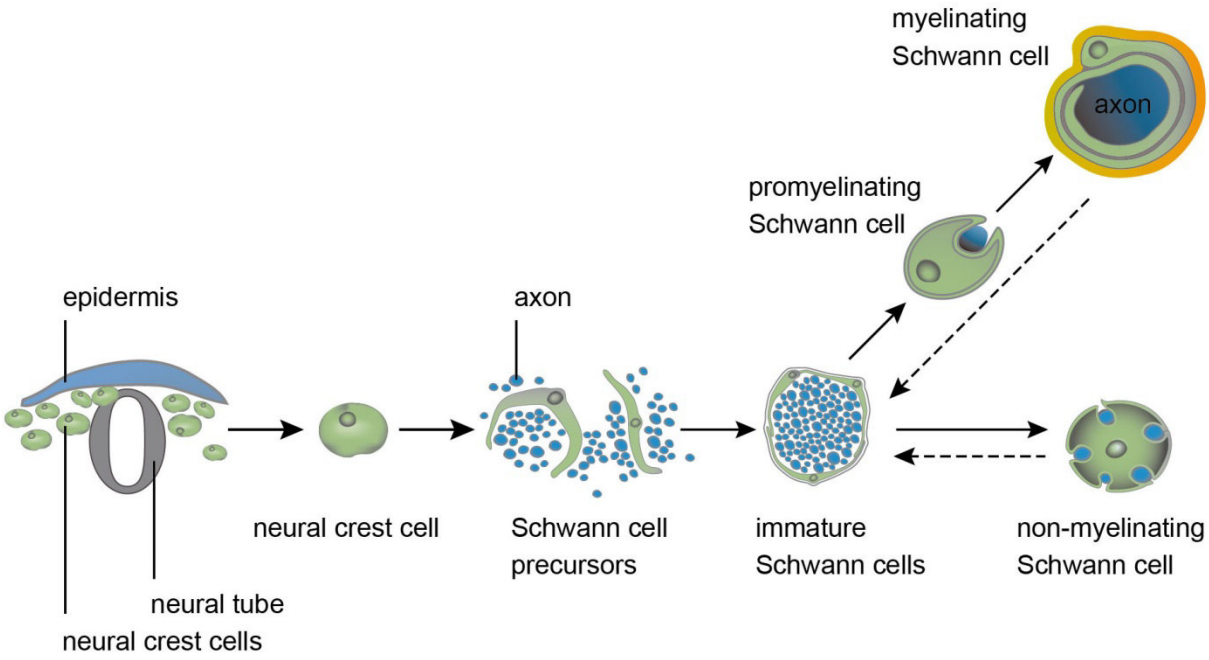

Figure 1. Schwann cell lineage development. Schwann cells undergo different developmental stages, which are schematically illustrated above. After formation of the neural tube, neural crest cells segregate from the dorsal site and start migrating in lateral and ventral directions. One part of the ventral migrating neural crest cells develops in Schwann cell precursors, which start expressing differentiation specific markers such as myelin protein zero (Mpz/P0) (Jessen and Mirsky, 2005). The next step of the embryonic development is the formation of immature Schwann cells. From this point on, the final differentiation to myelinating or non-myelinating Schwann cells depends on the diameter of the axon, with which they would shortly associate. Schwann cells that ensheath around large calibre axons (>1 µm) develop into myelinating cells, by going through a pro-myelinating stage. Schwann cells that meet small calibre axons (<1 µm) become non-myelinating (Remak bundles). The not interrupted arrows represent all developmental Schwann cell transitions. Dashed arrows mark the possible dedifferentiation potential of myelinating Schwann cells and Remak cells during repair processes after nerve injury.

Schwann cells have diverse functions, such as myelin formation, synaptic junctions ensheathment and bundling of small-diameter axons. Accordingly they can be divided into four different classes. The best-characterized group is the one of the myelinating Schwann cells, which wrap around single large-diameter peripheral axons in order to provide electrical insulation and accelerated signal propagation. This specific ensheathment then results in formation of distinct structures such as internodes, comprising 99 % of the myelinating Schwann cell membrane, and in nodes of Ranvier, representing the space between two internodes (Fig. 2) (Scherer, 1999). A large number of intracellular transcriptional and morphological changes take place in the Schwann cell to form the complex myelin membrane. Extrinsic information provided by the axons induces the myelination process and determines the amount of myelin that Schwann cells generate (Salzer, 2015). The primary

stimulus for Schwann cell myelination is provided by a signaling complex between axonal neuregulin-1 and glial ErbB receptors (also known as human epidermal growth factor receptors 2, Her2). This system has been shown to be active at all stages during the differentiation process (Nave and Schwab, 2005, Taveggia et al., 2005, Salzer, 2012). Small caliber axons (diameter <1 µm) are not myelinated, but rather ensheathed as bundles by a single Schwann cell (Fig. 1). In these Remak bundles each axon stays in contact with the Schwann cell processes (Griffin and Thompson, 2008). Absent myelination of Remak bundles correlates with the axonal diameter and the lower expression of neuregulin-1 in these axons (Taveggia et al., 2005). Remak Schwann cells usually cover both sensory and sympathetic axons and exhibit high plasticity, as they still have the ability to sprout and grow into denervated areas. This characteristic is important for often-renewable environments such as the skin, especially in the case of injury (Griffin and Thompson, 2008). There is no counterpart for Remak cells in the CNS (Nave, 2010).

Another group of non-myelinating cells is represented by the perisynaptic Schwann cells (also known as terminal Schwann cells). They are situated at the terminal ending of myelinated motor axons, the neuromuscular junctions, where their processes contact the surface of the nerve terminal. Their function is comparable to the one of astrocytes in the CNS, in which they can take up neurotransmitters and might have a role in the synaptogenesis and maintenance of synaptic activity, as well as in (modulation of) neurotransmission at the neuromuscular junction (Auld and Robitaille, 2003, Griffin and Thompson, 2008).

An additional peripheral glial cell type that shares various properties with astrocytes is the satellite glia. These cells reside in sensory, sympathetic, and parasympathetic ganglia, where several cells completely enclose the neuronal soma, connected by gap junctions. Satellite glial cells contribute to signal processing and transmission, and exert additional neuron supporting functions and electrical insulation, as they express receptors for neuroreactive molecules and neurotransmitter transporters, and were shown to release cytokines and adenosine triphosphate (ATP). They are also suggested to be responsible for chronic neuropathic pain as a result of injury to axons of sensory ganglia (Hanani, 2005, Ohara et al., 2009, Hanani, 2010, Vaegter, 2014).

2.2.2 Myelin sheath formation and myelin proteins

The establishment of myelin sheaths, as spirally wrapped plasma membranes of Schwann cells around axons, denotes an important evolutionary step of the vertebrate nervous system and largely occurs during postnatal development in mammals. Myelin sheaths provide the nervous system with numerous benefits. The most prominent one is the increased conduction velocity. This is given by the formation of salutatory action potential propagation that arises from one node of Ranvier to the next one as well as by indirectly enhancing the total nerve fibre diameter. Action potential and ion gradient formation is thus restricted to the nodal region of the axonal surface, which makes less than 0.5 %. Consequently, myelination strongly diminishes the energy consumption, required for signal transmission. Finally, myelin provides the axons with life-long protection and integrity, which is not given in demyelinating pathological conditions (Griffin and Thompson, 2008, Nave, 2010).

Myelin sheaths and corresponding membranes are very high in lipids, 70–85 %, whereas the protein content builds up the rest (Salzer, 2015). Their organization and distribution along the axon can be divided into nodal, paranodal, juxtaparanodal, and internodal regions (Fig. 2). Two myelin segments (internodes) are separated by a node of Ranvier, the unmyelinated part of the axon. Nodal regions are rich in voltage-gated sodium (Na^+) channels involved in the generation of action potentials. The paranodes are the lateral sites of the myelin sheath containing adhesion molecules such as contactin, Caspr, and neurofascin. Juxtaparanodes reveal a certain region between the inter- and paranode, where potassium (K^+) channels are concentrated (Fig. 2) (Scherer and Arroyo, 2002, Salzer et al., 2008).

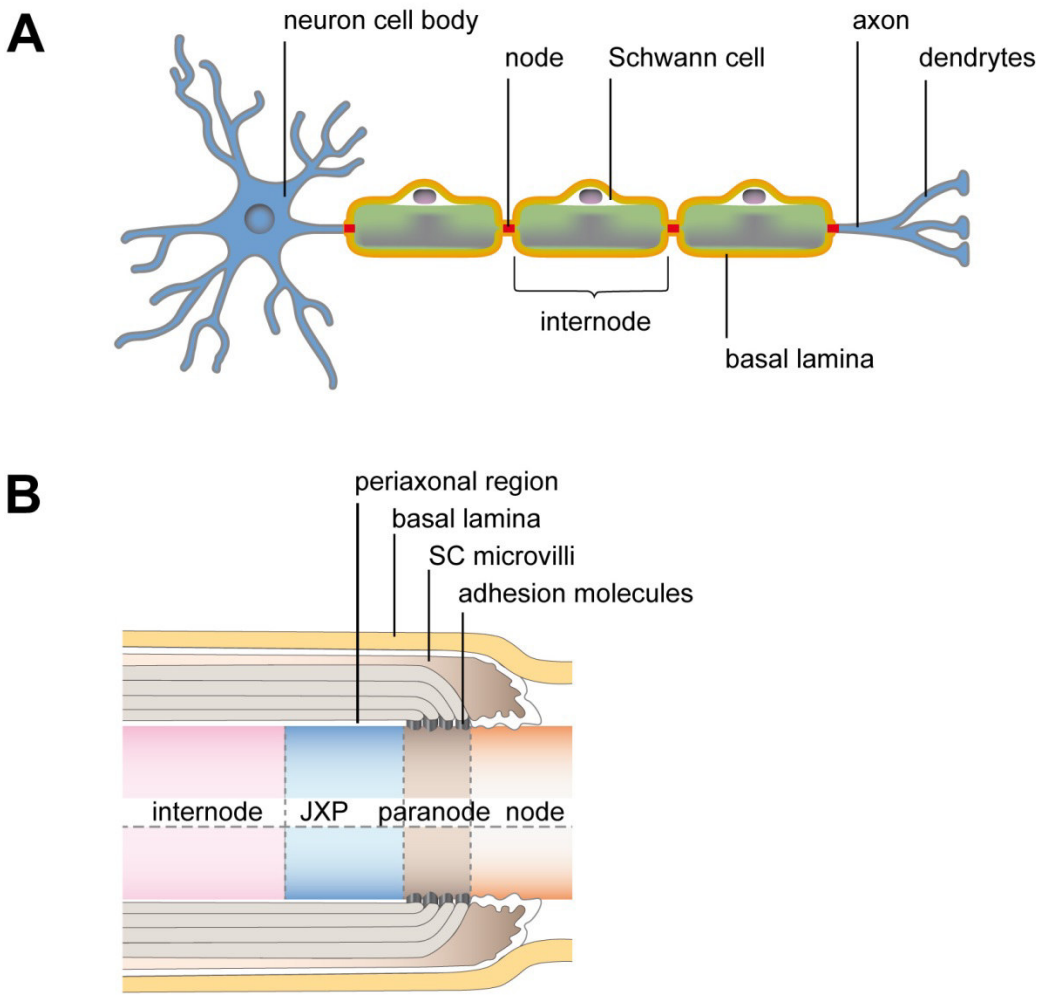

Figure 2. Structure of myelinated axons in peripheral nerves. (A) Single myelinating Schwann cells wrap around one axon several times and hence form the peripheral myelin sheath. Each myelinated segment builds the so-called internode, whereas the gaps between the single internodes represent the node of Ranvier. Myelinated fibres are covered by basal lamina. (B) Schematic longitudinal section of a myelinated peripheral nerve. The diagram is showing the following structures: the nodal region, where the Schwann cell microvilli terminate; the paranodal region containing the lateral loops of the myelin sheath, which connect to the axonal membrane via adhesion molecules; the juxtaparanode (JXP) and the internode, which are located under the compact myelin; the periaxonal region, the space between axon and myelin sheath.

At paranodes as well as at so-called Schmidt-Lanterman incisures, Schwann cell cytoplasm segments connected with gap junctions for better molecule transport through the spiral sheath, the myelin is not compacted. Non-compact myelin sheaths are hence characterized by the presence of Schwann cell cytoplasm. The internodal region mainly consists of compact myelin sheath, resulting from the tight circulatory wrapping of the Schwann cell around the axon. Both types of myelin exhibit a distinct protein expression. Compact myelin of the PNS is characterized by the expression of myelin protein zero (Mpz/P0), myelin basic protein (Mbp) and peripheral myelin protein 22 (Pmp22), whereas the non-compact myelin

contains myelin-associated glycoprotein (Mag), connexin-32 (Cx32) and E-cadherin (Fig. 3) (Scherer and Arroyo, 2002, Salzer, 2015).

P0 is the most abundant myelin protein of the PNS, estimated to comprise more than 50 % of the peripheral myelin proteins (Greenfield et al., 1973). It represents a single-pass transmembrane 30 kilodalton (kDa) molecule of the immunoglobulin gene superfamily, which is responsible for the adhesion of the extracellular myelin membrane surface. P0 is thus essential for the compaction of the extracellular space between the sheets of Schwann cell plasma membranes (Filbin et al., 1990, Scherer and Arroyo, 2002, Salzer, 2015). P0 deletion or overexpression leads to myelin degradation and severe neuropathological conditions, indicating that this protein is essential for myelin formation (Giese et al., 1992, Wrabetz et al., 2000). Its functional counterpart in the CNS is proteolipid protein 1 (Plp1/DM20), although myelinating Schwann cells also express small amounts of Plp1. It is of importance to point out that P0 is expressed in early embryonic development, and hence exhibits a possible function in gliogenesis. Detected in neural crest cells, SCPs and immature Schwann cells P0 is considered a highly specific lineage marker and is consequently upregulated in myelinating, but suppressed in non-myelinating Schwann cells (Lee et al., 1997).

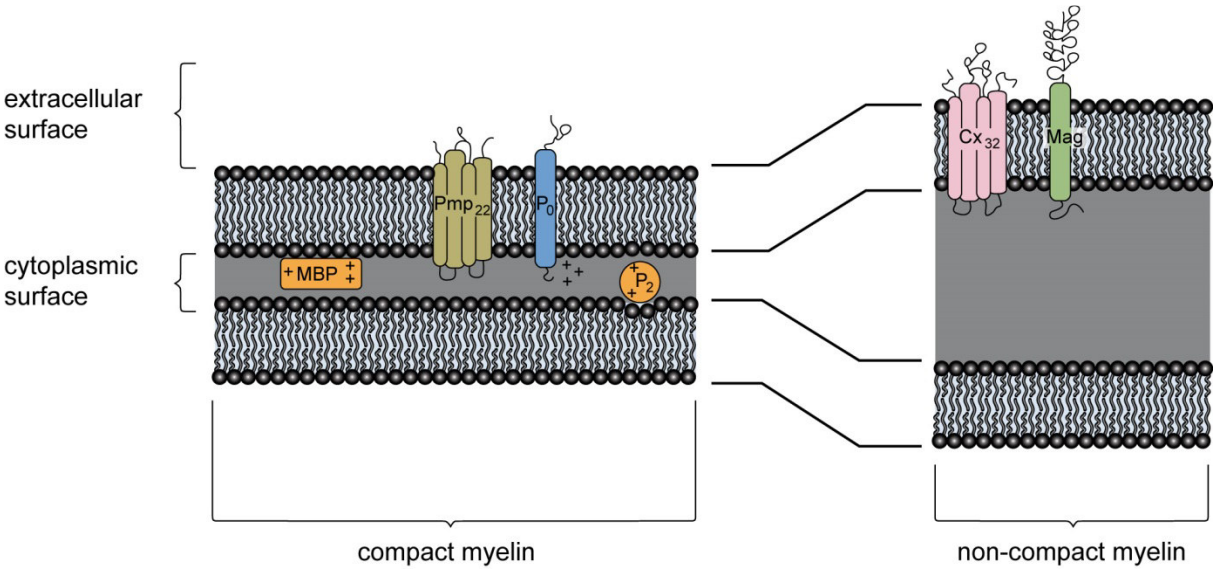

Figure 3. Structure of PNS myelin. Schematic illustration of the most abundant proteins in compact and non-compact peripheral myelin. Compact myelin is characterized by the expression of myelin protein zero (P0), representing a single-pass transmembrane molecule, responsible for adhesion of the extracellular myelin membranes and hence for myelin compaction; myelin basic protein (Mbp), a positively charged molecule, associated to the cytoplasmic site and mediating intracellular adhesion of the myelin layers; peripheral myelin protein 2 (P2), a lipid-binding protein located in the cytoplasm; and peripheral myelin protein 22 (Pmp22), a tetraspan membrane protein important for myelin formation. Non-compact myelin contains myelin-associated glycoprotein (Mag), which functions as stabilizer of axon-glia interactions and thus has a role in morphologically intact myelin formation, and connexin-32 (Cx32), a four-domain transmembrane protein, which assembles into gap junction channels and provides cytoplasmic transport of ions and metabolites across the myelin sheath.

Mbp is the second most abundant protein comprising between 5 to 18 % of the peripheral myelin proteins, and up to 30 % in the CNS. In rodents, four isoforms of the Mbp protein are known with molecular masses of 21, 18.5, 17 and 14 kDa, respectively, all of which can be found in the CNS and PNS myelin (Boggs, 2006). Mbp is not a transmembrane protein, but is rather associated to the cytoplasmic site of the cell membrane. In neutral pH it is largely positively charged, which allows it to interact with negatively charged phospholipids and to mediate intracellular adhesion of the myelin layers (Boggs, 2006, Inouye and Kirschner, 2015). Natural deletion of the Mbp gene in the CNS as it was described for the *shiverer* mouse, leads to severe hypomyelination and loss of compact myelin demonstrating that the Mbp protein plays a critical role in CNS myelination (Readhead and Hood, 1990). However, in the PNS this mutation does not result in serious consequences, but peripheral myelin devoid of Mbp reveals some morphological changes, such as increased Schmidt-Lanterman incisures and diminished diameter of myelinated axons. This indicates that Mbp also has an important function in the PNS myelin formation (Gould et al., 1995). Furthermore, Mbp appears to be involved in oligodendroglial signaling pathways, as it can bind cytoskeletal and other regulatory molecules and can react to changes of the extracellular environment by phosphorylation (Boggs, 2006). Similar functions have not been described in Schwann cells yet.

Peripheral myelin protein 2 (also termed Pmp2, P2 or Fabp8) belongs to the fatty acid binding protein family and is a lipid-associated protein located in the cytoplasm. Pmp2 was suggested to be the third most abundant of the PNS myelin proteins and is expressed in myelinating Schwann cells at the sites of compact myelin (Greenfield et al., 1973, Trapp et al., 1984). Clinically, Pmp2 has been established as a target antigen for immunization and induction of experimental autoimmune neuritis (EAN), an animal model of Guillain-Barré Syndrome (GBS) (Kadlubowski et al., 1980, Rostami et al., 1984). Its function in glial cells is not well described. A recent study revealed, however, that complete deletion of the Pmp2 gene does not induce any myelin disruption but results in a temporary reduction of motor nerve conduction velocity. The authors suggest a role for Pmp2 in lipid homeostasis, as it was shown to bind and transport fatty acids to the Schwann cell membrane (Zenker et al., 2014).

Another component of the compact myelin is Pmp22, a 22 kDa transmembrane protein consisting of four domains. Pmp22 comprises 2 to 5 % of the total myelin protein and was revealed to be important for myelin formation. Point mutations in the Pmp22 gene induce PNS hypomyelination accompanied by aberrant Schwann cell division, whereas chromosomal duplications lead to demyelinating peripheral neuropathies (Suter and Snipes, 1995, Müller, 2000). Unlike P0, which is nerve-specific, Pmp22 was found in other tissues, such as lung, gut, and heart (Suter and Snipes, 1995). Pmp22 is also expressed in neurons

and has been detected, similar to P0, in progenitor cells from embryonic dorsal root ganglia (DRG) (Hagedorn et al., 1999).

Connexin-32 (Cx32) is a four-domain transmembrane protein, expressed in myelinating Schwann cells, and is an important component of non-compact myelin structures. It assembles into gap junction channels and its purpose is to provide a continuous gateway for cytoplasmic transport of ions, metabolites and second messenger molecules across the myelin sheath. Although Cx32 is widely expressed in several tissues, functional consequence of various mutations are limited to the PNS giving rise to inherited peripheral neuropathies, in particular the X-linked form of Charcot-Marie-Tooth disease (Suter and Snipes, 1995, Fischbeck et al., 1999, Ressot and Bruzzone, 2000).

A second member of non-compact myelin proteins is the glycoprotein Mag (myelin-associated glycoprotein), which is expressed in both the CNS and PNS (Figlewicz et al., 1981). In myelinated axons, Mag is found in the periaxonal region, the space between axon and myelin sheath, and in the paranodal regions (Fig. 2). According to its location and the interaction with extracellular matrix components, one can infer that Mag has a crucial function in the stabilization of the axon-glia interactions and hence supports the formation of morphologically intact myelin sheaths. Although no peripheral neuropathy has yet been associated with Mag mutations, its depletion in the PNS leads to degeneration of myelinated fibres without effecting the initiation of myelination (Schachner and Bartsch, 2000).

Periaxin (Prx) is a scaffolding protein of myelinating Schwann cells, which alone has a role in Schwann cell elongation but in a complex with dystroglycans is responsible for proper myelin ensheathment. Loss of periaxin in mice leads to severe demyelination and gene mutations in humans cause demyelinating neuropathy (Sherman et al., 2012).

Recent proteome analysis of PNS fractions revealed the presence of many additional proteins, some of which are completely novel for the PNS (Patzig et al., 2011). Further characterization is needed, in order to assign their localization to compact myelin or to other sites of the Schwann cell, internodes or nodal structures. Importantly, this study showed for the first time, that the abundance of myelin proteins is different from the previously assumed numbers; namely that well-known proteins such P0, periaxin, and Mbp represent only 21, 16, and 8 %, respectively, of total peripheral myelin proteins. Approximately 50 % are composed of novel, not yet identified proteins (Patzig et al., 2011).

2.3 Regulation of the myelination process

2.3.1 Positive regulators of the myelination process

Myelination is a complex process, which is driven by extrinsic signals, intrinsic Schwann cell transcriptional changes and subsequent cytoskeletal rearrangements that direct glial membrane wrapping around axons. Some of the most important regulators of Schwann cell development and myelination process will be mentioned in this chapter.

One of the major regulators of Schwann cell development is SRY-related HMGbox-10 (Sox10). The transcription factor is expressed already in neural crest cells and then continuously present in all glial stages of the PNS, from SCPs to myelinating or non-myelinating Schwann cells. Sox10 is therefore important for the generation and specification of the Schwann cell lineage, as its deletion leads to impaired gliogenesis. Studies have revealed that Sox10 regulates the expression of ErbB receptors on Schwann cells. It thus controls their response to axonal neuregulin, an extrinsic regulator of SCP and Schwann cell survival, proliferation, and terminal differentiation (Jessen and Mirsky, 2005, Stolt and Wegner, 2015). In contrast, oligodendrocyte precursor development is not affected by Sox10 absence, but the oligodendroglial maturation process is impaired (Weider et al., 2013). In Schwann cells Sox10 is involved in the initiation of myelin gene expression, as well as myelin maintenance in fully differentiated cells and interacts with a variety of other transcriptional regulators. One of the well-known Sox10 interacting partners in immature Schwann cells is octamer-binding transcription factor-6 (Oct6/Pou3f1). Sox10 binds to the enhancer domain of Oct6 and, together with other factors, leads to its induction. This interaction is sufficient for the Schwann cell transition from immature to promyelinating but also throughout the promyelinating state, where both factors stay teamed up to escort the cells to their final differentiation. As a next step they activate together the transcription factor Krüppel box protein 20 (Krox20), also known as Egr2 (early growth response protein-2), while binding to its enhancer downstream of the gene. Krox20 activation requires additional factors and histone modifications by histone deacetylases and finally leads to induction of the myelination process. The role of Oct6 is restricted to early phases of Schwann cell differentiation and its expression is eventually downregulated, most probably in association with Krox20. Sox10 and Krox20 work synergistically, not only by directly interacting with each other, but also by binding to the same regulatory regions in order to maintain myelination. They activate the transcription of a number of prominent myelin genes, such as P0/Mpz, Mbp, Cx32, Mag and Pmp22 and furthermore control genes encoding enzymes involved in lipid biosynthesis. Krox20 is suspected to have a positive influence on Sox10 expression through a feedback loop, which suggests it to be a master regulator of the myelination process (Weider et al., 2013, Stolt and Wegner, 2015).

As introduced above axonal neuregulin-1 is an additional regulator of the myelination process. Depending on neuregulin-1 expression levels both myelin thickness and initiation of Schwann cell myelination are regulated. Signaling involving ErbB2/ErbB3 receptor complexes on Schwann cells activates a number of downstream pathways, including the phosphatidylinositol-3-kinase (PI3K) pathway. PI3K then catalyzes the formation of phosphatidylinositol-(3,4,5)-trisphosphate (PIP3) from phosphatidylinositol-(4,5)-bisphosphate (PIP2), which causes the activation of serine-threonine kinase (Akt) (Pereira et al., 2012, Glenn and Talbot, 2013). Activated Akt, on the other hand, was recognized as central signaling component for Schwann cell differentiation and the initiation of myelination (Maurel and Salzer, 2000, Ogata et al., 2004).

2.3.2 Negative regulators of the myelination process

The process of myelination is not only driven by stimulatory signals but is also seen as a highly controlled interplay between positive and negative regulators. The latter are mainly expressed during the immature stages of the Schwann cell lineage and subsequently downregulated when myelination is initiated. As dedifferentiation is required after nerve injury, negative regulators get reactivated and contribute to the high degree of plasticity of peripheral glial cells (Jessen and Mirsky, 2008). In this chapter, some of the differentiation inhibitors identified in the context of peripheral myelination will be described.

The transcription factor Sox2, belonging to the SRY-related HMG box family, is essential for maintaining Schwann cells in their immature state and has been defined as a negative regulator of Schwann cell differentiation. Sox2 expression is consequently downregulated during myelination, a transcriptional regulation in which Krox20 is involved (Le et al., 2005, Jessen and Mirsky, 2008). Interestingly, in the Schwann cell progenitor stage Sox2 expression is responsible for stabilizing the Schwann cell identity over melanocytes (Adameyko et al., 2012). Sox2 is also induced upon peripheral nerve injury together with cJun, another transcription factor found to act as inhibitor of Schwann cells differentiation (Parkinson et al., 2008). cJun inhibits myelin gene activation by negatively regulating Krox20 expression and drives differentiated Schwann cells back to an immature state (Parkinson et al., 2008). However, further studies indicate that this activity is not essential during development, as cJun is generally inactive in myelinating cells, but appears to be rather important in promoting the dedifferentiation process after nerve injury (Arthur-Farraj et al., 2012). The regulation between cJun and Krox20 is reciprocal and necessary for the balance between the differentiated and immature states, and is therefore important for axonal integrity (Jessen and Mirsky, 2008).

Another negative regulator of glial differentiation is p57kip2, which belongs to the family of

cyclin-dependent kinase inhibitors (CDKI), widely known as cell cycle inhibitors. Several publications from our lab have shown that p57kip2 is involved in the maturation and differentiation process of Schwann cells and oligodendrocytes (Heinen et al., 2008a, Heinen et al., 2008b, Kremer et al., 2009, Göttle et al., 2015). Suppression of the p57kip2 gene in cultured Schwann cells led to induction of myelin gene and protein expression, and decreased levels of Oct6, Sox2 and cJun expression, which relates to an initiated Schwann cell differentiation process (Heinen et al., 2008a, Heinen et al., 2013). Its activity was shown to be regulated by histone methyltransferases (Heinen et al., 2012). p57kip2 was downregulated during postnatal peripheral nerve development and transiently decreased short after sciatic nerve crush injury (Küry et al., 2002, Heinen et al., 2008a). p57kip2 suppression led to significant morphological changes in Schwann cells, comprising process elongation, and further induced their myelination potential when cultured *in vitro* together with neurons (Heinen et al., 2008a). Similar maturation-related phenotype and upregulated myelin gene expression were observed in oligodendrocytes upon suppression of p57kip2 (Kremer et al., 2009). Recent studies demonstrated that subcellular localization of the p57kip2 protein correlated with the differentiation competence of oligodendroglial cells. While nuclear accumulation of p57kip2 led to oligodendroglial differentiation arrest in their precursor stage, cytoplasmic distribution resulted in promotion of cell maturation and differentiation (Göttle et al., 2015). Finally, adult neural stem cells (NSCs) were also found to express p57kip2 and suppression of this gene led to oligodendroglial fate determination and significantly reduced the astroglial phenotype of NSCs (Jadasz et al., 2012). All these findings reveal p57kip2 as a prominent inhibitor of glial cell differentiation and foster its role beyond cell cycle control.

Another negative regulator of Schwann cell differentiation is the p38 mitogen-activated protein kinase (p38MAPK). Activation of p38MAPK can induce myelin breakdown and an immature Schwann cell phenotype hence promotes dedifferentiation. This kinase is involved in downregulation of Krox20 transcript levels and the subsequent decrease of myelin gene expression. On the other hand, p38MAPK stimulates cJun upregulation (Yang et al., 2012). p38MAPK expression was furthermore found to be induced upon crush injury in an animal model and suppression of kinase activity, which comprised oral administration of a specific p38MAPK inhibitor, led to faster nerve recovery (Myers et al., 2003).

As previously addressed, neuregulin signaling can drive the myelination process but it can also be involved in the inhibition of Schwann cell differentiation via activation of the lipid phosphatase and tensin homolog (PTEN). PTEN is recruited by interaction with the accessory protein Dlg1, and catalyzes the reaction from PIP3 to PIP2, resulting in downregulation of Akt activity. This negative regulation of the PI3K/Akt pathway leads to a myelin sheath growth arrest, hence preventing hypermyelination (Cotter et al., 2010, Pereira et al., 2012). PTEN deletion, on the other hand, leads to activation of the PI3K pathway and

results in enhanced Schwann cell wrapping and axonal hypermyelination (Goebbels et al., 2010). It is currently assumed that interactions between PTEN and Akt serve as important regulatory component of PNS myelination.

2.4 Regenerative processes in the PNS, Wallerian degeneration

In contrast to the CNS, axons of the PNS exert a remarkably high ability to regenerate after injury. Nerve injury induces a fast response of the surrounding non-neural cells and leads to degeneration of the detached distal nerve stump. This process is termed Wallerian degeneration (WD) according to Augustus Waller's initial description 165 years ago (Waller, 1850, Stoll et al., 2002). WD initiates and involves a cascade of glial-, macrophage-, fibroblast- and endothelial cell responses aiming at the clearance of inhibitory myelin debris and at generating an environment that permits axonal regrowth and successful nerve repair (Rotshenker, 2011). In the PNS, WD is a fast process enduring 7-14 days, whereas it remains limited and inefficient in the CNS where it can last for months to years (Vargas and Barres, 2007).

The initiation of WD begins with the degeneration of the axon, which does not start before 24-48 hours in rodents or even several days post lesion in humans. Axonal degeneration is induced by axonal membrane swelling and disruption, followed by intra- and extracellular calcium signals that trigger cytoskeletal disintegration in response to calpain-protease activation and ubiquitinilation. All these events are intrinsic to the axon and precede the course of myelin degeneration (Vargas and Barres, 2007, Gaudet et al., 2011).

Apart from their important role in providing accelerated signal conduction Schwann cells are also important in terms of trophic support of axons as well for guiding their growth in regenerating. They have the ability to sense axonal injury within minutes, before axonal degeneration has even started. Schwann cells in the distal nerve stump initiate a dedifferentiation process by altering their gene expression, so that myelin lipid and protein synthesis is ceased within the first 48 hours and subsequent regeneration-associated factors expression is upregulated. After the degenerated axons have disappeared myelin starts to be degraded, a process, which is coupled to phospholipase activation in Schwann cells. This is where another astonishing quality of Schwann cells is activated; they do not only degrade their own myelin but furthermore participate in the clearance of extracellular myelin debris and are thus the primary phagocytic cells within the first five days after injury. This cellular phenotype is also proliferating leading to the formation of Büngner bands. These bands represent Schwann cells dividing along the basal lamina and forming guiding tubes for better axonal growth support (Vargas and Barres, 2007, Gaudet et al., 2011). Both myelinating and

non-myelinating cells associated with injured axons are able to start the process of denervation (Griffin and Thompson, 2008).

Moreover, Schwann cells can also directly affect axonal regeneration processes. They secrete adhesion molecules that can stimulate neurite outgrowth and neurotrophic factors for improved axonal growth and survival. Furthermore, Schwann cells produce cytokines and chemokines for macrophage attraction to sites of injuries. Macrophages, which can be of endoneural or hematogenous origin, are guided to specific areas of damage and execute the final phase of myelin clearance. Cellular infiltration as well as complement protein uptake is possible because, as a consequence of nerve injury, the blood-nerve barrier is disrupted during the first 48 hours. The complement system is important for myelin opsonization and hence for macrophage recruitment. Circulating monocytes start infiltrating the endoneural tubes at five days post injury, whereas endoneural macrophages can be recruited earlier. Resident macrophages are also a source of proinflammatory molecules. In addition, T lymphocytes also reach the site of injury and by secreting pro- or anti-inflammatory cytokines they can modulate the immune response of the surrounding cells (Vargas and Barres, 2007, Gaudet et al., 2011).

All these observations demonstrate that Schwann cells are a central component of the peripheral nerve regeneration process and that they provide the PNS with a certain plasticity that exceeds the one of the CNS. Of note, oligodendrocytes are not able to adapt to injury and disease, cannot de- and redifferentiate, and are not involved in myelin clearance (Vargas and Barres, 2007). Apart from the Schwann cells features listed here these glial cells have recently been recognized to exert a high degree of immune competence, which is going to be described in detail in chapter 2.7.

2.5 Limitations of the regenerative process in the PNS[1]

The immune competence along with the plastic differentiation potential of Schwann cells provides the PNS with a high regeneration capacity and indicates that these glial cells are central components of many nerve pathologies. Nevertheless, nerve regeneration in the PNS faces limitations, in particular when it comes to inherited and inflammatory neuropathies or in peripheral nerve pathologies induced by toxins, drugs or in diabetic patients (Vincent et al., 2011, Diezi et al., 2013, Dalakas, 2015, Jerath and Shy, 2015). For most of these neurological conditions functional restoration of damaged axonal tracts and myelin sheaths represents the final therapeutic goal which is, however, currently unmet (Tzekova et al., 2015).

[1] for authorship notice please refer to chapter 9.2

2.5.1 Inherited peripheral neuropathies

Inherited peripheral neuropathies are generally termed as hereditary motor and sensory neuropathy (HMSN) or Charcot-Marie-Tooth disease (CMT). CMT is the most common inherited peripheral nerve disorder in humans, featuring up to 78 subtypes and more than 40 identified disease related genes with a multitude of diverse mutations (Jerath and Shy, 2015). These demyelinating peripheral neuropathies interfere with Schwann cell or neuronal cell body/axon structures and cause symptoms such as distal muscle weakness and atrophy, sensory loss, and slow nerve conduction velocity. The most common affected genes are peripheral Pmp22, Cx32, Mpz/P0, as well as mitofusin 2 (Mfn2). One of the best-investigated forms is CMT1A, caused by a duplication of the Pmp22 gene resulting in protein overexpression. Pmp22 then aggregates in the cytoplasm, disturbing wild type Pmp22 processing and transport and leading to myelin sheath destabilization. The second most abundant form is CMT1X, which occurs as consequence of mutations in the Cx32 gene. This results in loss of function, abnormal synthesis or disconnection of gap junctions between Schwann cells and neurons, leading to myelin disruption. Point mutations in the Mpz/P0 gene, also termed CMT1B, are characterized by reduced levels or overexpression of the protein, respectively resulting in myelin instability or excessive demyelination (Jerath and Shy, 2015). Current therapeutic approaches for inherited neuropathies are rather limited and are based on symptomatic treatment, rehabilitation, and genetic counseling (Jerath and Shy, 2015).

2.5.2 Autoimmune peripheral neuropathies: GBS, CIDP and MMN

Autoimmune peripheral neuropathies develop when the body's own immune system starts attacking different antigens on peripheral nerves, hence leading to acute inflammation and demyelination, damage of peripheral axons and of nodes of Ranvier. Key players of this inflammatory process are myelin-reactive antibodies, autoreactive T cells and activated macrophages (Dalakas, 2015).

Generally, inflammatory neuropathies can be divided into acute and chronic diseases and show an overall good response to immunotherapy. One of the most common inflammatory polyneuropathies is the GBS (Guillain-Barré Syndrome). Since this neurological condition develops fast, within 1-3 weeks, it is classified as acute peripheral nerve disease. The symptoms are represented by motor weakness in the lower limb, loss of neurological reflexes and sensory nerve abnormalities (Dalakas, 2015). GBS is generally subdivided into several subtypes depending on the affected structure, myelin- or axonal-type: acute inflammatory demyelinating polyneuropathy (AIDP) and acute motor axonal neuropathy (AMAN), respectively (Yuki and Hartung, 2012). AIDP represents the most common GBS subtype in

Europe and North America. The main target is myelin, which is recognized by autoantibodies, then most probably attacked via complement activation and later degraded in response to T cell and macrophage infiltration. However, the autoantigens on the myelin sheath have not been identified so far (Yuki and Hartung, 2012). AMAN is more prevalent in Asian countries and Mexico. The identified pathology affects axons and includes binding of activated complement complexes to nodal regions and initiation of direct axonal degeneration. To this end, the autoantibodies against targets have been characterized and appear to recognize various gangliosides (Yuki and Hartung, 2012, Dalakas, 2015). Gangliosides are highly abundant in peripheral nerves and are composed of a ceramide attached to an oligosaccharide core linked to sialic acid residues. The sugar-attached sialic acid, on the other hand, can induce an immune response, as it is directed to the extracellular space (Yuki and Hartung, 2012, Dalakas, 2015). Several GBS subtypes can be defined by the presence of anti-ganglioside antibodies in the serum but the connection between the clinical syndrome and the specific ganglioside has not been clarified yet (Dalakas, 2015). Some ganglioside antibodies are defined as pathogenic because when applied to rabbits or mice they are able to induce an acute neuropathy with histological features of AMAN (Yuki and Hartung, 2012). Further observations led to the conclusion that certain viral or bacterial pathogens can induce autoimmunity against myelin due to molecular mimicry (Yuki and Hartung, 2012, Dalakas, 2015). One classic example is the gram-negative bacterium *Campylobacter jejuni* (*C. jejuni*), which possesses ganglioside-like lipopolysaccharides in its membrane. *C. jejuni* induces diarrhea and is considered as cause of the axonal GBS subtype AMAN in 30 % of the patients (Dalakas, 2015). *C. jejuni* mimics gangliosides that are common on axons of motor nerves and infections with this bacterium induce the production of anti-ganglioside antibodies that may lead to GBS (Yuki and Hartung, 2012). Altogether, two third of the GBS patients have experienced previous infections with Cytomegalovirus (CMV), Epstein-Barr virus (EBV), herpes, hepatitis A virus (HAV), human immunodeficiency virus (HIV) or bacteria, such as *Hemophilus influenza*, *Mycoplasma pneumoniae* and *C. jejuni* (Dalakas, 2015). Infections with CMV or EBV are often connected with initiation of the demyelinating GBS variant (Yuki and Hartung, 2012).

Chronic inflammatory demyelinating polyneuropathy (CIDP) is the most abundant autoimmune peripheral neuropathy. CIDP has many clinical features in common with GBS and is therefore considered the chronic analogue of GBS. Nevertheless, it varies concerning disease development, prognosis, and responsiveness to treatments. Like GBS, CIDP affects motor and sensory nerves and is multifocal, meaning it can arise at different parts of the nerves and displays therefore various symptoms. Mostly macrophages and to a lesser degree T cells account for demyelination and conduction block in this disease but the specific targets remain largely unknown (Dalakas, 2015). In some CIDP patients P0 has been

identified as a target antigen (Yan et al., 2001). It has also been suggested that the attacked sites are rather at nodal/paranodal regions than in the compact myelin. No specific anti-ganglioside antibodies have been associated with the clinical course of CIDP, although some have been discovered in a minority of patients. In CIDP molecular mimicry has not been connected to pathogens but rather to melanoma cells, with melanoma patients having higher CIDP incidence, probably because of some carbohydrate epitopes shared with myelin (Dalakas, 2015).

Multifocal motor neuropathy (MMN) differs from the above-mentioned neuropathies, as in this clinical condition only motor- and no sensory nerves are affected. About half of the MMN patients exhibit specific anti-ganglioside antibodies, but the exact mechanism and immunopathology for this disease are still unclear (Dalakas, 2015). The responsiveness to therapy of immune-mediated neuropathies is overall very good and this includes plasma exchange (PE, also known as plasmapheresis) as first-choice treatment, intravenous immunoglobulins (IVIG) and in some cases corticosteroids (Dalakas, 2015). Plasmapheresis represents plasma separation and exchange to a substitute outside the body and serves to remove harmful, auto-reactive antibodies or other inflammatory agents from the blood of the patient. The possible IVIG mode of action and drug performance in different polyneuropathy patients will be explained in the following chapters (2.6.5 and 2.6.6).

2.5.3 Other peripheral neuropathies

It is worth mentioning that the range of peripheral neuropathies is wide and the patient's quality of life is affected by these disease conditions, which can lead to severe neuropathic pain and limb insensibility.

Toxic peripheral neuropathies often appear as a result of chemotherapies or as a side effect of certain drug use, and their main targets are neurons and their axons (Diezi et al., 2013). Diabetic neuropathy is one of the most common complications in more than half of the diabetes patients and it affects distal sensory, motor, autonomic or cranial nerves. Mechanistically this neuropathic disorder is based on glucose and lipid imbalances, which lead to oxidative stress, inflammation, and altered gene expression in sensory neurons and Schwann cells (Vincent et al., 2011, Vincent et al., 2013). The causes for infectious neuropathies can be different bacterial or viral microorganisms that have managed to pass the blood-nerve barrier. Among them are bacteria such as *Mycobacterium leprae*, an intracellular bacterium that causes leprosy and *Borrelia burgdorferi*, the inducer of Lyme disease. On the other hand, hepatitis C virus (HCV), HIV, varicella zoster virus, or herpes simplex virus can also lead to the generation of neuropathies. The main cause of infection-

related neuropathies is a direct nerve invasion or initiation of inflammatory reactions in the nerve itself, which subsequently lead to nerve injury (Sindic, 2013).
Unfortunately, approved therapeutic strategies for all these conditions are still missing and only individual symptomatic pain treatments and rapid diagnosis represent the current application choice.

2.6 Immunoglobulin applications in the nervous system

2.6.1 Immunoglobulins and their classes

Immunoglobulins (Igs) are heterodimeric proteins, structurally consisting of two heavy and two light chains. They consist of two highly variable Fab regions (Fragment, antigen-binding) and one Fc region (Fragment, crystallisable), and this structural dichotomy provides immunoglobulins with dual functional characteristics. The Fab region contains the binding site for antigens, also called paratope whereas the binding site on the antigen is called an epitope. The Fc region interacts with either Fc receptors (FcRs) or other effector molecules such as proteins of the complement system and thus ensures the so-called effector functions of immunoglobulins. Immunoglobulin glycosylation, in particular the one linked to the Fc region, plays an important role in antibody function and stability. Immunoglobulins are synthesized by B cell lymphocytes, which are thus responsible for the adaptive immune response of the immune system. These cells can produce different immunoglobulin isotypes, which vary in the composition of the heavy chain and are denoted as IgM, IgD, IgG, IgE and IgA (Schroeder and Cavacini, 2010).
IgG is the most abundant immunoglobulin isotype and has the highest specificity towards antigens. Four IgG subclasses exist in the corresponding abundance order in blood plasma: IgG1>IgG2>IgG3>IgG4. The diverse subclasses imply various functional properties in terms of complement fixation or binding to the complementary Fc gamma receptor (FcγR) for IgG recognition expressed on macrophages, neutrophils, and natural killer cells (NK). Whereas IgG1 and IgG3 bind to all receptors, IgG4 bind only to FcγR2 and FcγR3, and IgG2 only to FcγR2. The IgG subclasses exhibit also differences in antigen specificity (proteins or sugars), neutralization of toxins and viruses, and abundance in some diseases (Schroeder and Cavacini, 2010).
The second most common immunoglobulins are IgA. They exist as monomers in the serum but as dimers in secreted fluids such as saliva, colostrum, mucus, tears and others. IgA function comprises neutralization of pathogens directed to mucosal surfaces, while they are rather inefficient in activating the complement system. Two IgA subclasses (IgA1 and IgA2) have been described differing in sensitivity to bacterial proteases and antigen specificity

(Schroeder and Cavacini, 2010).

IgM are the third most common isotype of serum immunoglobulins. IgM are expressed as monomeric molecules in early B cell development and later on become pentameric, while cells mature, and are then being secreted. This pentameric structure provides IgM molecules with high avidity in recognizing multiple antigens and makes them therefore very efficient in labeling antigens for complement. They are also the first antibodies to be released during an immune response (Schroeder and Cavacini, 2010).

IgD antibodies are B cell membrane-bound when these cells leave the bone marrow in order to enter secondary lymphoid organs. At later time points IgD circulate in the serum at very low levels and the function of both forms (bound and soluble) has not been well defined yet (Schroeder and Cavacini, 2010).

Finally, IgE are immunoglobulins with the lowest serum abundance found in soluble or membrane bound forms on mast cells, basophils, or eosinophils. They are involved in allergic reactions, parasitic infections, or hypersensitivity (Schroeder and Cavacini, 2010).

2.6.2 Fc receptors

As indicated above, the Fc region of immunoglobulins can interact with receptors (FcRs) specific for the corresponding antibody class: FcαRs bind IgA, FcγRs bind IgG, FcδRs bind IgD, FcεRs bind IgE and FcμRs bind IgM. They are mainly expressed on immune cells and their activation initiates various biological responses such as for example induction or inhibition of B cell proliferation, phagocytosis by macrophages, degranulation of mast cells, cell lysis and stimulation of cytokine production (Takai, 2002). Immune complex internalization, followed by antigen presentation via class-I and class-II molecules, belongs to the secondary functions of the Fc receptors. Also does the transcellular antibody transport, which is carried out by the neonatal FcR (FcRn) responsible for the maternal IgG transports through the placenta (Takai, 2002).

For the current thesis it was most relevant to study receptors for immunoglobulin G binding, FcγRs. In humans and rats there are three and in mouse four FcγR classes described, (Nimmerjahn and Ravetch, 2008b) with different features (as summarized in table 1). FcγRs come with multiple isoforms and vary in their binding affinity to monomeric IgG or immune complexes. They also bind different IgG subclasses and initiate distinct signaling pathways that are associated with each FcγR (Raghavan and Bjorkman, 1996, Nimmerjahn and Ravetch, 2008b).

Table 1. IgG specific Fc receptors. The content of this table is adapted from (Raghavan and Bjorkman, 1996, Nimmerjahn and Ravetch, 2008b); and furthermore supplemented for *Rattus norvegicus* genes using information derived from the NCBI webpage (http://www.ncbi.nlm.nih.gov/pubmed).

FcγR class (CD)	***Rattus norvegicus* isoforms**	***Mus musculus* isoforms**	***Homo sapiens* isoforms**	**IgG binding specificity**	**Immune cells expression**
FcγR1 (CD64)	FcγR1a	FcγR1	FcγR1a, b*, c*	high-affinity receptor: binds monomeric IgG with high affinity, but also large immune complexes	neutrophils monocytes granulocytes macrophages
FcγR2 (CD32)	FcγR2a, b	FcγR2b FcγR3 (related to human FcγR2a)	FcγR2a, b, c	low-affinity receptor: low to undetectable affinity to monomeric IgG; it only binds complexed IgG (with lower affinity)	widely distributed among cells of the immune system; B cells (only FcγR2b), FcγR2b not on NK cells
FcγR3 (CD16) FcγR4 (only in mouse)	FcγR3a	 FcγR4 (related to human FcγR3a)	FcγR3a, b	low-affinity receptor: low to moderate affinity to monomeric IgG; binds complexed IgG (with decreasing affinity)	macrophages, neutrophils, mast cells, NK cells (only FcγR3)

FcγR: Fc gamma receptor; CD: cluster of differentiation; * not expressed as proteins; NK: natural killer cells.

FcγR1 is the only receptor that binds monomeric as well as complexed IgG with high affinity while all the other receptors preferably bind aggregated IgG or immune complexes and thus exhibit low affinity to monomeric IgG. Its unique feature compared to the low-affinity receptors is the capability to activate effector/immune responses at low IgG concentrations (Raghavan and Bjorkman, 1996). FcγRs can be further classified into activating and inhibitory receptors binding the same Fc portion of the IgG. FcγR1, FcγR2a and FcγR3 all translate activating signals upon IgG binding. These signals trigger the initiation of inflammatory responses such as phagocytosis by macrophages, antibody-dependent cellular cytotoxicity by NK cells, degranulation of mast cells and the transcription of cytokine-encoding genes (Takai, 2002). Activating FcγRs contain a transmembrane Fc receptor common gamma chain bearing an immunoreceptor tyrosine-based activation motif (ITAM) facing the cytoplasm. SRC-family protein tyrosine kinases that phosphorylate tyrosine

residues of the ITAM are crucial for the intracellular activating FcγR signaling. Phosphorylated ITAM then serves as binding site for the cytosolic protein kinase SYK (Takai, 2002). This signaling pathway initiates inflammatory responses, which are responsible for the development and pathogenesis of autoimmune diseases. By contrast, FcγR2b contains an immunoreceptor tyrosine-based inhibitory motif (ITIM) on its cytoplasmic site and is thus known as the inhibitory Fc receptor (Takai, 2002). FcγR2b transfers an inhibitory signal, which results in downregulation of the effector responses and might be responsible for the attenuation of autoimmunity (Takai, 2002). This well regulated signaling through activating and inhibitory FcγRs serves to control the activity of various immune cells. Effector cells of the innate immune system, such as monocytes, macrophages, dendritic cells, basophils, and mast cells express both activating and inhibitory FcγRs. The inhibitory FcγR2b is widely expressed on immune cells and in the case of B cells, it is the only FcγR found on their surface. Nevertheless, it is not found on natural killer cells as these exclusively express the activating receptor FcγR3 (Nimmerjahn and Ravetch, 2008b).

2.6.3 Fc receptor expression in the nervous system[2]

The association of Fc receptors with CNS neurological diseases is becoming more and more of interest, since several of these receptors were found to be expressed on microglia, astrocytes, oligodendrocytes and neurons (Okun et al., 2010). Yet, the function of the Fc receptors in cells of the CNS has not been solved. The expression of a unique Fc receptor for IgM, Fcα/μR, on mouse oligodendrocytes has been shown by Nakahara and colleagues (Nakahara et al., 2003a). This is in line with earlier studies, which already identified IgM binding on the oligodendroglial cell surface (Bieber et al., 2000, Warrington et al., 2000, Bieber et al., 2002, Warrington et al., 2007). Moreover, the same authors showed in a follow up study, that the common gamma chain of immunoglobulin Fc receptors, is expressed in mouse oligodendrocyte precursor cells (OPCs) and plays a role in their differentiation process via activation of Fyn tyrosine kinase and subsequent upregulation of Mbp expression, followed by morphological maturation (Nakahara et al., 2003b). Nevertheless, this study did not elucidate which type of Fc gamma receptor is actually involved in this signaling cascade, although some evidence was provided for the expression of FcγR1 and FcγR3 alpha subunits (Nakahara et al., 2003b). Microglial cells expressing FcγR1, FcγR2 and FcγR3 were found in active Multiple Sclerosis (MS) lesions, suggesting a role for these receptors in the pathogenesis of this demyelinating disease (Ulvestad et al., 1994). Fc gamma receptors are also involved in the activation and proliferation of microglia in ischemic stroke, thus contributing to the initiation and progression of neuronal damage

[2] for authorship notice please refer to chapters 9.1 and 9.2

(Komine-Kobayashi et al., 2004). Apart from this typical immunomodulatory function, Fc receptors are also found on astrocytes and upregulation of FcγR1 expression was detected in a transient BBB opening model mainly in microglia and astrocytes (Li et al., 2008). Interestingly, FcγR1 expression on neurons has primarily been identified on mouse DRG neurons and its possible role is associated with pain and inflammatory signaling following sensory neuron activation (Andoh and Kuraishi, 2004a). A follow up study of the same group detected also expression of the high affinity IgE receptor FcεR1 on DRG neurons, (Andoh and Kuraishi, 2004b). On the other hand, FcγR2b was found to be expressed on cerebellar neurons, and a possible neurodevelopmental role was suggested by the authors (Nakamura et al., 2007).

In the PNS, rather little information is currently available when it comes to FcR expression. Of note, Fc receptors could be identified in myelinating and non-myelinating human peripheral nerves (Vedeler, 1987) and expression was shown on the Schwann cell surface while no staining on axons and fibroblasts was found (Vedeler et al., 1989). FcR was also detected *in situ* in fetal peripheral nerve tissue. Since in cultured human Schwann cells the FcR signal vanished, it was suggested that downregulation of expression might be caused by the loss of axonal contact (Vedeler et al., 1990). In later observations, the detection of the Fc receptors on human Schwann cells was assigned to FcγR3, also known as CD16, a low affinity immunoglobulin binding receptor (Vedeler and Fitzpatrick-Klove, 1990, Vedeler et al., 1991). Gene expression analysis of cultured rat Schwann cells confirmed FcγR3 expression in rodent cells, however, to a much lower degree as compared to macrophages.

2.6.4 Intravenous immunoglobulins (IVIG)

Intravenous immunoglobulins are commercially available polyclonal IgG preparations for therapeutic use as infusion. Depending on the production method, it contains up to 98 percent intact IgG molecules including all four known subclasses in human serum (Kazatchkine and Kaveri, 2001, Buttmann et al., 2013). Additional components of commercially available IVIG can be small quantities of IgA, trace amounts of IgM and soluble CD4, CD8, HLA molecules, as well as cytokines (Blasczyk et al., 1993).[3]

IVIG are prepared from plasma pools of thousands of healthy donors (10.000-40.000) and as such comprise many different antigen-binding antibody regions reflecting the pathogens and foreign antigens to which the donors have been exposed (Radosevich and Burnouf, 2010). This characteristic feature is important for patients with immune deficiencies where immunoglobulin replacement therapy is applied (Kazatchkine and Kaveri, 2001). Nevertheless, the individual antigen reactivity and effector functions are influenced by the

[3] for authorship notice please refer to chapter 9.2

donor selection, the differences among each batch preparation, and the manufacturing processes. Moreover, non-IgG components may also exert additional immunomodulatory effects (Buttmann et al., 2013).[4]

The manufacturing process of pooled human immunoglobulins started in the 1940s with cold ethanol and pH fractionation. It then went through enzyme digestion and chemical modifications in order to minimize observed side effects such as acute allergic reactions or low blood pressure, most likely occurring due to high IgM and IgA concentrations, as well as capability of complement activation. However, these chemical modifications led to structural changes and loss of essential antibody functions and had to be replaced through improved purification methods. The modern IVIG preparation includes multiple steps, which ensure optimal safety and efficacy of the IVIG product. The first step is the blood collection, followed by plasma separation and freezing at less than -20°C within 72 hours after collection for several months storage. As a basic principle, virology testing of the donors has to be negative for HIV and HCV antibodies and hepatitis B surface antigen (HBsAg), but some manufacturers test the donor population for genomic viral markers of HIV, hepatitis B virus (HBV), HAV, and parvovirus B19 (B19). The following steps are responsible for the purification from possible contaminations with activated coagulation factors, components inducing IgG degradation or from protein impurities, and aim at reducing anti-complementary activity. A multistep fractionation process most commonly starts with cryoprecipitation (controlled thawing at 2-3°C), followed by several cold ethanol precipitation steps and ending with low pH/low pepsin treatment or anion and cation exchange chromatography. In addition, an important step is the inactivation and removal of viral contaminations, contributing to the further safety of the IVIG product. Some fractionation methods and low pH treatment during the production process already contribute to viral reduction but they seem to be insufficient for inactivation of all viruses. Introduction of pasteurization (treatment at 60°C for 10 hours) and solvent/detergent treatment were manifested for inactivation of lipid-enveloped viruses. Nanofiltration (using filters with pore size of 15, 20 or 35 nm) was found effective for both non-enveloped and enveloped viruses, as well as for prions. It is therefore often used in combination with the above-mentioned methods to ensure high viral safety (Radosevich and Burnouf, 2010).

The final formulation of IVIG aims at enhancing stabilization of the end product and is most commonly performed in a liquid form at low pH levels (pH 4.5-5.5), high protein concentrations (100 mg/ml) and in the presence of stabilizers such as sorbitol, sugars (maltose, glucose), or amino acids such as glycine, proline or isoleucine (Radosevich and Burnouf, 2010). Upon performance of several quality control assays IVIG preparations are then used for intravenous infusions. Subcutaneous injections have also recently been

[4] for authorship notice please refer to chapter 9.2

developed for easier application and less side effects accounted home treatment and have now become of increasing importance for chronic demyelinating disorders of the PNS (Radosevich and Burnouf, 2010, Buttmann et al., 2013).

2.6.5 IVIG applications in neurological diseases

IVIG have been used for more than 60 years as replacement therapy for prevention of microbial infections in patients with primary immune deficiencies, such as X-linked agammaglobulinemias and secondary immune deficiencies, caused by viral infections or as a result of chemotherapies (Nimmerjahn and Ravetch, 2008a, Schwab and Nimmerjahn, 2013). In the last 30 years its application range gradually expanded. In the 1980s IVIG were first shown to exert a beneficial effect on the autoimmune disease idiopathic thrombocytopenic purpura (ITP) (Imbach et al., 1981) and since then it has been applied for various acute and chronic autoimmune diseases. Meanwhile it is also used as therapy for a variety of neurological conditions and based on controlled clinical trials IVIG are now considered as first-line treatment in acute and chronic demyelinating neuropathies such as GBS, CIDP and MMN (Buttmann et al., 2013, Lünemann et al., 2015). In worsening myasthenia gravis (MG) it is applied as short-term therapy and is considered as second-line treatment in certain inflammatory myopathies and in stiff-person syndrome (Lünemann et al., 2015). The most common IVIG administration dose is set at high-dose (2 g/kg) and is given over two to five days. As the established half-life of infused immunoglobulins in humans is three weeks (Kazatchkine and Kaveri, 2001), the first treatment is usually followed by a lower maintenance dose of 1-2 g/kg after approximately one month (Lünemann et al., 2015).

In GBS patients IVIG are applied at low dose infusions (0.4 g/kg/day) for a period of five days and second treatment is only considered when the outcome from the first one was not positive. It is also successfully applied in AMAN, Miller-Fisher syndrome and childhood GBS, but controlled studies in these conditions have not been conducted yet. In CIDP, IVIG are recognized as first-line treatment for short-term as well as long-term applications. However, divergent amelioration of the respective diseases was observed in patients after IVIG application, plasmapheresis or steroids, and potential costs, side effects, patient age, and disease severity also have to be considered. Concerning MMN, IVIG are currently the only choice of therapy, as patients do not react to PE and steroids. IVIG are applied initially at high doses, continuing with reinfusions of lower doses for a three to six weeks (Lünemann et al., 2015).

In MS, the demyelinating immune-mediated disorder of the CNS, IVIG have also been tested in controlled randomized clinical trials. However, efficacy results were contradictory which is why IVIG are currently not being considered for patients with relapsing-remitting or

secondary progressive MS. Nevertheless, IVIG are occasionally recognized as an effective therapy in pregnant MS patients, as it managed to reduce the recurrence of MS relapses (Lünemann et al., 2015).

Finally, it should be recognized that, apart from the growing demand for novel applications and present therapies, IVIG are an expensive product with rather limited availability. Future studies focus on development of alternative IVIG replacement therapies or the identification of active components (Lünemann et al., 2015).

2.6.6 IVIG mode of action

IVIG are thought to exhibit multiple anti-inflammatory or immunomodulatory activities. Some of these have been revealed in detail in *in vivo* or *in vitro* studies, others are still hypothetical or based on information from the diverse clinical conditions that respond to IVIG. Nevertheless, several immunomodulatory mechanisms, such as the binding to pathogenic antibodies (anti-idiotype effect), inhibition of complement deposition and thus prevention of lytic attack, suppression of proinflammatory cytokines and modulation of cells of the immune system and their receptors have been extensively described (Kazatchkine and Kaveri, 2001, Dalakas, 2004, Siberil et al., 2007, Nimmerjahn and Ravetch, 2008a, Buttmann et al., 2013, Schwab and Nimmerjahn, 2013, Lünemann et al., 2015).[5]

The putative IVIG modes of action are categorically divided into two groups in connection to the structural functionality of the immunoglobulin molecules, namely Fc or Fab domain mediated mechanisms of action. Immunomodulation via the variable domain has been proposed to be dependent on the variety of foreign and self-antigens that have been identified in the IVIG preparations. Cytokines, T or B cell expressed antigens, Fas/CD95 (apoptosis receptor) and FasL/CD95L (Fas ligand), gangliosides and even epitopes on the variable domains of other antibodies (idiotypes) belong to the wide antigen range of autoreactive immunoglobulins. IVIG cannot only interfere with apoptosis mediated pathways of some cells, but most importantly can also neutralize a number of pathogenic antibodies by binding the corresponding idiotype (anti-idiotypic effect), a mechanism which is beneficial to GBS patients. Still, further investigations remain to be conducted in order to identify the full repertoire of mechanisms of action (Nimmerjahn and Ravetch, 2008a, Schwab and Nimmerjahn, 2013, Lünemann et al., 2015). Nevertheless, there is growing evidence that the immunomodulatory effect of IVIG is due to the Fc portion (Debré et al., 1993, Lin et al., 2007b). The Fc region is known to interact with classic pathways of activating and inhibitory Fc gamma receptors on macrophages, B cells, and other cells as well as with proteins of the complement system, which mediates the inflammation process or immune effector functions

[5] for authorship notice please refer to chapter 9.2

by these cells (Kazatchkine and Kaveri, 2001). Therefore, one of the assumed IVIG modes of action is blockade of activating Fc receptors on phagocytes by saturation and thus prevention of immune complex binding, or interfering with signaling pathways that are involved in these receptors' activation (Dalakas, 2004, Siberil et al., 2007, Schwab and Nimmerjahn, 2013). Most studies deal with modulation of the effector function of low affinity FcγR3 receptor and some argue that IgG monomers or possible dimers and aggregates in the IVIG preparation might exhibit the actual inhibitory effect (Aschermann et al., 2010, Schwab and Nimmerjahn, 2013). On the other hand, there is evidence that the inhibitory FcγR2b plays a crucial role in the immunomodulatory activity of IVIG. By blocking or depleting the FcγR2b in an ITP model in mice, the authors could show that the IVIG responsiveness was lost (Samuelsson et al., 2001). Furthermore, FcγR2b expression in effector macrophages as well as their number were increased after IVIG application (Nimmerjahn and Ravetch, 2008a, Schwab and Nimmerjahn, 2013). Other studies demonstrated that in CIDP patients the expression level of the receptor on B cells was downregulated and IVIG treatment led to improvement of this deregulation (Tackenberg et al., 2009, Quast et al., 2015).

In vitro studies as well as animal models and patient data have shown that IVIG can interfere with proteins of the complement system. IVIG can directly bind to activated complement components and thus prevent the subsequent formation of the membrane attack complex (MAC) on target cells. Importantly, an accidental activation of the complement system cascade may be involved in the pathogenesis of demyelinating inflammatory neuropathies such as GBS (Yuki and Hartung, 2012). It is therefore considered that this particular mechanism may lead to inhibition of complement-mediated tissue damage in demyelinating autoimmune diseases (Dalakas, 2004, Siberil et al., 2007, Buttmann et al., 2013).

In GBS patients it has also been demonstrated that IVIG treatment can reduce serum levels of proinflammatory cytokines such as tumor necrosis factor alpha (TNFα) and interleukin-1 beta (IL-1β) (Sharief et al., 1999, Reuben et al., 2003). Moreover, diminished expression of adhesion molecules and other pro-inflammatory cytokines in T cells, accompanied by an upregulation of the anti-inflammatory molecule transforming growth factor beta (TGF-β), was reported as an immunomodulatory key function (Dalakas, 2004, Siberil et al., 2007, Buttmann et al., 2013).

Neutralizing antibodies against receptors and other membrane-expressed proteins, such as co-stimulatory and antigen-presenting molecules on T cells, B cells and monocytes have also been identified in IVIG preparations. Several proposed modes of action of these antibodies involve the inhibition of autoreactive and cytotoxic T cells, induction of protective regulatory T cells and suppression of IgG production in B cells. IVIG have been shown to suppress the differentiation and maturation of dendritic cells, which are important antigen-presenting

mediators for T cell activation. Altogether, IVIG lead to attenuation of the effector functions of cells of the innate and the adaptive immune system (Dalakas, 2004, Siberil et al., 2007, Buttmann et al., 2013).

A novel anti-inflammatory activity of IVIG has been associated with a sialic acid modification on the Fc-linked glycan. Such modifications are not fundamental structures of the Fc region, however, they play a role in immunoglobulin effector functions. Interestingly, IVIG preparations with digested whole glycans or digested sialic acid residues in the Fc region lost their anti-inflammatory activity in a model of rheumatoid arthritis (Kaneko et al., 2006). On the other hand, IVIG fractions enriched in sialic acid revealed a 10-fold protective anti-inflammatory effectiveness and the proposed mechanism of action appeared to involve upregulation of the FcγR2b receptor expression on effector macrophages (Kaneko et al., 2006). A novel receptor that specifically binds sialic acid-rich Fc fragments on immunoglobulins, the C-type lectin SIGN-R1 (specific ICAM-3 grabbing non-integrin-related 1), was found to be expressed on regulatory macrophages (Anthony et al., 2008). SIGN-R1 appears to have a role in the process of inflammation inhibition through pooled immunoglobulins as receptor deletion or blockade did not induce beneficial IVIG effects in a mouse model for ITP and inflammatory arthritis (Anthony et al., 2008, Schwab and Nimmerjahn, 2013).

2.6.7 Immunoglobulin effects CNS cells[6]

There is convincing evidence that immunoglobulins may directly affect oligodendroglial cells, the myelinating glial cells of the CNS. Several studies showed that monoclonal oligodendrocyte-reactive IgMκ antibodies directed to oligodendrocyte antigens have the potential to enhance CNS remyelination in an animal MS model induced by the Theiler's murine encephalomyelitis virus (TMEV) (Miller et al., 1994, Asakura et al., 1996, Asakura et al., 1998). The IgMκ antibodies were obtained by immunization of mice with mouse spinal cord homogenate and screened for auto-antigen binding capacity (Miller et al., 1994, Asakura et al., 1996, Asakura et al., 1998). Only these autoantibodies that successfully bound to oligodendrocyte antigens promoted remyelination in TMEV induced lesions (Asakura et al., 1998). Specific IgMκ antibodies directed against well-known oligodendrocyte surface antigens such as lipids, gangliosides and carbohydrates were also tested and disclosed a positive differentiation potential (Asakura et al., 1998).

A number of additional studies revealed that treatment of non-immune, toxin-induced, as well as TMEV induced models of demyelinating diseases with polyclonal human IgG and IgM molecules results in a significantly enhanced oligodendrocyte differentiation reaction (Bieber

[6] for authorship notice please refer to chapter 9.2

et al., 2000, Warrington et al., 2000, Bieber et al., 2002). In the TMEV model for induced demyelination, both IVIG and polyclonal human IgM promoted remyelination but IgM molecules appeared to be more potent (Bieber et al., 2000, Warrington et al., 2000). Using the same disease model, though by administration of human monoclonal serum-derived IgM antibodies, the authors could demonstrate binding to the oligodendrocyte surface for all molecules but remyelination potential was restricted to a few immunoglobulins (Warrington et al., 2000). In a different demyelination model, induced by toxic lysolecithin injection in the spinal cord and thus less immune system dependent, the results were comparable. Application of polyclonal human IgM or serum-derived human monoclonal antibodies accelerated the process of remyelination, however pooled IgG did not show any effect (Bieber et al., 2002). Of note, lesions treated with the serum derived monoclonal antibody exhibited larger macrophage infiltration, suggesting a role for this immune cell recruitment in myelin repair (Bieber et al., 2002). Altogether, these studies showed that the specific binding to oligodendroglial surface antigens and thus acceleration of oligodendroglial remyelination was restricted to monoclonal IgM molecules (Bieber et al., 2000, Warrington et al., 2000, Bieber et al., 2002).

Interestingly, a specific Fc receptor for IgM, Fcα/μR, is expressed on oligodendrocytes, their precursor cells and myelin, suggesting a possible direct interaction between receptor and immunoglobulins (Nakahara et al., 2003a). On the other hand, recombinant human monoclonal IgM antibodies were shown to have an effect on hippocampal neurons, in which they manage to initiate rearrangement of membrane lipids and microtubules, hence inducing axonal outgrowth (Xu et al., 2011).

Recent studies on human IgG application in an animal model of spinal cord injury revealed that single dose application enhanced functional recovery and diminished the inflammation process in the scar (Nguyen et al., 2012). In connection to this study, IVIG are now being considered as a potential pharmacological treatment of spinal cord injury (Tzekou and Fehlings, 2014).

2.6.8 Immunoglobulin effects on PNS cells[7]

An indirect effect of human immunoglobulins in demyelinating disease models of the PNS has been demonstrated via IVIG treatment of rats with EAN, an inducible inflammatory GBS like disease (Gabriel et al., 1997, Lin et al., 2007a). In these studies EAN was induced by immunization of rats with bovine peripheral nerve myelin (Gabriel et al., 1997, Lin et al., 2007a). IVIG treatment reduced EAN severity, from the onset of first neurological signs, by preventing disease development and inducing a faster and more complete recovery (Gabriel

[7] for authorship notice please refer to chapter 9.2

et al., 1997, Lin et al., 2007a). The same authors could demonstrate that the Fc- and not the Fab portion of the IgG molecule was responsible for the reduced demyelination and inflammation leading to shorter disease duration, although complete IVIG preparations were slightly superior to all fractions (Lin et al., 2007b). However, disease amelioration is currently thought to result from immune system modulation whereas no studies on neural regeneration and glial maturation have been conducted within cells of the PNS.

Interestingly, recent studies point to a role of endogenous antibodies in rapid myelin clearance and axon regeneration after nerve injury by promoting macrophage entrance and phagocytotic activity (Vargas et al., 2010). The authors used a model of B cell depleted JHD mice, which lack endogenous antibodies. Upon sciatic nerve injury, they could observe delayed myelin clearance accompanied by significantly reduced macrophage infiltration and phagocytic activity, finally resulting in decreased axonal regeneration. It was further shown, that this process could be rescued by passive transfer of purified IgG and IgM molecules from wild type mice or exogenous antibodies directed against myelin. Vargas and colleagues therefore concluded that endogenous myelin-reactive autoantibodies are sufficient for effective and fast clearance of degenerated myelin (Vargas et al., 2010).

2.7 Schwann cells are immune competent glial cells[8]

Schwann cells have been recognized as immune competent cells primarily based on their involvement in peripheral neuropathies, but also in light of the fact that they express specific pattern recognition receptors (PRR) for the detection of pathogens, their role in initiating and regulating local immune responses by antigen presentation and cytokine secretion and due to a number of described interactions with immune cells or proteins of the complement system. Although peripheral nerve disorders are heterogeneous by nature, including inflammation mediated damage, genetic causes, or in response to acute injuries, these pathologies have interactions between glial and immune cells in common (Tzekova et al., 2014).

Major histocompatibility complex (MHC) genes encode specialized molecules for the presentation of antigenic protein fragments to T cells. There are two classes of MHC molecules, namely class I and II, which vary in function and expression patterns. Whereas all nucleated cells express MHC class I molecules, MHC class II is usually expressed on specialized antigen presenting cells of the immune system such as dendritic cells, macrophages, and B lymphocytes. It has long been known that rat and human Schwann cells express MHC class I and II molecules on their surface and that they could therefore be

[8] for authorship notice please refer to chapter 9.1

considered as accessory antigen presenting cells (Fig. 4) (Samuel et al., 1987, Armati et al., 1990). The expression of MHC class II on the Schwann cell surface was shown to be interferon gamma (IFNγ) and TNFα dependent and these cytokines most likely originate from the interactions between Schwann- and T cells (Kingston et al., 1989). MHC I is constitutively expressed at low levels on Schwann cells and can in contrast to MHC II be upregulated by IFNγ (Lilje and Armati, 1997). Moreover, a recent study confirmed that human Schwann cells are able to process as well as present endogenous and exogenous antigens *in vivo* and *in vitro*, thus them being equipped with the full antigen presenting machinery. This indicates antigen processing and presentation as possible functions of Schwann cells that may contribute to (auto)immune responses within peripheral nerves (Meyer Zu Horste et al., 2010). The capacity of Schwann cells to act as antigen presenting cells is of additional importance in immune-mediated disorders of the PNS such as GBS or CIDP. MHC class II antigen reactivity was detected on Schwann cells of patients suffering from GBS, CIDP, toxic or metabolic neuropathies, with the strongest expression in CIDP (Pollard et al., 1986, Pollard et al., 1987, Mancardi et al., 1988, Mitchell et al., 1991). These findings strongly indicate that these glial cells act as facultative antigen presenting cells and are further corroborated by studies on the expression of co-stimulatory molecules by Schwann cells which are essential for proper antigen presentation and are involved in T cell regulation within the inflamed nerve (Murata and Dalakas, 2000, Spierings et al., 2001, Duan et al., 2007).

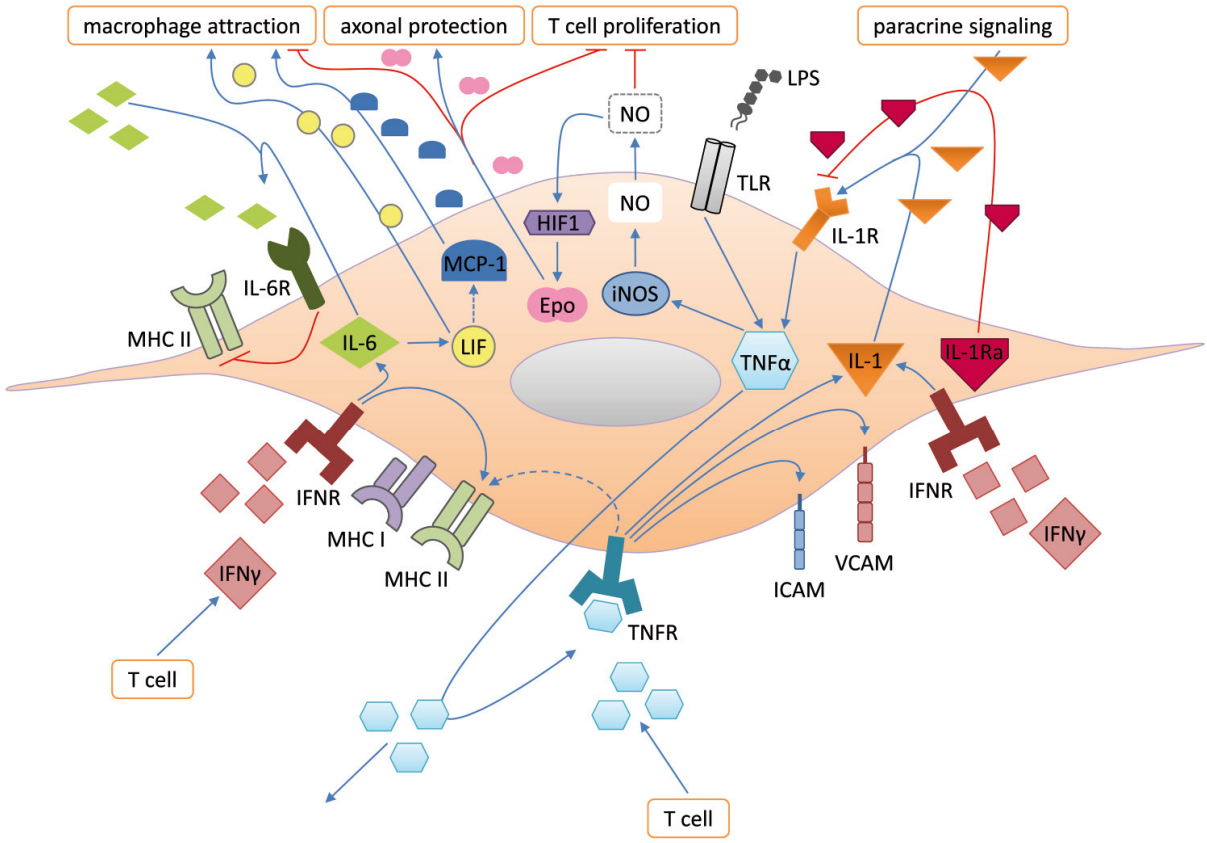

Figure 4. Secreted molecules and receptors expressed by Schwann cell. Schwann cells are well known to express a number of immune-related receptors on their surface. Among these are Toll-like receptors (TLR), that can be activated by lipopolysaccharide (LPS); TNF receptors (TNFR) involved in TNFα para-/autocrine signaling; cell adhesion molecules such as intercellular adhesion molecule (ICAM) and vascular cell adhesion protein (VCAM), important for host defense after injury; IL-1 receptor (IL-1R) and IL-6 receptor (IL-6R), and MHC class I and II antigen presenting molecules. Schwann cells release proinflammatory cytokines such as tumor necrosis factor-α (TNFα), interleukin-1 (IL-1) and interleukin-6 (IL-6) in response to nerve injury; and express the proinflammatory chemokine monocyte chemoattractant protein (Mcp-1), which attracts macrophages to pathogenic peripheral nerves. Schwann cells release also anti-inflammatory molecules such as erythropoietin (Epo), which protect myelin against immune attacks and degradation by inhibiting T cell and macrophage proliferation.
"With kind permission from Springer Science+Business Media: Journal of Clinical Immunology, Molecules involved in the crosstalk between immune- and peripheral nerve Schwann cells, 34 Suppl 1, 2014, S86-104, Tzekova N., Heinen, A., Küry, P., original figure 2."

Apart from the above mentioned Fc receptors Schwann cells were shown to express various other immunologically relevant surface molecules and receptors (Fig. 4). PRRs such as toll-like receptor 1 (TLR1), TLR3, TLR4, TLR2 and TLR6 induced by bacterial surface antigens or viral RNA, cell adhesion molecule I-CAM, proposed to be important for host defense after PNS injury, mannose receptor, suggested to be involved in Schwann cell phagocytosis, and lectins, carbohydrate-binding proteins belong to their repertoire, reviewed in (Tzekova et al., 2014).

Schwann cell interactions with proteins of the complement system are various. In demyelinating inflammatory neuropathies as well as the corresponding animal model EAN the membrane attack complex could be described on Schwann cell surface, revealing that complement activation participates in demyelination (Stoll et al., 1991, Putzu et al., 2000, Yuki and Hartung, 2012) (Fig. 5). Activation of complement factors plays a central role in Wallerian degeneration by means of macrophage activation and subsequent myelin debris removal (Dailey et al., 1998, Ramaglia et al., 2007). In addition, Schwann cells actively express complement factors C1r, C1s and C3 (Dashiell et al., 1997, de Jonge et al., 2003) as well as control proteins (Nose et al., 1990, Funabashi et al., 1994), complement receptor 1 (CR1) (Vedeler and Matre, 1988, Vedeler et al., 1989, Vedeler et al., 1990, Vedeler et al., 1992, Funabashi et al., 1994) and some inhibitors of C3 and C5 convertases (Koski et al., 1996, de Jonge et al., 2003), which are mediators that attenuate or suppress complement factor activation. The expression and tight regulation of complement activating and inhibiting molecules suggests that Schwann cells, when not directly affected by inflammation or injury, can actively protect themselves against accidental complement dependent myelin phagocytosis (Nose et al., 1990, Funabashi et al., 1994) (Fig. 5).

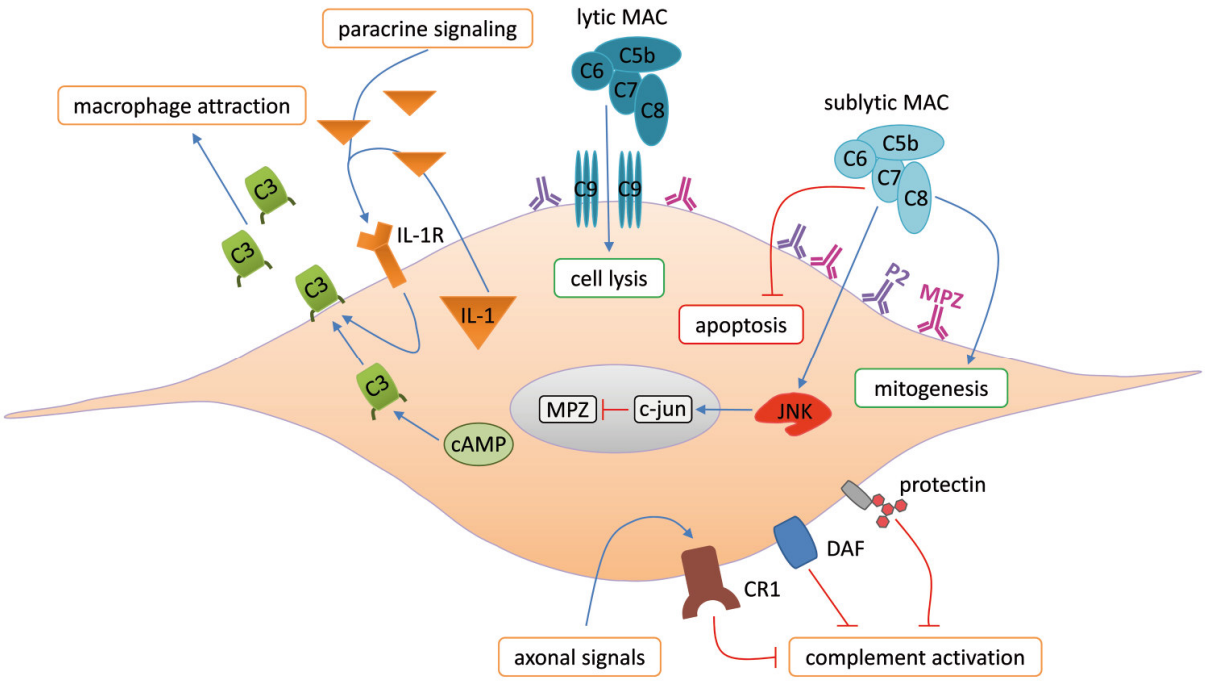

Figure 5. Expression of complement system components by Schwann cell. Antibodies against myelin proteins P2 and Mpz/P0 can initiate the complement cascade on Schwann cells, which finally leads to assembly of the membrane attack complex (MAC) on the cell surface. MAC consists of complement components C5b, C6, C7 and C8 and its activation either leads to cell lysis by pore formation through C9, or when present at sublytic concentrations, protects against apoptosis, induces mitogenesis and interferes with Schwann cell differentiation by jun N-terminal kinase (JNK) activation. Schwann cells also express and release complement factor C3, which leads to macrophage attraction

and myelin debris clearance in Wallerian degeneration. An important Schwann cell protection mechanism against complement system mediated lysis is the expression of complement inhibiting molecules such as complement receptor 1 (CR1), decay accelerating factor (DAF) and protectin.
"With kind permission from Springer Science+Business Media: Journal of Clinical Immunology, Molecules involved in the crosstalk between immune- and peripheral nerve Schwann cells, 34 Suppl 1, 2014, S86-104, Tzekova N., Heinen, A., Küry, P., original figure 1."

Schwann cells can also directly interact with different cells of the immune system such as via the FasL/Fas receptor pathway with T lymphocytes. FasL is a cytokine shown to induce apoptosis upon binding to the Fas receptor, a mechanism that is primarily used by the immune system to eliminate remaining effector T cells. However, Schwann cells were shown to express FasL and can thus participate in this elimination process with a possible function in amelioration of the inflammatory immune response (Wohlleben et al., 2000, Bonetti et al., 2003). Indirect studies also provide evidence of glial Fas expression as FasL on T cells or macrophages could induce their death (Dace et al., 2009). In this context, a direct connection between Schwann cells and macrophages was suggested following the identification of the chemokine monocyte chemoattractant protein-1 (Mcp-1), the expression of which was increased in Schwann cells from heterogeneously deficient P0/Mpz mice, an animal model of inherited neuropathies. Mcp-1 turned out to be an important chemoattractant for macrophages, as reduced levels of Mcp-1 ameliorated genetically caused damaged of the peripheral nerve (Fischer et al., 2008a).
These immune cell interactions are further stimulated by the glial expression of pro-inflammatory and anti-inflammatory cytokines, cytokine receptors, and chemokines (Fig. 4). The secretion of the pro-inflammatory cytokines interleukin-1 alpha (IL-1α) and IL-1β by Schwann cells has been demonstrated to stimulate macrophage recruitment and T cell activation in EAN models, GBS patients, and Wallerian degeneration (Putzu et al., 2000, Skundric et al., 2001, Shamash et al., 2002). IL-1α also serves as inducer of Schwann cell proliferation (Lisak et al., 1994), while IL-1β role was designated in instructing rapid WD (Shamash et al., 2002). In GBS nerve biopsies, IL-1β signals colocalized with TNFα, a mainly macrophage and lymphocyte derived pro-inflammatory cytokine, which is, however, also expressed by Schwann cells, axons and fibroblasts (Murwani and Armati, 1998, Putzu et al., 2000). IL-1 and TNFα are constitutively expressed in intact peripheral nerves and become rapidly induced in Schwann cells upon nerve transection (Shamash et al., 2002). Interestingly, treatment of GBS patients using IVIG led to reduction of TNFα serum levels and clinical improvement (Sharief et al., 1999), supporting the notion that TNFα prolongs immune attacks. Schwann cells also express both TNF receptors (Bonetti et al., 2000) and this process appears to be TNFα dependent (Qin et al., 2008), suggesting the existence of a feedback loop for this cytokine. Interleukin-6 (IL-6) is another pro-inflammatory cytokine

expressed by Schwann cells (Rutkowski et al., 1999, Ozaki et al., 2008), which functions as glial co-mitogen (Lisak and Bealmear, 1994, Lisak et al., 1994) and contributes together with IL-1 to the immune response induction upon nerve injury (Bolin et al., 1995). IL-6 was shown to promote neurite extension in sensory neurons (Hirota et al., 1996) and is supposed to directly influence Schwann cell maturation (Hirota et al., 1996) as well as to diminish their antigen presenting properties (Kitamura et al., 2005). Since Schwann cells also express IL-6 receptor (IL-6R), this fact supports a regulation of cytokine expression in an auto-/paracrine loop (Lara-Ramirez et al., 2008).

Following nerve injury, a sequential expression of pro- and anti-inflammatory mediators is observed, where a decline in pro-inflammatory cytokine expression is accompanied by upregulation of anti-inflammatory cytokines several days post transection. Interleukin-10 (IL-10) belongs to the late induced anti-inflammatory cytokines during Wallerian degeneration, where it exerts a possible role in diminishing inflammatory responses (Jander et al., 1996, Be'eri et al., 1998). This was also confirmed in EAN sciatic nerves where IL-10 upregulation correlated with clinical improvement (Zhu et al., 1997). Schwann cells were shown to secrete erythropoietin (Epo), primarily known to stimulate erythrocyte maturation (Fig. 4). They also express the Epo receptor (EpoR), and Epo stimulation was demonstrated to induce MAPK/ERK signaling and to promote Schwann cell proliferation (Li et al., 2005). Furthermore, Epo release by Schwann cells was shown to ameliorate axonal degeneration (Keswani et al., 2004) and to protect peripheral myelin against immune attacks and degradation by diminishing T cell and macrophage proliferation. Exogenously applied Epo subsequently increased Schwann cell proliferation as well as migration to the lesion site (Li et al., 2005, Inoue et al., 2010). Another potent anti-inflammatory cytokine constitutively expressed by Schwann cells is TGF-β with a role in T cell differentiation inhibition, suppression of myelin phagocytosis in WD and protection of Schwann cells against apoptosis upon nerve transection (Ahn et al., 2010, Luo et al., 2013).

Schwann cells also express a number of chemotaxic cytokines, termed chemokines. Their secretion upon infection or injury can lead to immune cell attraction, therefore certain chemokines are considered as pro-inflammatory mediators. Macrophage inflammatory protein (MIP) is strongly induced by Schwann cells after nerve transection and is responsible for neuropathic pain in sciatic nerve lesions (Taskinen and Roytta, 2000, Kiguchi et al., 2010). A number of chemokines from the CXC family, such as CXCL9, CXCL10 and CXCL11 are induced in diabetic neuropathies (Tang et al., 2013), in Schwann cells of acutely injured nerves (Küry et al., 2002), or in cerebrospinal fluids of GBS patients (Kieseier et al., 2002, Press et al., 2003) leading to local pro-inflammatory immune reactions. As mentioned earlier, in peripheral nerves the expression of the chemokine Mcp-1 (CCL2) is restricted to Schwann cells (Toews et al., 1998, Rutkowski et al., 1999) (Fig. 4). Mcp-1 was upregulated

following sciatic nerve transection and crush injury, followed by macrophage attraction to the demyelinated nerve, suggesting that Mcp-1 expression correlates with macrophage infiltration upon demyelination (Toews et al., 1998, Rutkowski et al., 1999). Mcp-1 also participates in macrophage-mediated attack to peripheral myelin in autoimmune neuropathies as revealed by correlation of increase in its expression and disease severity in GBS patients (Orlikowski et al., 2003). This chemokine is probably also involved in the disease development of inherited neuropathies based on studies in animal models, where upregulated expression levels of Mcp-1 correlated with increased macrophages numbers within peripheral nerves (Fischer et al., 2008a, Fischer et al., 2008b, Groh et al., 2010, Kohl et al., 2010). Considering the variety of inflammation-related molecules that are either expressed or sensed by Schwann cells this strengthens the evidence for their broad physiological and pathological role and defines them as immune-competent glial cells (reviewed in (Tzekova et al., 2014)).

2.8 Aim of the thesis

Intravenous immunoglobulins are currently used as first-choice treatment for a variety of inflammatory neuropathies, such as GBS, CIDP, and MMN (Buttmann et al., 2013, Lünemann et al., 2015). In animal models of autoimmune neuropathies IVIG were also shown to induce amelioration of the disease course (Gabriel et al., 1997, Lin et al., 2007a, Lin et al., 2007b). However, despite these observed beneficial effects no immunoglobulin related role in modulating the nerve's own regeneration activity has been described. Along this line, so far no direct studies investigated a potential impact of immunoglobulins on the glial cells of the PNS. This is even more surprising since numerous publications reported beneficial immunoglobulin mediated effects on myelinating glial cells of the CNS (Bieber et al., 2000, Warrington et al., 2000, Bieber et al., 2002).

The focus of this thesis was therefore to determine whether intravenous immunoglobulins exert direct effects on Schwann cell homeostasis and maturation, and whether observed reactions could be correlated with a potential influence on nerve regeneration processes as they were shown to depend and to be regulated by Schwann cells. For this purpose the impact of stimulation with IVIG was studied using various primary cell culture models including primary Schwann cells, differentiation-competent Schwann cells (Heinen et al., 2008a) as well as myelinating neuron/glia cocultures.

3 MATERIALS AND METHODS

3.1 Material

3.1.1 Animals[9]

For the preparation of primary Schwann cell cultures sciatic nerves from newborn Wistar rats of either sex (postnatal day zero, P0) were used. Myelinating neuron/glia dissociation cocultures were prepared from dorsal root ganglia (DRG) of C57BL/6 mouse embryos (embryonic day 15, E15), whereas DRG explant cultures were prepared from Wistar rat embryos (E17/18).

The animals were ordered from Janvier Labs (Saint Berthevin Cedex) or/and bred within the animal facility of the Heinrich-Heine-University (Düsseldorf) under pathogen free standard conditions (temperature 21°C; humidity 50 %; 12 h light/ 12 h dark cycle). Food and water were available ad libitum. For this study no animal *in vivo* experiments were performed. Animal sacrifice and tissue elevation were conducted with approval by the local animal facility of the Heinrich-Heine-University (registration numbers: O82/12, O69/2011, O53/11) in accordance with the German Animal Protection law (State Office, Environmental and Consumer Protection of North Rhine-Westphalia, LANUV NRW).

3.1.2 Escherichia coli (E. coli) bacteria strains

Following *E.coli* strains were used for transformations:

Strain	Supplier
One Shot TOP10 Genotype: F-*mcrA* Δ(*mrr-hsd*RMS-*mcr*BC) Φ80*lac*ZΔM15 Δ*lac*X74 *rec*A1 *ara*D139 Δ(*araleu*)7697 *gal*U *gal*K *rps*L (StrR) *end*A1 *nup*G	Invitrogen Thermo Fisher Scientific

[9] for authorship notice please refer to chapter 9.2

3.1.3 Chemicals

3.1.3.1 Reagents and chemicals

Chemical/reagent	Supplier
2-mercaptoethanol/ β-mercaptoethanol	Sigma-Aldrich
2-propanol	Merck
4,6-diamidino-2-phenylindole (DAPI)	Sigma-Aldrich
Agarose	Sigma-Aldrich
Arabinosyl cytosine hydrochloride (AraC)	Sigma-Aldrich
Avastin (Bevacizumab)	Roche Pharma
Bacto agar	Gibco Thermo Fisher Scientific
Bovine serum albumin (BSA)	Carl ROTH
Citifluor	Science Services
Deoxynucleotide (dNTPs)	Applied Biosystems Thermo Fisher Scientific
Dimethylsulfoxide (DMSO)	Sigma-Aldrich
Ethanol abs.	Merck
Ethylendiamintetraacetic acid (EDTA)	Sigma-Aldrich
Fcgr1 recombinant Rat Protein, His Tag, 5µg (rrFcgr1)	Invitrogen Thermo Fisher Scientific
Fluromount G	Southern Biotech
Forskolin	Sigma-Aldrich
Gammagard Liquid [Immune Globulin Intravenous (Human)] 10%, 100mg/ml protein; Lot LE12J270AB	Baxter Healthcare Corporation
Gammagard Liquid [Immune Globulin Intravenous (Human)] 10%, 100mg/ml protein; Lot LE12L341AA (IVIG2)	Baxter Healthcare Corporation
Gammagard Liquid [Immune Globulin Intravenous (Human)] 10%, 100mg/ml protein; Lot LE12L341AA (IVIG3)	Baxter Healthcare Corporation
Gammagard Liquid formulation buffer (0.25 M glycine, pH 4.5)	Baxter Healthcare Corporation
Glycerol	Sigma-Aldrich
Herceptin (Trastuzumab)	Roche Pharma
Hydrochloric acid (HCl)	Merck
Isofluran	DeltaSelect
LiChrosolv Water	Merck
Methanol	Merck
Milk powder	Carl ROTH
Paraformaldehyde	Merck
Pepsin	Sigma-Aldrich
Ponceau S staining solution	Sigma-Aldrich
Recombinant interleukin-18 (rrIL-18)	R&D Systems
Recombinant Ra IL-18/IL-1F4, 25 µg	R&D Systems

Sodium chloride (NaCl)	Merck
Sodium dodecyl sulphate (SDS)	Merck
Sodium hydroxide (NaOH)	Merck
Sucrose	Merck
Synagis (Palivizumab)	Abbott SRL
Trishydroxymethylaminomethan (Tris)	Merck
Triton X-100	Sigma-Aldrich
Trypton	Difco
Tween 20	Sigma-Aldrich
Yeast extract	Difco

3.1.4 Buffers and solutions

3.1.4.1 Buffers, solutions and reagents for cell culture

Buffer/reagent	Supplier	Composition
Deoxyribonuclease I (DNase)	Sigma-Aldrich	8 mg/ml stock solution in DMEM
Dulbecco´s phosphate buffered saline (PBS)	Sigma-Aldrich	
L-glutamine, 200 mM	Gibco	1:100 dilution in DMEM
penicillin/streptomycine, 5000 U (pen/strep)	Gibco	1:100 dilution in DMEM
Poly-D-lysine (PDL)	Gibco Thermo Fisher Scientific	10 mg/ml stock solution in PBS
Laminin 1 mg/ml	Sigma-Aldrich	dilution to 13 µg/ml in PBS
Collagen Typ I Rat Tail, 100mg	Becton-Dickinson	1:7 dilution in 0.02 N acetic acid
NGF-β from rat, 1mg	Sigma-Aldrich	1 mg/ml stock in 0.1 % BSA
D-(+)-Glucose solution, 100 g/L in H2O, sterile-filtered, BioXtra, suitable for cell culture	Sigma-Aldrich	
L-Ascorbic acid, cell culture tested, 25g	Sigma-Aldrich	5 mg/ml fresh stock in H2O
Baby Rabbit Complement, 1 ml lyophylised	BIOZOL (Cedarlane)	ad 1 ml sterile ddH2O
Bovine pituitary extract (BPE; GGF), 50mg	Millipore (Upstate Biotechnologies)	10 mg/ml stock in PBS
0.05 % Trypsin	Gibco Thermo Fisher Scientific	
Collagenase type 1, 100 mg	Sigma-Aldrich	6 mg/ml stock in PBS (0.6%)
Forskolin	Sigma-Aldrich	2 mM stock in EtOH absolute
0.6 % sucrose	Merck	0.6 g in 100 ml in PBS
Recombinant Ra IL-18/IL-1F4, 25 µg	R&D Systems	100 µg/ml stock in 1 % FCS (FCS diluted in sterile PBS)
Mouse anti rat CD90 (THY1) monoclonal antibody; 0,25 mg	AbD Serotec	0.4 ml mouse anti THY1 antibody diluted with 1.6 ml DMEM (use 1:10 diluted in DMEM)
Synagis (Palivizumab)	Abbott SRL	dilution in Schwann cell medium to 20 mg/ml

Herceptin (Trastuzumab)	Roche Pharma	dilution in Schwann cell medium to 20 mg/ml
Avastin (Bevacizumab)	Roche Pharma	dilution in Schwann cell medium to 20 mg/ml
Gammagard Liquid [Immune Globulin Intravenous (Human)] 10%, 100mg/ml protein; Lot LE12J270AB	Baxter Healthcare Corporation	dilution in Schwann cell medium to 20 mg/ml
Gammagard Liquid [Immune Globulin Intravenous (Human)] 10%, 100mg/ml protein; Lot LE12L341AA (IVIG2)	Baxter Healthcare Corporation	dilution in Schwann cell medium to 10 or 5 mg/ml
Gammagard Liquid [Immune Globulin Intravenous (Human)] 10%, 100mg/ml protein; Lot LE12L341AA (IVIG3)	Baxter Healthcare Corporation	dilution in Schwann cell medium to 10 or 5 mg/ml
Gammagard Liquid formulation buffer (0.25 M glycine, pH 4.5)	Baxter Healthcare Corporation	corresponding dilution in Schwann cell medium

3.1.4.2 Buffers, solutions and reagents for molecular biology

Buffer/reagent for DNA/RNA	**Composition**
Tris-acetate-EDTA (TAE) buffer, 50x stock solution	121 g Tris 28.55 ml glacial acetic acid 50 ml 0.5 M EDTA, pH 8.0 ddH_2O ad 500 ml
BlueJuic Gel Loading Buffer (10x)	Invitrogen Thermo Fisher Scientific
RLT lysis buffer	Qiagen

Buffer/reagent for proteins	**Supplier**	**Composition**
RIPA Buffer (10x)	Cell Signaling Technology	dilute to 1x solution with ddH_2O
Halt Protease Inhibitor Cocktail, containing Protease Inhibitor Cocktail (100x), EDTA Solution, 0.5 M (100x)	Thermo Scientific Thermo Fisher Scientific	
Halt Phosphatase Inhibitor Cocktail (100x)	Thermo Scientific Thermo Fisher Scientific	
Halt Protease and Phosphatase Inhibitor Cocktail (100x)	Thermo Scientific Thermo Fisher Scientific	
NuPAGE LDS Sample Buffer (4x)	Novex Thermo Fisher Scientific	
NuPAGE Sample Reducing Agent (10x)	Novex Thermo Fisher Scientific	
RunBlue RAPID SDS Run Buffer 500 ml (20x)	Expedeon, BIOZOL	40 ml unBlue RAPID SDS Run Buffer 760 ml ddH2O
RunBlue TGS Blot Stock Buffer 500 ml (10x)	Expedeon, BIOZOL	100 ml TGS Blot Stock Buffer 200 ml methanol 720 ml ddH2O
1x Tris buffered saline (TBS)		20 mM Tris base

		150 mM NaCl
		ad 1000 ml ddH2O
		pH adjusted to 7.6 using HCl
TBS Tween (TBST)		1x TBS
		0.05 % (v/v) Tween 20
Blocking buffer 1 % milk		1x TBS
		1 % milk powder
		0.05% Tween 20
Blocking buffer 2 % milk		1x TBS
		2 % milk powder
		0.05% Tween 20
Fcgr1 recombinant Rat Protein, His Tag, 5 µg (rrFcgr1)	InvitrogenTM Thermo Fisher Scientific	reconstituted to 0.2 mg/ml in sterile ddH2O; 2-4 µg protein unsed in SDS PAGE

3.1.4.3 Buffers, solutions and reagents for staining procedures

Buffer/reagent	**Composition**
8 % paraformaldehyde, pH 7.4 (PFA)	80 g PFA
	ad 1 L 1xPBS
	adjust pH with NaOH and HCl
4 % paraformaldehyde, pH 7.4 (PFA)	dilute 8 % stock in PBS
2 % normal rabbit serum (NRS)	100 % NRS diluted 1:50 in 1xPBS
5 % normal rabbit serum (NRS)	100 % NRS diluted 1:20 in 1xPBS
2 % normal goat serum (NGS)	100 % NGS diluted 1:50 in 1xPBS
10 % normal goat serum (NGS)	100 % NGS diluted 1:10 in 1xPBS
5 % low background solution (LBS)	100 % LBS diluted 1:20 in 1xPBS
0.5 % bovine serum albumin (BSA)	0.5 g BSA
	ad 100 ml 1xPBS
0.1 % Triton X-100	100 % Triton X-100 diluted 1:1000 in 1xPBS
0.5 % Triton X-100	100 % Triton X-100 diluted 1:200 in 1xPBS
1 % Triton X-100	100 % Triton X-100 diluted 1:100 in 1xPBS
Phalloidin-TRITC	5 mg/ml stock in DMSO; for staining dilute to 50 µg/ml with PBS
4,6-diamidino-2-phenylindole (DAPI)	10 mg DAPI
	3 ml EtOH
	ad 500 ml PBS for 20µg/ml stock
	stock dilution 1:10 in 1xPBS for final use

3.1.5 Materials

Gels/Membranes/Culture Dishes	Supplier
Amersham Hyperfilm ECL	GE Healthcare
Cell Culture Dish, ø 100 mm	Greiner bio-one
Cell Culture Flask, 250 ml, 75 cm²	Greiner bio-one
Cell Culture Flask, 50 ml, 25 cm²	Greiner bio-one
Cell Culture Multiwell Plate, 12 Well	Greiner bio-one
Cell Culture Multiwell Plate, 24 Well	Greiner bio-one
ø 13 mm microscope cover glasses	Assistent
ø 15 mm microscope cover glasses	Assistent
RunBlue Blot Sandwich nitrocellulose, 90x85mm	Expedeon, BIOZOL
RunBlue SDS Gel 4-12 %, 12 well	Expedeon, BIOZOL
x-well slide, 2-well on PCA detachable	Sarsted

3.1.6 Media

3.1.6.1 Media for cell culture

Medium	Supplier/composition
Dulbecco's modified eagle medium (DMEM)	Gibco
DMEM GlutaMax-I (4.5 g/l glucose)	Gibco
Fetal calf serum (FCS)	Lonza
Heat inactivated horse serum (HS)	Gibco Thermo Fisher Scientific
Leibovitz's medium (L15)	Gibco Thermo Fisher Scientific
Minimum essential medium (MEM)	Gibco Thermo Fisher Scientific
N2 supplement	Invitrogen Thermo Fisher Scientific
Growth medium for myelinating neuron/glia cocultures	2 ml 10 % glucose (0.4 %) 5 ml horse serum (10 %) 0.5 ml pen/strep ad 42.5 ml MEM * 2.5 µl NGF (50 ng/ml)
Myelination medium for myelinating neuron/glia cocultures	2 ml 10 % glucose (0.4 %) 2.5 ml horse serum (5 %) 0.5 ml N2 supplement 0.5 ml pen/strep ad 44.5 ml MEM * 2.5 µl NGF (50 ng/ml) added freshly * 0,5 µM forskolin added freshly * 20 µg/ml GGF added freshly

	* 50 µg/ml L-Ascorbic acid added freshly
Myelination medium for myelinating neuron/glia cocultures with 20mg/ml IVIG/ buffer control	1 ml 10 % glucose (0.4 %)
	1.25 ml horse serum (5 %)
	0.25 ml N2 supplement
	0.25 ml pen/strep
	5 ml IVIG/ buffer control
	ad 17.25 ml MEM
	* 1.25 µl NGF (50 ng/ml) added freshly
	* 0,5 µM forskolin added freshly
	* 20 µg/ml GGF added freshly
	* 50 µg/ml L-Ascorbic acid added freshly
Schwann cell medium	5 ml L-glutamine
	5 ml pen/strep
	50 ml FCS
	ad 500 ml DMEM
	* 2 µM forskolin added freshly
Schwann cell proliferation medium	Schwann cell medium
	* 2 µM forskolin
	* 100 µg/ml GGF
Schwann cell cryopreservation medium	4 ml Schwann cell medium
	4 ml FCS
	2 ml DMSO

3.1.6.2 Media for the cultivation of *E. coli*

Medium	**Supplier/composition**
Luria Broth (LB) medium	1.0 % (w/v) bacto trypton 0.5 % (w/v) yeast extract 0.5 % (w/v) NaCl ad 1000 ml ddH_2O
LB agar	1.5 % (w/v) bactoagar in LB
LB with ampicillin	50 µg/ml ampicillin in LB
LB with kanamycin	50 µg/ml kanamycin in LB
LB agar with ampicillin	50 µg/ml ampicillin in LB agar
LB agar with kanamycin	50 µg/ml kanamycin in LB agar
SOC medium	Invitrogen

3.1.7 Antibiotics

Antibiotic	Supplier
Ampicillin (stock 50 mg/ml in H2O)	Roche
Hygromycin B (50mg/ml)	Invitrogen Thermo Fisher Scientific
Kanamycin (stock 50 mg/ml in H2O)	Sigma-Aldrich
Penicillin/streptomycine, 5000 U/ml	Gibco Thermo Fisher Scientific

3.1.8 Molecular weight standards

Standard	Supplier
MagicMark XP Western Protein Standard	Novex Thermo Fisher Scientific
Novex Sharp Pre-stained Protein Standard	Novex Thermo Fisher Scientific
TrackIt 1 Kb Plus DNA Ladder	Invitrogen Thermo Fisher Scientific

3.1.9 Vectors

Vectors	Supplier	Sequence (Species)
pcDNA3.1/hyg-citrine	see Heinen et al., 2008a	
pCMV6-Entry	OriGene	
pCMV6-Entry-cDNA-CD64 (pCD64)	OriGene	1059 nucleotides Fcgr1a cDNA (*Rattus norvegicus*)
pSUPER	OligoEngine	
pSUPER-kip2	see Heinen et al., 2008a	64 nucleotides p57kip2 insert (*Rattus norvegicus*)

3.1.10 Kits

Kit	Supplier
5-Bromo-2′-deoxy-uridine Labeling and Detection Kit I	Roche
Bacis Glial Cell Nucleofector Kit	Lonza
DC Protein Assay	Bio-Rad
EndoFree Plasmid Maxi Kit	QIAGEN
High-Capacity cDNA Reverse Transcription Kit with RNase Inhibitor	Applied Biosystems Thermo Fisher Scientific
IL-18 ELISA Kit, Rat	Novex Thermo Fisher Scientific
RNase Free DNase Set	QIAGEN
RNeasy Mini Kit	QIAGEN
Slide-A-Lyzer Dialysis Cassettes, 3.5K MWCO, 0.5-3ml	Thermo Scientific Thermo Fisher Scientific
Slide-A-Lyzer Dialysis Cassettes, 3.5K MWCO, 3-12ml	Thermo Scientific Thermo Fisher Scientific

SuperSignal West Pico Chemiluminescent Substrate	Thermo Scientific Thermo Fisher Scientific

3.1.11 Technical devices and software

Technical device/software	Supplier
Axioplan 2 Fluorescence microscope	Zeiss
Axiovision 4.2 software	Zeiss
BioPhotometer	Eppendorf
E.A.S.Y. RH transilluminator	Herolab
EBA 12R table top centrifuge	Hettich
Eppendorf Centrifuge 5804	Eppendorf
GeneAmp® PCR System 9700	Applied Biosystems Thermo Fisher Scientific
GSA rotor	Sorvall
HAT Minitron shaker incubator	Infors HAT
Heraeus Hera Safe incubator BBD 6220	Thermo Fisher Scientific
ImageJ software	National Institutes of Health
Infinite M200 Pro plate reader	TECAN
Lonza Nucleofector II device	Lonza
NanoDrop 1000 spectral photometer	Thermo Fisher Scientific
Nikon Eclipse TE 200 microscope	Nikon Instruments Europe BV
NIS-Elements AR 3.10 software	Nikon Instruments Europe BV
Odyssey infrared imaging system scanner	LI-COR Biosciences
Odyssey software	LI-COR Biosciences
Power Pac200 Power supply	BioRad
Primer express software	Applied Biosystems Thermo Fisher Scientific
RC-5B Plus centrifuge	Sorvall
RunBlue Dual Run&Blot Unit	Expedeon, BIOZOL
Sonifier Cell Disrubtor B15	Branson
Table top centrifuge 5417C	Eppendorf
Thermomixer comfort	Eppendorf
Veriti Thermal Cycler	Applied Biosystems Thermo Fisher Scientific

3.2 Molecular biological methods

3.2.1 Transformation of plasmids into *E. coli*

Transformation was performed using One Shot® TOP10 *E. coli* strain (Invitrogen). The chemically competent cells were transformed with plasmid desoxyribonucleic acid (DNA) according to the specifications of the supplier with slight changes in the used volumes. 25 µl

of the competent cells were thawed on ice and mixed with maximum 100 ng plasmid DNA (≥ 1/10 of the total reaction volume). Cells were incubated on ice for 30 min and after that heat shock was performed for 30 sec at 42°C. 125 µl pre-warmed SOC medium were added to the cells and then incubated for 1 hour (h) at 225 rounds per minute (rpm) in a shaking incubator. 10 µl of each cell suspension were plated on pre-warmed Luria-Bertani (LB) agar plates and these were incubated inverted at 37°C overnight. Selection was performed by adding the corresponding antibiotics to the LB agar medium prior plate preparation.

3.2.2 Glycerol stocks

Transformed bacteria can be stored by generating glycerol stocks. Single bacterial colony was picked from the LB plate of the transformed bacteria and incubated at 37°C for 6-8 h in 3 ml LB medium with the corresponding antibiotics. Alternatively, bacteria enriched LB medium can be taken directly from the overnight culture before the plasmid maxi preparation (see 3.2.3.2). 500 µl of bacteria enriched LB medium was mixed with 500 µl of 50 % glycerol solution (v/v) (prepared with Ampuva H_2O, sterile filtered) and then immediately frozen on dry ice. Transformed bacteria were stored at -80°C.

3.2.3 Isolation of nucleic acids

3.2.3.1 Bacterial culture preparation for plasmid DNA isolation

Following plasmid transformation, single colonies were picked with a sterile toothpick and transferred into a 14 ml polypropylene round bottom falcon tube (Becton Dickinson) filled with 3 ml LB medium containing antibiotics dependent on the encoded plasmid resistance. Incubation was performed for 6-8 h in a shaking incubator at 37°C and 225 rpm. After incubation, 200 µl of the bacteria enriched LB medium was transferred to 200 ml fresh LB medium (with antibiotics) for overnight culture. Incubation was performed for 14-16 h in a shaking incubator at 37°C and 225 rpm. Following incubation, glycerol stocks were prepared (see 3.2.2). Otherwise the bacteria enriched medium was centrifuged in 200 ml plastic tubes at 6000xg and 4°C for 15 min in a GSA rotor (Sorvall).

3.2.3.2 Isolation of plasmid DNA

For isolation of endotoxin free plasmid DNA the EndoFree Plasmid Maxi Kit (QIAGEN) was used). All steps for plasmid DNA isolation were performed according to the protocol of the supplier. Plasmid DNA was dissolved in 200-500 µl (depending on the pellet size) nuclease-free water (H_2O). DNA concentration was adjusted to 1 µg/µl, aliquoted and stored at -20°C.

3.2.3.3 Restriction digestion of plasmid DNA

Restriction enzyme digestion was performed in order to identify if the correct plasmid DNA was isolated or if the plasmid contains a specific insert sequence. The reaction was performed as follows, according to the manufacturer's protocol (Fermentas FastDigest):

Components	Reaction volume (total 20 µl)
plasmid DNA	x µl (1 µg)
FastDigest enzyme	1.0 µl (1-5 units per µg plasmid DNA)
10x FastDigest green buffer	2 µl
Nuclease free H_2O	ad 20 µl

3.2.3.4 Agarose gel electrophoresis

Following restriction digestion the fragmented plasmid DNA was analysed by agarose gel electrophoresis. 1-2 % (w/v) agarose gels were prepared depending on the size of the designated fragments to be separated. Agarose (Sigma-Aldrich) was weight and the corresponding volume 1x Tris-acetate-EDTA buffer (TAE) was added to the powder. The solution was brought to boil in a microwave oven in order to dissolve the agarose. After cooling down to 60°C, 5 µl ethidium bromide or Roti-GelStain (Carl ROTH) were added per 100 ml agarose solution. The agarose solution was led to polymerize in a gel rack and then transferred into a tank filled with 1x TAE buffer. Each sample was mixed with 10x BlueJuice gel loading buffer (1x final concentration; Invitrogen) and 8-10 µl TrackIt 1 Kb Plus DNA ladder (Invitrogen) was applied for each gel. Electrophoresis was performed at 100-120 volts (V) for approximately 30-60 min. The separated DNA fragments were detected using a ultra violet (UV) transilluminator (Herolab) and documented using a CSC camera.

3.2.3.5 Preparation of total RNA[10]

Prior cell lysis, the Schwann cells were washed three times with Dulbecco´s phosphate buffered saline (PBS; Sigma-Aldrich). 350 µl RLT lysis buffer (QIAGEN) was supplemented with 0.1 M β-mercaptoethanol (dilution 1:100) and added to the cells. Cells debris were scraped, and used immediately or frozen on dry ice and then stored at -20°C. Total RNA (ribonucleic acid) from cultured rat Schwann cells was isolated using the RNeasy Mini Kit (QIAGEN). All steps were performed according to the protocol of the supplier. After the first step of washing with 350 µl RW1 buffer (QIAGEN) an additional step was added to avoid contamination with genomic DNA. On each spin column 80 µl deoxyribonuclease (DNAse) solution was added, contained 10 µl DNAse (prepared from RNase Free DNase Set;

[10] for authorship notice please refer to chapter 9.2

QIAGEN) and 70 µl RDD buffer (QIAGEN) and incubated for 15 min at room temperature (RT). Then the protocol was preceded with the second washing step with RW1 buffer. RNA Elution was done by adding 31 µl ribonuclease (RNase) free H_2O (QIAGEN) to the center of each column and incubating for 5 min at RT. Finally, the columns were spun down at 10.000 rpm for 2 min. RNA was stored at -20°C on a short-term and -80°C for a long-term.

3.2.3.6 Determination of nucleic acid concentration

Concentration determination of total RNA and plasmid DNA was performed by NanoDrop 1000 spectral photometer (Thermo Scientific). Measurements were done using 1 µl of undiluted nucleic acid samples. RNase free H_2O was used as reference. Plasmid DNA concentration was adjusted to 1 µg/µl for transfection purpose with nuclease-free H_2O.

3.2.4 Reverse transcription of total RNA[11]

The isolated RNA (see 3.2.3.5) was reverse transcribed using the High-Capacity cDNA Reverse Transcription Kit with RNase Inhibitor (Applied Biosystems) according to the specifications of the supplier. For each reverse transcription, maximal 250 ng of total RNA were used in a 30 µl total reaction volume. Reverse transcription was then performed in Veriti Thermal Cycler (Applied Biosystems) by applying the following steps: Step 1 for 10 min at 25°C, Step 2 for 120 min at 37°C, Step 3 for 5 sec at 85°C, Step 4 for process termination at 4°C. Finally, copy DNA (cDNA) was diluted to a total volume of 200 µl for quantitative real-time polymerase chain reaction (PCR) purposes.

Components	Reaction volume (total 30 µl)
10x RT buffer	3.0 µl
10x RT random primers	3.0 µl
25x dNTP mix (100 mM)	1.2 µl
RNase inhibitor	1.5 µl
MultiScribe reverse transcriptase, 50 U/µl	1.5 µl
250 ng total RNA	x µl
RNase free H2O	ad 30 µl

3.2.5 Quantitative real time PCR (qRT-PCR)[12]

Prior to the quantification, RNA was reverse transcribed into cDNA (see 3.2.4). Real time PCR amplification and quantification was performed using the Power Sybr Green Mastermix

[11] for authorship notice please refer to chapter 9.2
[12] for authorship notice please refer to chapter 9.2

(Applied Biosystems) according to the manufacturer's protocol with each primer at a final concentration of 0.30 pmol on GeneAmp PCR System 9700 (Applied Biosystems). The default two-step amplification profile used was 45 cycles of 15 seconds at 95°C and 1 minute at 60°C. Glyceraldehyde-3-phosphate dehydrogenase (GAPDH) and ornithine decarboxylase (ODC) were used as endogenous reference genes and relative gene expression levels were determined according to the ΔΔCt method (Applied Biosystems). Each cDNA sample was measured in duplicates.

Components	Reaction volume (total 30 µl)
cDNA sample	5.0 µl
SybrGreen Mix	15.0 µl
forward primer	1.8 µl
reverse primer	1.8 µl
LiChrosolv H_2O	6.4 µl

The oligonucleotide sequences, used as qRT-PCR amplification primers, were designed using PrimerExpress 2.0 software (Applied Biosystems). Synthetic oligonucleotides were manufactured by MWG Biotech and delivered in a lyophilized state. 100 pmol stock solutions were prepared by dissolving the oligonucleotides in LiChrosolv H_2O (Merck) according to datasheet information, provided by MWG Biotech. For the qRT-PCR reaction working stock solutions of 5 pmol were used (1:20 dilution of the 100 pmol stock solution in LiChrosolv H_2O). Following primers were applied in the qRT-PCR:

Primer name	Forward sequence	Reverse sequence
CD16/Fcgr3a_1	CCA TGC AGA CTG GCT ATT GCT	GGG TCC CCC TCC TGG AA
CD16/Fcgr3a_2	CGA CGT CTC CCT CCA GCT T	AGA GTC CTA TCA GCA GGC AGA AA
CD32a/Fcgr2a_1	AGC ATA CAG CTG GCC AGG AT	AGA TGG AGT AGC TAA CAT TAT AAG GAT GA
CD32b/Fcgr2b_1	GCT GAG AAA AAT GAG GTG GAG AA	CCG GAG CTT CAG GAT GCT T
CD64/Fcgr1a_1	TGG ATC ATA CTG GTG CGA GGT A	TTG GTG CTG CGC TTA AGG A
CD64/Fcgr1a_2	GGG AGT CTG GTC ATC CTG AAC T	AAA GCC GTA AGC CAG GAC TCT
Syk_1	GGA GAG CAA TTT TGT GCA CAG A	CGT AGT GCT GGG TGA CCA GAA
Syk_2	GTG CGC ATG ATC GGA ATC T	GCC ATC TCC ATC ACC AGC AT
P0/Mpz	ACC TTC AAG GAG CGC ATC C	GCC ATC CTT CCA GCT AGG GT
MBP	CAA TGG ACC CGA CAG GAA AC	TGG CAT CTC CAG CGT GTT C
Prx	CGC CCG TGT GTT CTT TGA G	AGG GCT CGG CAC ATT GC
Pmp22	GCG GAA CAC TTG ACC CTG AA	TCA TTT AAA CAT GTG GCC CCA
Pmp2	TGC AGA AGT GGG ATG GTA AAG A	TCC ACT ACC ATT TTC CCA TCC A
Plp1	CTT TGG AGC GGG TGT GTC AT	TGT CGG GAT GTC CTA GCC AT
Cx32	CCT CCG GCA TCT GCA TTA TC	AGG CCC GGA TGA TGA GGT A

Mag	CGC CTT TGC CAT CCT GAT T	TGT GAC GTT CTT TTT TCT TCT TGT CT
Sox10	GCA GGC TGG ACA CTA AAC CC	GTG CGA GGC AAA GGT AGA CTG
Krox20/Egr2	TTT TTC CAT CTC CGT GCC A	GAA CGG CTT TCG ATC AGG G
Oct6	GGC ACC CTC TAC GGT AAT GTG T	TTG AGC AGC GGT TTG AGC T
p57kip2	CAG GAC GAG AAT CAG GAG CTG A	TTG GCG AAG AAG TCG TTC G
Tyrp1_1	CTT CGT CAG GGC CTT GGA	GCA ATG ACA AAT TGA GGG TGA GT
Tyrp1_2	GGC TCA GTT TCC ACG AGA ATG	GGG VAA CAC ACC CCA CTT C
Olig1_1	ATG CAG GAC CTG AAC TTG GC	GGG TAG GAT AAC TTC GCG CAG
Olig1_2	ACA TCA AGG GTG TTG CCG A	GAC ACC GGA CTC TGG GCT T
IL-18	TGT GTT CGA GGA CAT GCC TG	GTC TGG GAT TCG TTG GCT GT
Mcp-1	ATG ATC CCA ATG AGT CGG CT	CCT GCT GCT GGT GAT TCT CTT
GAPDH	GAA CGG GAA GCT CAC TGG C	GCA TGT CAG ATC CAC AAC GG
ODC	GGT TCC AGA GGC CAA ACA TC	GTT GCC ACA TTG ACC GTG AC

3.2.6 SDS gel electrophoresis and Western blot analysis[13]

3.2.6.1 Isolation of soluble proteins

For the purpose of soluble protein isolation $2.5x10^6$ - $3x10^6$ Schwann cell were seeded on one ø (diameter) 100 mm dish. Non-differentiating Schwann cells were stimulated for 1 day with IVIG/buffer control treated, whereas differentiating (p57kip2 suppressed and control transfected) cells were stimulated for 7 days IVIG/buffer control. Per each condition, 5.10^6 cells (two ø 100 mm dishes) were used. When treatment was terminated, cells were washed three times with PBS and each dish was incubated with 2 ml 0.05 % trypsin (Gibco) at 37°C for maximal 3 min. The reaction was stopped with 10 ml Schwann cell medium per dish, cells were scraped gently, collected in 30 ml tubes and centrifuged at 1500 rpm, at RT for 5 min. The harvested pellets were washed three times with PBS (once with 20 ml PBS, then two times with 10 ml PBS) by centrifugation at 1500 rpm, at 4°C for 5 min, and were either used directly or frozen on dry ice and then stored at -80°C for further analysis.

Harvested cell pellets were lysed on ice with 1x RIPA buffer for 5-10 min (Cell Signaling Technology) according to the specifications of the manufacturer. Prior use, RIPA buffer was supplemented with 1x Halt protease and 1x Halt phosphatase inhibitor cocktails, with addition of 1x Ethylenediaminetetraacetic acid (EDTA) (all Thermo Scientific). Whole cell lysates were subjected to two sonification cycles of once 10 sec and once 15 sec, while stored on ice for 1-2 min between cycles; sonifyer settings: cycle at 5x (10 %), power at 50 %. Lysates were then centrifuged at 14.000xg, 4°C for 10 min to obtain the soluble protein fraction. Samples were either frozen on dry ice (then stored at -80°C), or used directly

[13] for authorship notice please refer to chapter 9.2

for further analysis. Protein concentrations were determined using the DC Protein Assay (Bio-Rad) following the guidelines for microplate assay protocol according to the manufacturer's protocol. Prior concentration determination, the protein samples were diluted 1:5 with supplemented RIPA buffer. After 15 min incubation, the protein concentration was measured on an Infinite M200 Pro plate reader (TECAN) at 750 nm.

3.2.6.2 SDS PAGE

For the purpose of SDS PAGE (sodium dodecyl sulfate polyacrylamide gel electrophoresis) analysis, protein samples were mixed with 1x NuPAGE LDS Sample Buffer (Novex) and 1x NuPAGE Sample Reducing Agent (Novex). Protein lysates were heated at 90°C for 5 min. The following protein standards were used once per each gel: 3.5 µl MagicMark XP Western Protein Standard and 8 µl Novex Sharp Pre-stained Protein Standard (all Novex). Samples (20-30 µg protein per lane) were subjected to standard SDS PAGE using 4-12 % RunBlue SDS gel (Expedeon). The gels run was performed on a RunBlue Dual Run&Blot unit (Expedeon) in 1x RunBlue RAPID SDS run buffer (Expedeon) at 50-60 milliampere (mA) per gel starting current, and 45 mA/gel ending current, for 70-90 min using Power Pac200 Power supply (BioRad).

3.2.6.3 Western blot

SDS PAGE separated proteins were transferred onto RunBlue Blot Sandwich nitrocellulose membranes (Expedeon) by electroblotting using 1x RunBlue TGS Blot buffer (Expedeon) with 20 % methanol (Merck) at 200 V for 1 h in the RunBlue Dual Run&Blot unit. To verify successful protein transfer and note the position of the marker, the nitrocellulose membrane was stained for 1-2 min in Ponceau S staining solution (Sigma-Aldrich) and destained first in double-distilled water (ddH_2O) and then in 1x Tris buffered saline (TBS). Membranes were blocked with 1-2 % milk powder (Carl ROTH) in TBS or Starting block (in PBS; Thermo Scientific) for 1h at RT, depending on the used antibody. After the blocking procedure membranes were incubated with primary antibodies overnight at 4°C by slightly shaking. Upon primary antibody incubation, the membranes were washed four times with TBS with 0.05 % Tween (TBST) for 5 min by slightly shaking. Incubation with secondary antibodies was performed for 2 h at RT, in the dark, by slightly shaking. As antibody diluent the corresponding blocking buffers in TBST for milk powder, or PBS with 0.05 % Tween (PBST) for Starting block were prepared. Following primary and secondary antibodies were used:

Antibody	Supplier	Dilution
goat anti-CD64	R&D Systems	1:1000
rabbit anti-CD64	BIOSS	1:500
mouse anti-DDK/Flag tag	OriGene	1:1000
rabbit anti-Syk	Cell Signaling Technology	1:500
mouse anti-P0	(Archelos et al., 1993), kindly provided by Dr. M. Stettner	1:500
rabbit anti-MBP	Millipore	1:500
rabbit anti-p38MAPK	Cell Signaling Technology	1:1000
rabbit anti-phospho-p38MAPK	Cell Signaling Technology	1:400
rabbit ant-PTEN	Cell Signaling Technology	1:2000
rabbit anti-phospho-PTEN	Cell Signaling Technology	1:1000
rabbit anti-Akt	Cell Signaling Technology	1:4000
rabbit anti-phospho-Akt	Cell Signaling Technology	1:500
rabbit anti-cJun	Cell Signaling Technology	1:1000
rabbit anti-phospho-cJun	Cell Signaling Technology	1:500
mouse anti-actin	Becton-Dickinson	1:1000
mouse anti-GAPDH	Millipore	1:1000 Odyssey detection
mouse anti-GAPDH	Millipore	1:4000 HRP detection
goat anti-rabbit IgG, HRP-linked	Cell Signaling Technology	1:2000
peroxidase horse anti-mouse IgG	VECTOR Laboratories	1:5000
peroxidase horse anti-goat IgG	VECTOR Laboratories	1:2000
IRDye 800CW donkey anti-mouse IgG	LI-COR Biosciences	1:15000
IRDye 800CW goat anti-rabbit IgG	LI-COR Biosciences	1:10000

3.2.6.4 Signal detection

After incubation with secondary antibodies, membranes were washed four times with TBST for 5 min by slightly shaking. Membranes were kept in the dark the whole time. Visualization of signals using IRDye 800CW secondary antibodies was done on an Odyssey infrared imaging system scanner (all LI-COR Biosciences). For visualization of signals using peroxidase-labeled (VECTOR Laboratories) or horse-radish-peroxidase (HRP)-linked antibodies (Cell Signaling Technology) secondary antibodies, nitrocellulose membranes were incubated for 5 min with SuperSignal West Pico Chemiluminescent Substrate (Thermo Scientific) according to the manufacturer's protocol. Membranes were then exposed to Amersham Hyperfilm ECL (GE Healthcare) to detect the HRP signal. Protein band quantifications were performed using the Odyssey software. The intensity for each band was determined and normalized to the intensity of the GAPDH band of the corresponding probe.

3.2.7 GeneChip Array analysis

In order to identify further transcriptional changes induced by IVIG treatment in rat Schwann cells a GeneChip Array analysis was performed on differentiation competent (p57kip2 suppressed) and control transfected (pSUPER transfected) cells, which have been stimulated by IVIG or buffer control for 7 days (see 3.3.5). Each experiment used for the array analysis comprised four samples: pSUPER transfected Schwann cells stimulated with buffer control; pSUPER transfected Schwann cells stimulated with IVIG; p57kip2 suppressed Schwann cells stimulated with buffer control; p57kip2 suppressed Schwann cells stimulated with IVIG. Total RNA samples from four independent experiments were adjusted to a concentration of 50 ng/µl. In total, 550 ng RNA per sample were sent for analysis. Gene expression analysis with all 16 rat RNA samples was performed by Miltenyi Biotec using one color Agilent Whole Rat Genome Oligo Microarrays (Agilent Technologies) according to the manufacturer's protocol. Ratio building, data pre-processing, statistical analysis, and functional discriminatory gene analysis (DGA) was done by Miltenyi Biotec. Statistical analysis was carried out via Student's *t*-test. Multiple testing correction was performed by the method of Benjamini and Hochberg (Benjamini, 1995). The threshold to which genes were considered significantly regulated were higher than 2.0 (fold-change) and smaller than 0.01 (*p*-values).

3.3 Cell culture methods[14]

3.3.1 Coating of flasks and cell culture dishes

For cultivation of Schwann cell on culture flasks, dishes and multiwall plates surface coating was performed with 0.1 mg/ml sterile filtered poly-D-lysine solution (PDL; Sigma-Aldrich) in PBS over night at 4°C. Plastic surfaces were then washed three times with PBS before cell plating. For staining analysis of Schwann cells, ø 15 mm microscope cover glasses (Assistant) in a 12 well cell culture multiwell plate (Greiner bio-one) were coated with 0.1 mg/ml PDL and incubated over night at 4°C. Microscope cover glasses were then washed three times with PBS before cell plating.

DRG explants were cultivated as follows: two pieces of DRG explants were seeded on 1 mg/ml PDL coated ø 13 mm microscope cover glasses in a 24 well cell culture multiwell plate (Greiner bio-one). After 24 h the plates were washed three times with PBS and then each cover glass was coated with 500 µl laminin (end concentration 13 µg/ml in PBS). Laminin coating was let to dry under sterile laminar flow for 24 h at RT.

[14] for authorship notice please refer to chapter 9.2

Myelinating neuron/glia dissociation cocultures were cultivated on 2-well cell culture slides (Sarstedt). These were coated with collagen, 1:7 diluted with 0.02 N acetic acid, and let to dry for 30 min at RT under sterile laminar flow.

3.3.2 Immunoglobulin preparations

3.3.2.1 Immunoglobulin specifications

Gammagard Liquid [Immune Globulin Intravenous (Human)] 10 % containing 100 mg/ml protein lot LE12J270AB (Baxter Healthcare Corporation) was used in the majority of the experiments. Of note, two further IVIG lots (IVIG2: LE12L068AB and IVIG3: LE12L341AA, all Baxter Healthcare Corporation) were tested and showed similar results in binding assays and functional analyses. In all experiments, IVIG lot LE12J270AB were used at a final concentration of 20 mg/ml protein in Schwann cell medium. IVIG2 lot LE12L068AB and IVIG3 lot LE12L341AA were used at final concentrations of 10 mg/ml or 5 mg/ml protein in Schwann cell medium. Gammagard Liquid formulation buffer (0.25 M glycine, pH 4.5) was included as a control and used in the same dilutions as the corresponding IVIG preparations. $F(ab')_2$ fragments (Fragment, antigen-binding, including hinge region/both arms) were generated by Baxter Healthcare Corporation from Gammagard Liquid (lot LE12L341AA) as follows: IVIG3 was incubated with pepsin (Sigma-Aldrich) at pH 4 and 37°C under pyrogenic-free conditions. The reaction was halted by changing to pH 7, then the $F(ab')_2$ fragments were purified using size exclusion chromatography, filtered and adjusted to a final concentration of 31 mg/ml in 0.25 M glycine buffer, pH 4.5. The resulting $F(ab')_2$ fraction revealed an endotoxin concentration of 0.436 EU/ml and 2.3 % of Fc binding in comparison to IVIG was determined. Purified $F(ab')_2$ fragments were applied at a final equimolar concentration of 3.65 mg/ml $F(ab')_2$, corresponding to 5 mg/ml IVIG3. The low molar concentration was used to prevent aggregate formation. The following human monoclonal antibodies were used as IgG1 controls: Avastin (Roche Pharma), Herceptin (Roche Pharma) and Synagis (Abbott SRL) all at final concentrations of 20 mg/ml. All above mentioned immunoglobulin preparations were kindly provided by Baxter Healthcare Corporation.

3.3.2.2 Dialysis of immunoglobulins

Prior to cell culture application all immunoglobulin preparations (IVIG, $F(ab')_2$, IgG1), as well as the corresponding control buffer, were dialysed over night at 4°C to 200x-500x volume of non-supplemented DMEM using Slide-A-Lyzer Dialysis Cassette 3.5 K MWCO (molecular weight cut-off 3.5 K; Thermo Scientific) according to the manufacturer's protocol. Dialysis was performed for 24 h altogether with one medium exchanged with fresh non-supplemented DMEM after the first 6 h. Dialysis was done in order to balance minor effects, which resulted

from the IVIG formulation buffer. All immunoglobulin preparations were stored at 4°C post dialysis and used for cell culture applications shortly after. If longer storage was required, it did not exceed 2 weeks. Of note, the distribution of IgG monomers, dimers, and oligomers was analyzed in IVIG preparations before and after dialysis by size exclusion chromatography (SEC-HPLC). The SEC-HPLC analysis was performed by Baxter Healthcare Corporation. An average of 89.35 ±1.16 % monomers, 10.53 ±1.14 % dimers and 0.12 ±0.02 % oligomers was found, which changed to 87.32 ±1.97 % monomers, 12.78 ±1.66 % dimers and 0.15 ±0.05 % oligomers after dialysis and subsequent storage of IVIG in cell culture media for one to seven weeks. However, a number of initial experiments were performed with non-dialysed IVIG and revealed them to be as effective as dialysed ones regarding proliferation, gene expression, and morphological maturation.

3.3.2.3 Cell culture application

For the purpose of IVIG (all lots), IgG1 controls and buffer control binding studies, 120.000 Schwann cells per condition were seeded on ø 15 mm 0.1 mg/ml PDL coated microscope cover glasses in a 12 well cell culture multiwell plate in Schwann cell medium. One day after plating, Schwann cells were decorated with IVIG and control buffer for 24 h in culture. Decoration of Schwann cells with purified $F(ab')_2$ fragments was performed for 4 h. Cells were then fixed with 4 % paraformaldehyde (PFA; Merck) and subjected to immunostaining (see 3.3.9).

Short-term gene expression analysis of non-differentiating Schwann cells was done on 100.000-150.000 cells (per condition) seeded on 0.1 mg/ml PDL coated 12 well cell culture multiwell plates. Stimulation with IVIG (all lots), IgG1 controls and buffer control was performed one day after cell plating for a period of 1 and 3 days. Stimulation of Schwann cells with purified $F(ab')_2$ fragments was performed for 1 day only. For protein expression analysis, $2x10^6$ Schwann cells per condition were seeded on ø 100 mm dishes. 24 h after cell plating, IVIG/buffer control stimulation was undertaken for 1 day.

Long-term IVIG/buffer control treatment was performed on differentiating competent Schwann cells transfected with p57kip2 suppression and control vectors (see 3.3.5). For gene and protein expression analysis, $2.5x10^6$ or $5x10^6$ transfected cells, respectively, were seeded per condition on ø 100 mm dishes. For staining analysis approximately 150.000-200.000 transfected cells per condition were seeded on ø 15 mm microscope cover glasses in 12 well cell culture multiwell plates. Cells were subjected to 7 days IVIG/buffer control treatment in Schwann cell medium with 50 µg/ml hygromycin B (Invitrogen); while IVIG/buffer control stimulation was initiated 2 days post transfection. Medium was exchanged at day 4 after treatment and consisted of Schwann cell medium with IVIG/buffer control,

supplemented with 50 µg/ml hygromycin B. All further IVIG/buffer control cell culture applications have been described in the corresponding chapters.

3.3.3 Preparation of primary rat Schwann cells

Primary rat Schwann cells were dissected from sciatic nerves of P0 Wistar rats according to the protocol of (Brockes et al., 1979). Nerves were cut into small pieces, transferred into a 50 ml tube containing DMEM medium and centrifuged at 2000 rpm for 5 min (Eppendorf Centrifuge 5804). Cell pellets were digested with 0.05 % trypsin and 0.6 % collagenase (Sigma-Aldrich) mix for 60 min at 37°C and the reaction was stopped with Schwann cell medium. The cell suspension was centrifuged at 1500 rpm for 5 min and cell pellets were carefully resuspended in Schwann cell medium, followed filtration through a 60 µm filter. The cell filtrate was filled up with Schwann cell medium and centrifuged in a 50 ml tube at 1500 rpm for 5 min. Cell pellets were again resuspended in Schwann cell medium and were then transferred into an uncoated 25 cm² cell culture flask (T25 flask; Greiner bio-one) in 5 ml total medium volume. After 24 h incubation at 37°C, 98 % humidity and 10 % CO_2, 10 µM arabinosyl cytosine (AraC) was added to the culture medium and treatment was performed for 7 days, with medium exchange every second day. After 7 days, complement lysis was performed to eliminate fibroblasts. Schwann cells were detached from the T25 flask using 3 ml 0.05 trypsin at 37°C. The reaction was stopped by adding 8 ml Schwann cell medium and cells were then centrifuged at 1800 rpm for 5 min. Cell pellet was resuspended in 2 ml baby rabbit complement (BIOZOL) supplemented with mouse anti-THY1 antibodies (AbD Serotech) and was then incubated for 20 min at 37°C. Complement lysis was stopped by addition of 7 ml Schwann cell medium and cells were then centrifuged at 1800 rpm for 5 min. Cells pellets were resuspended in 5 ml Schwann cell proliferation medium and transferred into a PDL coated T25 flask. Medium was exchanged every second day with proliferation medium. After reaching confluence, an additional complement lysis was performed and cells were then transferred into a PDL coated 75 cm² cell culture flask (T75 flask; Greiner bio-one) with 20 ml total volume of proliferation medium. Cells were further propagated and distributed into four and later into eight PDL coated T75 flasks.

Schwann cells were then prepared for cryopreservation. Confluent cells were detached from the T75 flask by applying 4 ml prewarmed (37°C) 0.05 % trypsin for 2 min at 37°C. The reaction was stopped by addition of 20 ml Schwann cell medium and cells were centrifuged at 1500 rpm for 5 min. Cell pellets were resuspended in 500 µl Schwann cell medium and then carefully mixed with 500 µl Schwann cell cryopreservation medium. Cells were immediately frozen at -80°C and 24 h after freezing cells were transferred to and stored in liquid nitrogen.

3.3.4 Culturing of primary rat Schwann cells

For cultivation, primary rat Schwann cells (see chapter 3.3.3) were thawed, transferred into 50 ml Schwann cell medium and centrifuged at 1500 rpm for 5 min. Cell pellets were resuspended in 20 ml Schwann cell medium, freshly supplemented with 2 µM forskolin (Sigma-Aldrich). Cell cultivation was performed on PDL coated T75 culture flask at 37°C, 98 % humidity and 10 % CO_2. Medium was exchanged every second day with Schwann cell medium, freshly supplemented with 2 µM forskolin. Cell propagation was performed as follows: cells were washed three times with PBS, then treated with 4 ml prewarmed (37°C) 0.05 % trypsin and incubated at 37°C for 2 min. Trypsin reaction was stopped by addition of 20 ml Schwann cell medium and centrifugation at 1500 rpm for 5 min. Cell pellets were resuspended in 3 ml Schwann cell medium with 2 µM forskolin. The cells suspension was splitted into three PDL coated T75 culture flasks containing 20 ml Schwann cell medium with forskolin.

3.3.5 Transfection procedures

Transfections procedures were carried out by vector-based RNA interference (p57kip2 gene suppression) or vector-based cDNA expression (CD64/Fcgr1a overexpression) using the Bacis Glial Cell Nucleofector Kit (Lonza). Prior transfection the PDL coated ø 100 mm dishes were washed three times with PBS and 10 ml Schwann cell medium was added to each dish followed by medium equilibration at 37°C, 98 % humidity and 10 % CO_2. For the purpose of transfection, Schwann cells were collected by trypsinisation, counted and $5x10^6$ cells were distributed in separate tubes to be used per single transfection. The cells were centrifuged at 1200 rpm for 7 min and the supernatant was discarded. Cell pellets were then mixed with 100 µl nucleofector solution (Lonza) and 10 µg plasmid DNA. Cells were cotransfected with a vector of interest and pcDNA3.1/hyg-citrine vector in a 9:1 ratio. The plasmid combinations are listed below:

1 µg pcDNA3.1/hyg-citrine + 9 µg pSUPER (control vector)
1 µg pcDNA3.1/hyg-citrine + 9 µg pSUPER-kip2 (p57kip2 gene suppression vector)
0.5 µg pcDNA3.1/hyg-citrine + 4.5 µg pCMV-6-Enrty (control vector)
0.5 µg pcDNA3.1/hyg-citrine + 4.5 µg pCMV6-Entry-cDNA-CD64 (CD64/Fcgr1a overexpression vector)

The pcDNA3.1/hyg-citrine vector was used for cotransfection as it allows the selection of the transfected cells with hygromycin B and their identification via citrine (green fluorescent protein) expression. The DNA-cell mixture was then subjected to nucleofection using Lonza Nucleofector II device (Lonza). Prewarmed Schwann cell medium (1 ml) was added to the transfected cells and after that the cell suspension was distributed equally to two ø 100 mm dishes (500 µl or $2.5x10^6$ cells per dish). Cells were incubated at 37°C, 98 % humidity and 10 % CO_2. For all conditions, Schwann cell medium was exchanged by selection medium with hygromycin B (final concentration 50 µg/ml) 24 h after transfection.

For cells transfected with pSUPER-kip2 and control vectors the second medium exchange with selection medium containing IVIG/buffer control was undertaken 2 days after transfection. Next medium exchange (selection medium with IVIG/buffer control) was performed 6 days after transfection (4 days IVIG/buffer control stimulation). Cells were harvested or stained for further investigations at day 9 after transfection (7 days IVIG/buffer control stimulation).

The second medium exchanged for Schwann cells transfected with pCMV6-Entry-cDNA-CD64 overexpressing and control vectors was performed on the second and the fourth day after transfection with selection medium. Cells were harvested or stained for further investigations at 5 days after transfection.

3.3.6 Culturing of mouse myelinating neuron/glia dissociation cocultures

Mouse DRG cultures were prepared from embryonic day 15 (E15) C57BL6 mouse embryos according to the protocol described in (Päiväläinen et al., 2008). All embryos were separated from the mouse uterus and stored in Leibovitz's medium (L15 medium; Gibco) on ice during the dissection procedure. DRGs of six embryos (approximately 15 DRGs per embryo) were collected as explants in 2 separate 30 ml tubes filled with L15 medium and then centrifuged at 1500 rpm for 5 min. DRG tissue dissociation was performed in 0.05 % trypsin and 0.05 % collagenase for 20 min at 37°C. Dissociated DRGs were resuspended in 40 µg/ml Deoxyribonuclease I (DNase; Sigma-Aldrich) diluted in L15 medium, and the digestion was stopped with L15 medium containing 10 % heat inactivated horse serum (HS; Gibco). The cell suspension was centrifuged at 190xg for 5 min and then washed two times by further centrifugation (5 min, 190xg) and resuspension in 10 ml of L15 medium containing 10 % HS. For each condition approximately 500.000 cells were seeded onto one collagen (Becton-Dickinson) coated 2-well cell culture slide and incubated in growth medium at 37°C, 98 % humidity 10 % CO_2 for four to five days. Myelination was induced by changing to myelination medium supplemented with dialysed IVIG/buffer control. Treatment was performed for 7 days with one medium exchange at day 3 with myelination medium supplemented with IVIG/buffer

control. Cocultures were fixed at day 7 with 4 % PFA and stained against MBP and β-tubulin (TUJ1). MBP positive internodes were counted in both conditions and the average number was determined.

3.3.7 Culturing of rat dorsal root ganglion (DRG) explant cultures

DRGs were dissected from three E17/E18 Wistar rat embryos (around 15 DRGs per embryo) and stored in 0.6 % sucrose in PBS on ice. Each dissected DRG was cut into 2 to 4 explants and plated on PDL and laminin coated microscope cover glasses (see 3.3.1). Two DRG explants were then positioned carefully onto one cover glass with the help of a needle in the corresponding medium. Explants were cultured for 24 h as follows: (a) non-conditioned Schwann cell medium alone or supplemented with different concentrations of recombinant rat interleukin-18 (10 ng/ml, 25 ng/ml and 50 ng/ml rrIL-18; R&D Systems); (b) Schwann cell conditioned medium alone or of Schwann cells treated with 10 ng/ml, 25 ng/ml or 50 ng/ml rrIL-18 for 3 days; (c) conditioned medium of Schwann cells treated with either buffer control or IVIG preparations for 3 days. DRG explants were incubated at 37°C, 98 % humidity and 10 % CO_2.

After 24 h cell fixation was performed in culture medium, without washing: 600 µl 8 % PFA were added to 600 µl cell culture medium very carefully and incubated for 10 min at RT. DRG explants were then washed three times in PBS. Axons were visualized using neurofilament immunofluorescence staining. For quantification of axon outgrowth, microimages were taken (AxioVision software; Zeiss) and axonal length was measured from the borders of the inner DRG core to the maximal axon spread using ImageJ software (National Institutes of Health). Statistical analysis was performed by applying a student Student's *t*-test.

3.3.8 Preparation of Schwann cell conditioned medium

10^6 Schwann cells were seeded onto ø 100 mm dishes per condition in Schwann cell medium. After 4 h the medium was exchanged as follows for experiments with rrIL-18 Schwann cell conditioned medium: untreated cells + Schwann cell medium (control cells); untreated cells + Schwann cell medium supplemented with 10 ng/ml rrIL-18; untreated cells + Schwann cell medium supplemented with 25 ng/ml rrIL-18; untreated cells + Schwann cell medium supplemented with 50 ng/ml rrIL-18. For experiments with IVIG/buffer control Schwann cell conditioned medium: untreated cells + Schwann cell medium supplemented with IVIG; untreated cells + Schwann cell medium supplemented with buffer control. Schwann cells were incubated in these media for 3 days. After that the Schwann cell

conditioned medium was removed from the dishes and used directly for cultivating of rat DRG explant cultures (see 3.3.7).

3.3.9 Immunocytochemistry

Immunostaining on paraformaldehyde-fixed cultured Schwann cells, myelinating neuron/glia cocultures and DRG explants was performed as described below: Cells were washed three times with PBS, fixed for 10 min at RT with 4 % PFA and then again washed three times with PBS. Unspecific staining of surface antigens was blocked with normal rabbit serum (NRS; Invitrogen) or normal goat serum (NGS; Sigma-Aldrich). On the other hand, unspecific staining of intracellular proteins was blocked with the above-mentioned sera in the presence of Triton X-100 (Sigma-Aldrich) for cell permeabilisation. All different staining procedures are described in detail below. Blocking was performed for 40 min and cells were then incubated with primary antibodies in the corresponding buffers overnight at 4°C (primary antibodies are listed below). After 24h, cells were washed three times with PBS and then incubated with secondary antibodies in PBS for 2 h at RT (secondary antibodies are listed below). Cell nuclei were visualized by means of 4,6-diamidino-2-phenylindole (DAPI, Sigma) and microscope cover glasses were mounted using Citifluor mounting medium (Citifluor). Stained cell cultures were visualized using an Axioplan 2 fluorescence microscope (Zeiss) and Axiovision 4.2 software (Zeiss).

For surface staining against the CD64/Fcgr1 receptor cells were blocked in 2 % NRS, then incubated with primary antibody in 2 % NRS. CD64 overexpressing cells were blocked and incubated with primary antibody in 5 % NRS.

For intracellular Olig1 staining cells were blocked in 2 % NGS with 0.5 % Triton X-100, then incubated with primary antibody in 2 % NGS with 0.1 % Triton X-100.

Myelinating neuron/glia cocultures were blocked in 10 % NGS with 1 % Triton X-100 and incubated with primary antibodies in 10 % NGS with 0.1 % Triton X-100.

DRG explants were blocked in 5 % low background solution (Inotech Biosystems) with 0.1 % Triton X-100 and then incubated with primary antibody in the same blocking buffer.

Immunostaining for IVIG binding studies was performed as follows: living Schwann cells were decorated with IVIG and buffer control for 24h (see 3.3.2.3) and then fixed with 4 % PFA. Immunocytochemical staining and visualization was performed directly after cell fixation, without any blocking procedures, by applying Cy3- or Alexa Fluor 488-conjugated secondary antibodies specific to human $F(ab')_2$ or human Fcγ fragments in PBS for 4 h at RT.

For intracellular actin filament staining a phalloidin-tetramethylrhodamine B isothiocyanate (phalloidin-TRITC) conjugate was used. PFA fixed cells were dehydrated with cold acetone

(Merck) for 3 min at -20°C and then washed three times with PBS. Cell permeabilisation was performed with 0.1 % Triton X-100 for 10 min at RT. Following three times washing with PBS, cells were stained for 40 min at RT (in the dark) with 50 µg/ml phalloidin-TRITC (red fluorescence). Before mounting, cells were washed five times with PBS.

The following antibodies and reagents were used for the immunostaining procedures:

Antibody/ reagent	Supplier	Dilution
goat anti-CD64	R&D Systems	1:500
mouse anti-MBP	Covance	1:500
rabbit anti-β-tubulin	Covance	1:1000
mouse anti-neurofilament	Covance	1:1000
mouse anti-Olig1	Millipore	1:500
goat anti-rabbit IgG secondary antibody, Alexa Fluor 488 conjugate	Invitrogen Thermo Fisher Scientific	1:500
goat anti-rabbit IgG secondary antibody, Alexa Fluor 594 conjugate	Invitrogen Thermo Fisher Scientific	1:500
goat anti-mouse IgG secondary antibody, Alexa Fluor 488 conjugate	Invitrogen Thermo Fisher Scientific	1:500
goat anti-mouse IgG secondary antibody, Alexa Fluor 594 conjugate	Invitrogen Thermo Fisher Scientific	1:500
$F(ab')_2$-rabbit anti-goat IgG secondary antibody, Alexa Fluor® 594 conjugate	Invitrogen Thermo Fisher Scientific	1:500
Cy3 AffiniPure $F(ab')_2$ fragment goat anti-human IgG, $F(ab')_2$ fragment specific	Jackson ImmunoResearch	1:500
Alexa Fluor 488 AffiniPure $F(ab')_2$ fragment goat anti-human IgG, Fcγ Fragment Specific	Jackson ImmunoResearch	1:500
phalloidin-TRITC conjugate	Sigma-Aldrich	50 µg/ml

3.3.10 Proliferation assays

Cellular proliferation rates were determined either via 5-bromo-2´-deoxy-uridine (BrdU) incorporation using the 5-Bromo-2′-deoxy-uridine Labeling and Detection Kit I (Roche), or using anti-Ki67 immunostaining. 120.000 Schwann cells were seeded on ø 15 mm 0.1 mg/ml PDL coated microscope cover glasses in a 12 well cell culture multiwell plate. IVIG and buffer control we added to the culture medium 1 day after cell plating and stimulation was performed for 2 days altogether. BrdU application (10 µM final concentration) was done by adding the substance directly to the culture medium, and mixing carefully. Labeling with BrdU was undertaken for 8 h (40 h after cell plating and at the same time 8 h before experiment end) or 24 h (24h after cell plating and at the same time 24h before experiment end). Cells were fixed for staining after 2 days IVIG/buffer control treatment as follows: fixation in acid ethanol (pH 2; Merck) for BrdU staining and in 4 % PFA for Ki67 staining. BrdU staining was performed according to the manufacturer's protocol (Roche). Ki67 staining was done as follows: after cell fixation cells were blocked for 2-3 h at RT in 10 % NGS and 0.5 % bovine serum albumin (BSA, Carl Roth) with 0.5 % Triton X-100; over night incubation was

performed at 4°C with a primary Ki67 antibody (Abcam) in PBS; after 24 h a secondary antibody was applied in PBS for 4 to 6 h at RT; cell nuclei were counterstained with DAPI.
Caspase-3 staining was performed using the same culture conditions as mentioned above but with different staining procedure: cell were blocked for 2-3 h at RT in 10 % NGS with 0.1 % Triton X-100 and then incubated over night at 4°C with primary caspase-3 antibody in PBS. Stained cells were visualized using an Axioplan 2 fluorescence microscope (Zeiss) and Axiovision 4.2 software (Zeiss). Images were analyzed with ImageJ software (National Institutes of Health).

Antibody	Supplier	Dilution
rabbit anti-Ki67	Abcam	1:100
rabbit anti-cleaved caspase-3	Cell Signaling Technology	1:100
goat anti-rabbit IgG secondary antibody, Alexa Fluor 488 conjugate	Invitrogen Thermo Fisher Scientific	1:500
goat anti-rabbit IgG secondary antibody, Alexa Fluor 594 conjugate	Invitrogen Thermo Fisher Scientific	1:500

3.3.11 Morphological measurements

For the purpose of morphological process measurements 9 days p57kip2 suppressed versus control transfected Schwann cells (see 3.3.5) were used. Cells were cultivated on ø 100 mm cell culture dishes. For the analysis of Schwann cell growth IVIG and buffer control were added to the culture medium two days post transfection and treatment was pursued for 3 to 7 days under selection conditions (hygromycin), with one medium exchange at day 4. Morphological measurement of cell processes was done on living cells (expressing fluorescent citrine protein) at day 3 or day 7 after IVIG/buffer control stimulation on Nikon Eclipse TE 200 microscope using NIS-Elements AR 3.10 software (Nikon Instruments Europe BV, Amsterdam, Netherlands).

3.3.12 ELISA

For the purpose of concentration measurements of secreted IL-18 from cultured non-differentiating Schwann cells, 120.000 cells per condition were seeded on 0.1 PDL coated 12 well cell culture multiwell plates. Treated with IVIG and buffer control was performed one day after cell plating for up to 9 days, with one medium exchange at day 4. Concentration measurements of secreted IL-18 from cultured differentiating Schwann cells (p57kip2 suppressed and control transfected cells) were performed, as indicated earlier, for 7 days starting two days after transfection. Medium exchange was done at day 4 upon IVIG/buffer control treatment. Culture media were collected at days 1, 4, 7 and 9 for non-differentiating

Schwann cells and at days 4 and 7 for p57kip2 and control suppressed cells. The medium for time point day 4 was collected before the above-mentioned medium exchange. Collected media were then centrifuged at 2000 rpm for 10 min (4°C), frozen on dry ice and stored at -80°C prior further analysis. ELISA measurements were performed with non-diluted media supernatants using rat IL-18 ELISA kit (Invitrogen) according to the manufacturer's protocol. Detection of the optical density was done at 450 nm on an Infinite M200 Pro plate reader (TECAN).

3.4 Statistics[15]

Unless otherwise stated, data is presented as mean values +/- standard error of the mean (SEM) and significance was assessed by two-sided Student's *t*-test, unpaired comparison for means (GraphPad Prism). Experimental groups were considered significantly different at $*p<0.05$, $**p<0.01$, $***p<0.001$; ns, not significant. n represents the number of independent experiments.

[15] for authorship notice please refer to chapter 9.2

4 RESULTS

4.1 Human immunoglobulins specifically bind to the rat Schwann cell surface[16]

Several studies indicate that immunoglobulins may directly affect oligodendroglial cells, the myelinating glial cells of the CNS. Natural oligodendrocyte-autoreactive IgMk antibodies were shown to bind to oligodendrocytes and to promote CNS remyelination, most likely by enhancing macrophage clearance (Asakura et al., 1998, Warrington et al., 2000, Bieber et al., 2002). Other studies reported the expression of a certain Fc receptor for IgM on oligodendroglial precursor cell, oligodendrocytes and myelin, implicating a direct receptor immunoglobulin interaction on CNS glial cells (Nakahara et al., 2003a).

These observations prompted us to address the question whether immunoglobulins also bind to the Schwann cell surface and could thus exert a positive effect on their regeneration potential. For this purpose we decorated alive, non-differentiating primary rat Schwann cells with 20 mg/ml dialysed human IVIG for 24 h in culture. Anti-human $F(ab')_2$-specific and anti-human Fc gamma-specific antibodies were applied, all of them being $F(ab')_2$ molecules as to minimize possible cross-reactivity, in order to detect human immunoglobulins on the cell surface. We could show that IVIG specifically bind on the Schwann cell surface (Fig. 6A-J). Immunofluorescent signals, corresponding to surface bound immunoglobulins, were localized mainly concentrated around the perinuclear region but also all over the cell surface. Similar binding patterns were observed when aditional IVIG lots were applied for decoration (Fig. 14I-N) and also with differentiation competent Schwann cells (by means of suppressed p57kip2 gene expression as shown by (Heinen et al., 2008a); data not shown).

We next investigated how IVIG bind on the Schwann cell surface. To examine possible binding via the Fab domain of immunoglobulins, pepsin digested IVIG preparations enriched in human $F(ab')_2$ fragments were used for cell decoration, revealing a detection of a related binding pattern on the Schwann cell surface (Fig. 6J). This indicates that IVIG binding could take place via the Fab part of the immunoglobulins. However, two human monoclonal IgG1 controls, the antibodies Avastin and Herceptin, revealed a similar binding pattern on the Schwann cell surface (Fig. 6G-I), suggesting that in addition IVIG binding may be mediated via Fc gamma receptors. Altogether, these findings implicated that IVIG surface recognition (representing a large pool of polyclonal IgG molecules with different specifications) could take place either via Fc parts interacting with Fc gamma receptors (Fig. 6K-M) or via Fab domains recognizing Schwann cell epitopes (Fig. 6O-Q).

[16] for authorship notice please refer to chapter 9.2

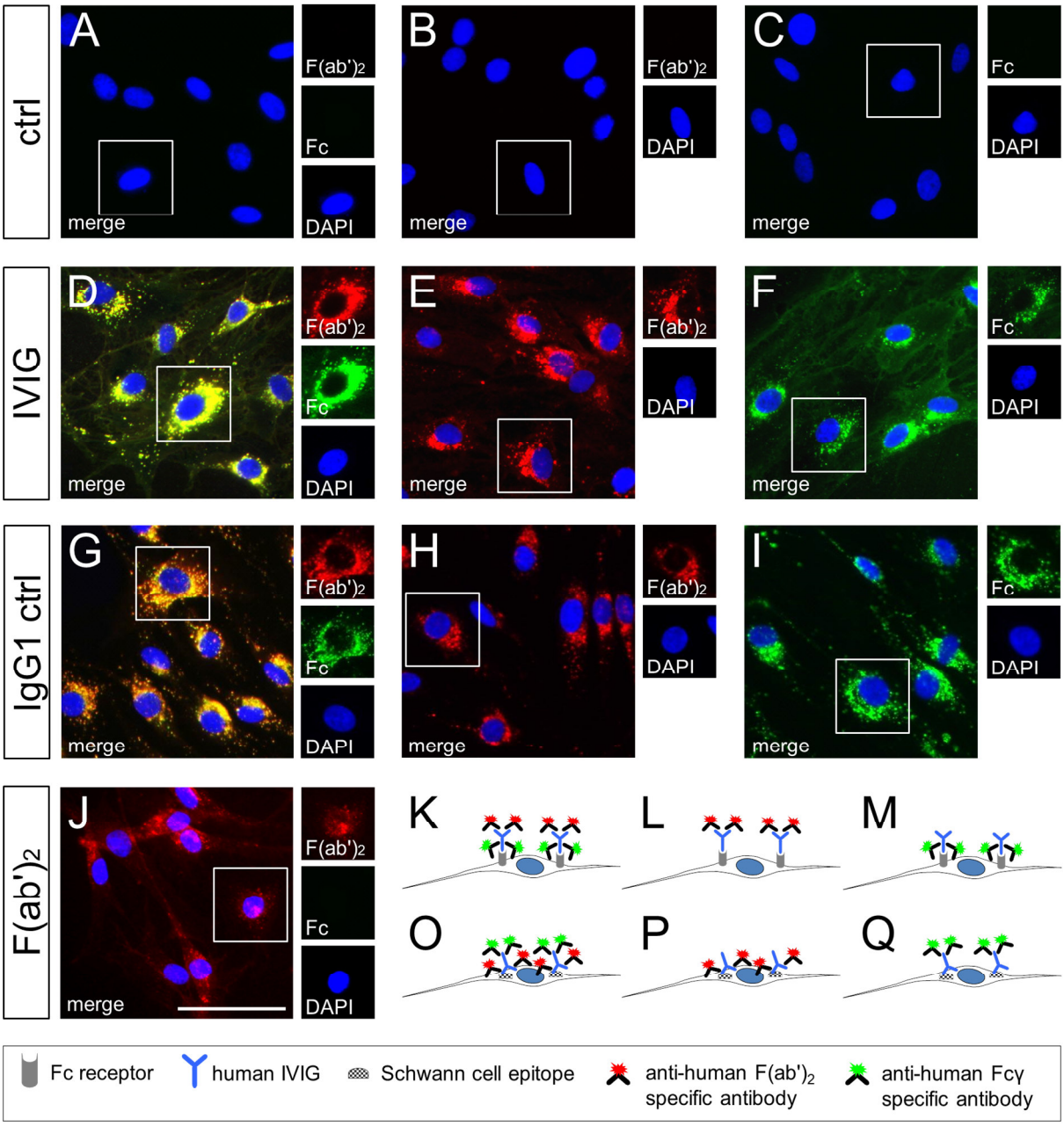

Figure 6. IVIG bind specifically to the Schwann cell surface. (A-G) Living Schwann cells were decorated either with dialysed control buffer (ctrl) (A-C), 20 mg/ml dialysed IVIG (D-F), 20 mg/ml dialysed IgG1 control (IgG1 ctrl, Herceptin) (G-I) or dialysed $F(ab')_2$ fragments, corresponding to 5mg/ml IVIG (J) for a duration of 24 h. After fixation the cells were stained against human $F(ab')_2$ (red) and human Fc parts (green), and nuclei were labelled with DAPI (blue). IVIG, IgG1 ctrl and $F(ab')_2$ fragments binding could be detected by means of co-immunostaining (A, D, G, J) or single staining against human $F(ab')_2$ (B, E, H) or human Fc fragments (C, F, I). Application of dialysed control buffer (A-C) resulted in no staining. (K-Q) The lower right panel represents the two possible hypotheses which might apply for the binding mode of human IVIG on Schwann cells, namely via certain Fc gamma receptors (K-M) or via recognition of epitopes on the cell surface (O-Q). It is further illustrated which potential recognition patterns the anti-human $F(ab')_2$ or anti-human Fc specific antibodies could exhibit in a co-immunostaining against both $F(ab')_2$ or Fc fragments (K, O), or in a single staining against $F(ab')_2$ (L, P) or Fc fragments (M, Q) of human immunoglobulins. Scale bar: 50 µm. n=8 for (A-F), n=2 for (G-I), n=4 for (J).

4.2 Schwann cells express CD64 encoding a high affinity immunoglobulin receptor[17]

In order to verify our assumption that IVIG can bind on the cell surface via its Fc part, we investigated whether Schwann cells express the corresponding FcγR for IgG binding. Previous studies demonstrated that Fc gamma receptors are expressed on human Schwann cells (Vedeler and Fitzpatrick-Klove, 1990), in particular FcγR3, also known as CD16 (Vedeler et al., 1991). Interestingly, cultured rat Schwann cells were also found to express FcγR3, according to transcriptional analysis, however to a much lesser extent as compared to macrophages (Vedeler et al., 1992).

To further characterize which Fc receptors for immunoglobulin binding are indeed expressed by rat Schwann cells, we performed quantitative RT-PCR (qRT-PCR) measurements of Fcgr1a, Fcgr2a, Fcgr2b and Fcgr3a transcripts (corresponding gene names for *Rattus norvegicus*), encoding rat CD64, CD32a, CD32b and CD16 Fc receptors, respectively. Interestingly, only expression of CD64 could be detected. For this purpose we used a cell culture model of differentiating competent Schwann cells, which has been previously established in our group (Heinen et al., 2008a). By suppressing the p57kip2 gene, a cyclin-dependent kinase inhibitor, Schwann cells undergo morphological and transcriptional changes, which lead to cell cycle exit and promotion of a differentiation related phenotype (Heinen et al., 2008a). We used this model in order to monitor transcriptional changes that might be induced by IVIG not only in non-differentiating but also in differentiating Schwann cells. Of note, CD64 expression was significantly upregulated in differentiation competent rat Schwann cells (Fig. 7D). Treatment with IVIG led to significant downregulation of the receptor gene expression in non-differentiating Schwann cells, whereas receptor expression in differentiated cells was not influenced. In order to address the question whether the CD64 receptor protein is also expressed on the Schwann cell surface we next performed staining experiments using a polyclonal CD64 antibody, directed to the extracellular domain of the mouse protein. Specific staining signals were detected dispersed over the cell surface of the non-differentiating cells (Fig. 7A-C). Compared to that, the receptor staining on differentiating cells was mainly located on the cell soma above the perinuclear region (Fig. 7E-G). To further validate these data, the same polyclonal CD64 antibody was applied in a Western blot analysis. This led to the detection of a specific signal between 50 and 60 kDa, demonstrating upregulation in differentiation competent Schwann cells, consistent with the CD64 receptor regulation represented by the qRT-PCR data (Fig. 7H).

[17] for authorship notice please refer to chapter 9.2

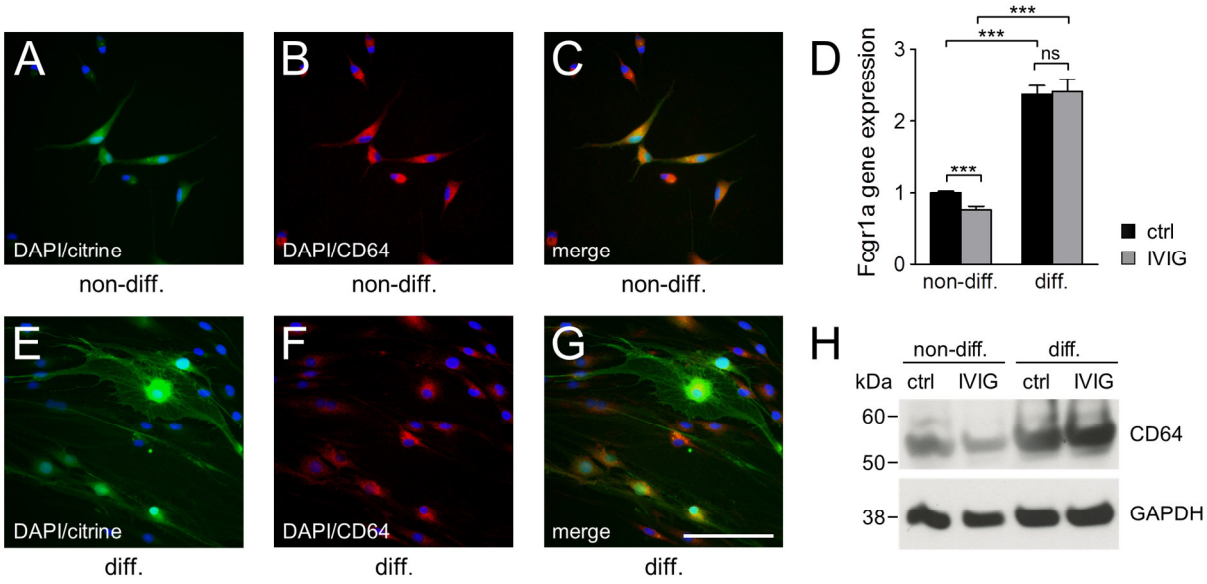

Figure 7. Schwann cells express the Fc gamma receptor CD64. CD64 protein expression was detected on the surface of non-differentiating (non-diff.; A-C) as well as differentiating Schwann cells (diff.; E-G). Differentiation was induced by means of p57kip2 suppression and modulated cells were visualized via citrine (green-fluorescent protein) expression. Cell nuclei were visualized by DAPI (blue). (D) Significant induction of rat Fcgr1a gene expression (CD64) under differentiation promoting conditions as determined by quantitative RT-PCR. Seven days stimulation with 20 mg/ml dialysed IVIG (grey bars) in comparison to control buffer (ctrl; black bars) significantly decreased the expression of CD64 in non-differentiating Schwann cells, only (D). (H) Western blot analysis of differentiating and non-differentiating Schwann cells stimulated with both IVIG and control buffer (ctrl) confirmed CD64 protein expression. Protein molecular weights are indicated in kDa (kilodalton). GAPDH expression was used for normalization. *t*-test (ns, not significant, ***p<0.001). Error bars represent SEM. Scale bar: 100 µm. n=7 for (A-C), n=6 for (E-G), n=8 for (D), n=4 for (H).

To determine whether the signals detected with the above mentioned polyclonal CD64 antibody can in fact be assigned to the rat CD64 protein, several control experiments were performed. Western blot analysis revealed that the antibody is specific as it recognized a rat recombinant CD64 protein (rrFcgr1a) in two different concentrations, 2.5 µg and 5 µg (Fig. 8A). Of note, the recombinant protein used for control experiments represents a truncated version of the whole CD64 receptor, leading to the detection of signals below 50 kDa, and not between 50 and 60 kDa, as previously mentioned. A second antibody (designated CD64*; Fig. 8A) with multiple species reactivity (human, mouse and rat) though raised against a synthetic peptide derived from human CD64 also recognized the rrFcgr1a protein but did not detect the receptor in rat Schwann cells and was therefore not applicable for future experiments.

In addition, we overexpressed the full-length Fcgr1a/CD64 receptor as a flag-tagged fusion protein in cultured rat Schwann cells and compared these to control transfected cells by means of qRT-PCR, Western blot analysis and immunostaining (Fig. 8B-I). Fcgr1a/CD64 transcript measurements revealed successful overexpression (data not shown). Moreover,

by applying the polyclonal CD64 antibody to Western blot analysis, we could repeatedly detect a signal between 50 and 60 kDa, respectively. This signal was much stronger in the CD64 overexpressing cells when compared to control transfected cells (Fig. 8B). A band of the same apparent molecular weight was detected when an anti-flag antibody was applied to the overexpressing cells (Fig. 8C), furthermore indicating that the overexpression was also successful at protein level. Immunostaining revealed a diffusely distributed expression of CD64 on control transfected cells (Fig. 8D-F), whereas CD64 overexpressing cells exhibited a much stronger signal all over the cell surface (Fig. 8G-I).

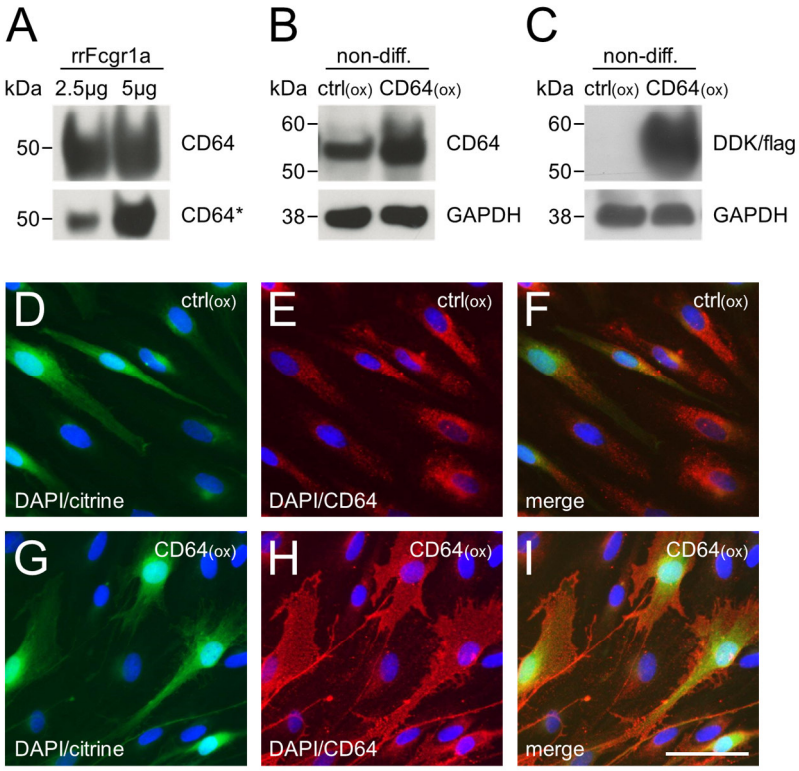

Figure 8. Verification of Fc gamma receptor expression CD64 in Schwann cells. Detection of rat CD64 by means of Western blot analysis (A-C) and immunostaining (D-I) in rat Schwann cells overexpressing the corresponding receptor. (A) Application of two different polyclonal CD64 antibodies (CD64: goat-anti-mouse antibody; CD64*: rabbit-anti-mouse/human/rat antibody) to two different concentrations (2.5 and 5 µg protein) of commercially available rat recombinant Fcgr1a/CD64 protein (rrFcgr1a). This truncated CD64 protein was used as a positive control for detection of the rat CD64 protein. Of note, the goat-anti-mouse antibody was used for all additional Western blot and staining experiments. (B-C) Western blot analysis of CD64 overexpressing Schwann cells ($CD64_{(ox)}$) versus control transfected cells ($ctrl_{(ox)}$) revealed successful protein overexpression of the rat CD64 receptor. Overexpression was induced by means of transfection using a construct encoding the full-length Fcgr1a/CD64 protein with a fused C-terminal DDK/flag-tag. Application of either anti-CD64 (B) or anti-DDK/flag (C) antibody revealed a significant protein upregulation in CD64 overexpressing cells. CD64 expression was detected in the control cells (B), whereas the DDK/flag-tag was only translated, as expected, in the CD64 overexpressing cells (C). Protein molecular weights are indicated in kDa (kilodalton). GAPDH expression was used for normalization. (D-I) Surface protein expression of the CD64 receptor was detected on control transfected cells (D-F) as well as CD64 overexpressing Schwann cells (G-I) by means of immunostaining with the goat-anti-mouse-CD64 antibody (red).

Modulated cells were visualized by means of citrine (green-fluorescent protein) co-expression. Cell nuclei were visualized by DAPI (blue). Scale bar: 50 µm. n=1 for (A), n=4 for (B), n=3 for (C), n=3 for (D-I).

Based on these results, we searched for further molecules directly involved in the signaling pathway following ligand-engaged activation of Fc gamma receptors. The spleen thyrosine kinase (SYK) is well known to be expressed in all haematopoietic cells (Turner et al., 2000). In addition evidence exists for expression in some nonhematopoietic cells (Yanagi et al., 2001). SYK is recruited and activated in the downstream signaling pathways of FcγR1, FcγR3 and FcγR2a (Kim et al., 2001) and other immunoreceptors, such as B cell receptors, T cell receptors, and other Fc receptors. However, more recently large number of new SYK functions in immune cell signaling and beyond has been identified (Mocsai et al., 2010). Measurements of SYK gene and protein expression in CD64 overexpressing versus control transfected cells were performed by means of qRT-PCR and Western blot analysis (data not shown). Of note, on transcriptional as well as protein level, no SYK expression was detected, indicating that SYK might not be involved in the downstream Fc receptor signaling in rat Schwann cells.

4.3 IVIG stimulation affects Schwann cell proliferation[18]

As a next step we examined whether IVIG affect Schwann cell proliferation. Stimulation with dialysed IVIG preparations for 2 days revealed a significant reduction of the proliferation rate of non-differentiating cells (Fig. 9). Application of BrdU to cultured Schwann cells for 8 or 24 hours displayed significantly reduced BrdU incorporation in cells treated with IVIG after both time points (Fig. 9A, C, D), indicating that cells are dividing less frequently upon IVIG stimulation. We confirmed these findings by staining against an additional proliferation marker, Ki67 (Fig. 9B, staining data not shown). Calculation of the Ki67/DAPI ratio also revealed significantly less proliferative cells after IVIG treatment (Fig. 9B). In order to exclude that reduced Schwann cell numbers upon IVIG treatment were due to effects on cell survival, staining for activated caspase-3, a common cell apoptosis marker, was performed after the same stimulation conditions described above. No evidence of induction of apoptosis after treatment with IVIG was found, as the caspase-3 staining turned out to be negative (data not shown).

[18] for authorship notice please refer to chapter 9.2

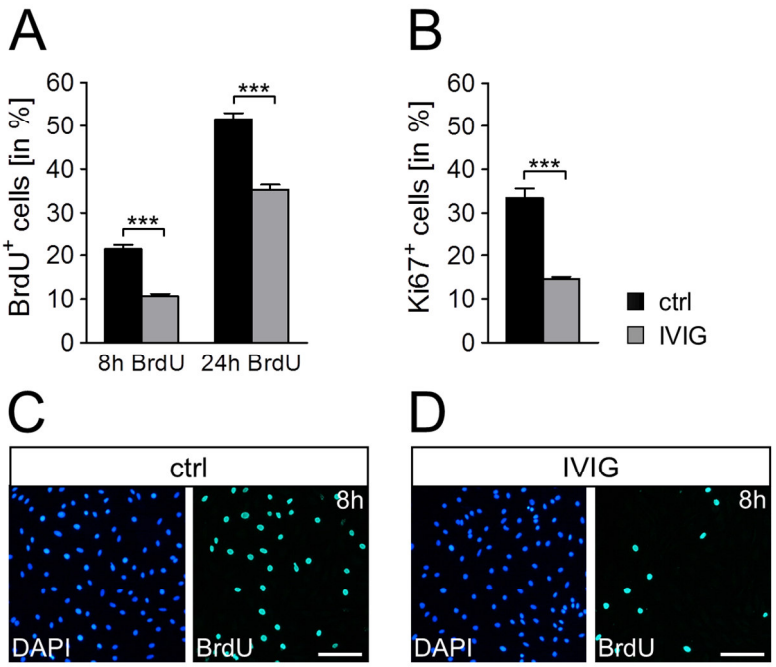

Figure 9. IVIG stimulation reduces Schwann cell proliferation rate. (A-D) Schwann cell proliferation is reduced after 2 days of stimulation with 20 mg/ml dialysed IVIG (grey bars) compared to control buffer (ctrl) preparations (black bars). (A) BrdU labelling was performed within the last 8 or 24 hours (8 h, 24 h) of IVIG treatment and evaluation of the percentage of BrdU/DAPI double positive ($BrdU^+$) nuclei compared to total number of DAPI nuclei revealed a significant reduction of proliferating cells. (C, D) Representative photographs of DAPI (blue) and BrdU (green) labeled nuclei after 8 h BrdU pulse of control buffer (C) and IVIG (D) stimulated cells. (B) These results were confirmed by staining against further proliferation marker Ki67 2 days after IVIG stimulation and determination of the percentage of Ki67/DAPI double positive ($Ki67^+$) nuclei in relation to total number of DAPI positive nuclei. *t*-test (***p<0.001). Error bars represent SEM. Scale bar: 100 µm (C, D). n=4 for (A, C, D), n=2 for (B).

4.4 IVIG accelerate the growth of cellular processes in differentiation competent Schwann cells[19]

We could demonstrate that IVIG treatment had an impact on Schwann cell morphology. Morphological alterations in Schwann cells, comprising process extensions are observed during the myelination process, where Schwann cells grow along and wrap around axons.

As previously published by our group, long-term suppression of p57kip2 in Schwann cells leads to morphological differentiation in absence of axons (Heinen et al., 2008a), which is why we used this model for examinations regarding a potential influence of IVIG on the maturation process. Significantly accelerated growth of cellular processes was measured upon stimulation with IVIG using differentiation competent Schwann cells (Fig. 10). Along with an induction of myelin expression, differentiating Schwann cells also exhibit somatic and

[19] for authorship notice please refer to chapter 9.2

process growth (Heinen et al., 2008a). Here, we observed that, after 5 days suppression and 3 days of IVIG stimulation, the mean length of cellular processes was significantly increased, while non-differentiating cells did not respond (Fig. 10A, C, D). The effect was no longer observed with further progression of the differentiation process and after 7 days of IVIG incubation (Fig. 10B), indicating that the IVIG effect on process extension kinetics was restricted to early stages of the differentiation process.

Cytoskeletal rearrangements involving actin polymerization have been shown to be engaged in myelin-related gene expression and thus in Schwann cell differentiation processes (Fernandez-Valle et al., 1997). No disruption of actin filament assembly and structure could be observed after IVIG stimulation as revealed by staining with TRITC-conjugated phalloidin (data not shown). However, cultured non-differentiating Schwann cells displayed dark cell structures around the nuclei in presence of IVIG, when observed in phase-contrast microscopy. It is currently unclear whether this is a direct impact on cell shape and cytoskeleton, or it reflects discrete cell surface alterations possibly connected to the IVIG binding sites on the cell surface (data not shown).

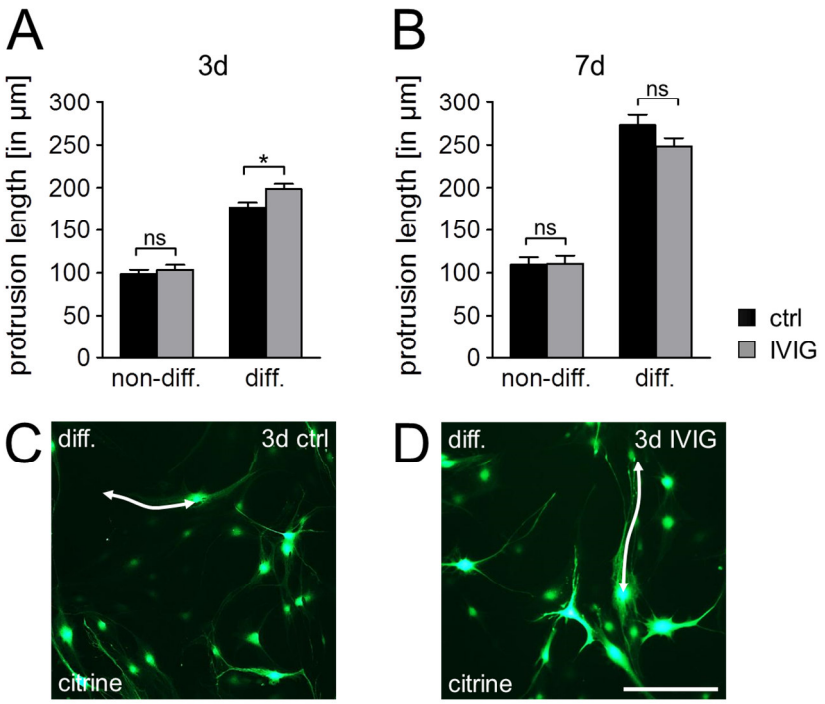

Figure 10. IVIG induce the growth of cellular processes in differentiation competent Schwann cells. (A-D) Quantification of the average Schwann cell processes lengths revealed significantly accelerated growth of cellular processes in early stages of the differentiation process. (A) The cell processes of p57kip2 suppressed cells (diff.) were significantly longer after 3 days (3d) IVIG stimulation (grey bars) and 5d suppression, when compared to control buffer treated cells (black bars). However, no difference was observed in control suppressed cells (non-diff.). (B) In later stages of the differentiation process (9d suppression and 7d of IVIG stimulation) the measurement of the cellular processes did not reveal the same effect. (C, D) Representative photographs of differentiating citrine

positive Schwann cells after 3d control buffer (C) or IVIG (D) treatment; cell processes are marked by white arrows. *t*-test (ns, not significant, **p*<0.05). Error bars represent SEM. Scale bar: 200 µm. n=10 for (A-D).

4.5 IVIG lead to induction of myelin gene expression and maturation activation related signaling pathways[20]

Next, we investigated whether IVIG treatment affects the expression of essential Schwann cell transcription factors, myelin (-related) genes, and signaling molecules. To this end we examined the transcriptional regulation of genes such as myelin protein zero (Mpz/P0), myelin basic protein (Mbp), periaxin (Prx), peripheral myelin protein-22 (Pmp22), peripheral myelin protein 2 (Pmp2), proteolipid protein 1 (Plp1), connexin 32 (Cx32) and myelin-associated glycoprotein (Mag) (Fig. 11A-H), comprising some of the most prominent genes encoding peripheral myelin (Patzig et al., 2011). We found that stimulation of differentiation incompetent cultured Schwann cells with dialysed IVIG led to a significant upregulation of myelin gene expression within the first day of treatment (Fig. 11A-H). Note that for most genes this induction was transient and restricted to the first 24 hours of treatment. Nevertheless, the expression of Plp1 and Cx32 remained upregulated after 3 days of IVIG stimulation (Fig. 11F, G). Consistent with the observed myelin induction, IVIG remarkably induced the expression of transcription factors Sox10 (SRY-related HMGbox-10), Oct6 (octamer-binding transcription factor-6) and Krox20/Egr2 (early growth response protein-2) after the first day of treatment (Fig. 11I-K). These genes are key regulatory players in Schwann cell differentiation processes and positively regulate myelination (Svaren and Meijer, 2008).

[20] for authorship notice please refer to chapter 9.2

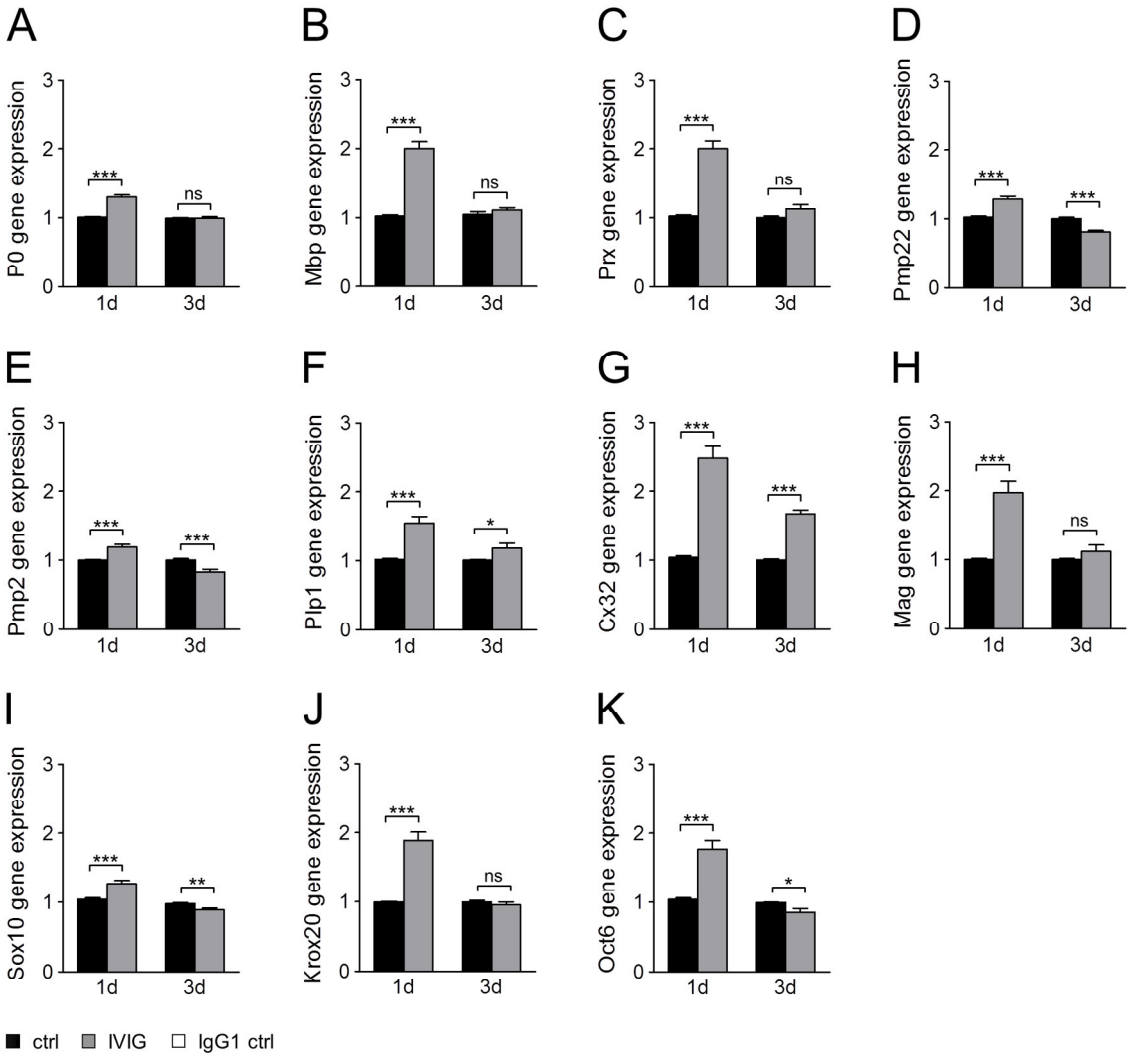

Figure 11. Short-term IVIG effect on myelin gene expression. (A-K) Gene expression measurements of non-differentiating Schwann cells (non-diff.) were performed after 1 and 3 days of IVIG and control buffer (ctrl) treatment. (A-H) Quantitative RT-PCR measurements showed consistent and significant upregulation of myelin genes expression after 1 day (1d) stimulation with 20 mg/ml dialysed IVIG (grey bars) as opposed to control buffer (black bars) stimulations. Myelin gene expression after 3d IVIG stimulation was rather not significant or diminished, apart from Plp1 (F) and Cx32 (G). (I-K) Gene expression of important Schwann cell differentiation-related transcription factors was also increased upon 1d IVIG stimulation. GAPDH was used for normalization. *t*-test (ns, not significant, **p*<0.05, ***p*<0.01, ****p*<0.001). Error bars represent SEM. Number of experiments: n=18 for (A, B), n=7 for (C, D, G), n=4 for (E, H), n=11 for (F), n=5 for (I, J, K).

Serine-threonine kinase Akt activation plays a central role in the course of Schwann cell differentiation and peripheral myelination, a process triggered by phosphatidylinositol 3,4,5-trisphosphate (PIP_3) which is a product of the phosphatidylinositol 3-kinase (PIP_3K) (Ogata et al., 2004). On the other hand, PTEN (phosphatase and tensin homolog) catalyses the opposite reaction of PIP_3 to phosphatidylinositol 4,5-bisphosphate (PIP_2), and can thereby act as indirect inhibitor of Akt activation and myelination (Cotter et al., 2010,

Goebbels et al., 2010). We therefore determined expression levels of these signaling proteins. Western blot analysis revealed enhanced phosphorylation of Akt (Fig. 12A) and downregulation of the phosphorylated PTEN protein (Fig. 12B) after 1 day of stimulation with IVIG, an observation, which supports an IVIG dependent induction of the differentiation process. Interestingly, expression of cJun and phospho-cJun proteins, an important regulator of Schwann cell dedifferentiation in injured nerves (Parkinson et al., 2008, Arthur-Farraj et al., 2012) and predemyelination in CMT-1 models (Klein et al., 2014) was not altered upon IVIG treatment (Fig. 12B). An additional Schwann cell differentiation inhibitor and thus regulator of the myelination process, p38 mitogen-activated protein kinase (p38MAPK) (Yang et al., 2012), was downregulated in its phosphorylated form after IVIG stimulation (Fig. 12A). Together, these results indicate that immunoglobulin treatment initiates differentiation events.

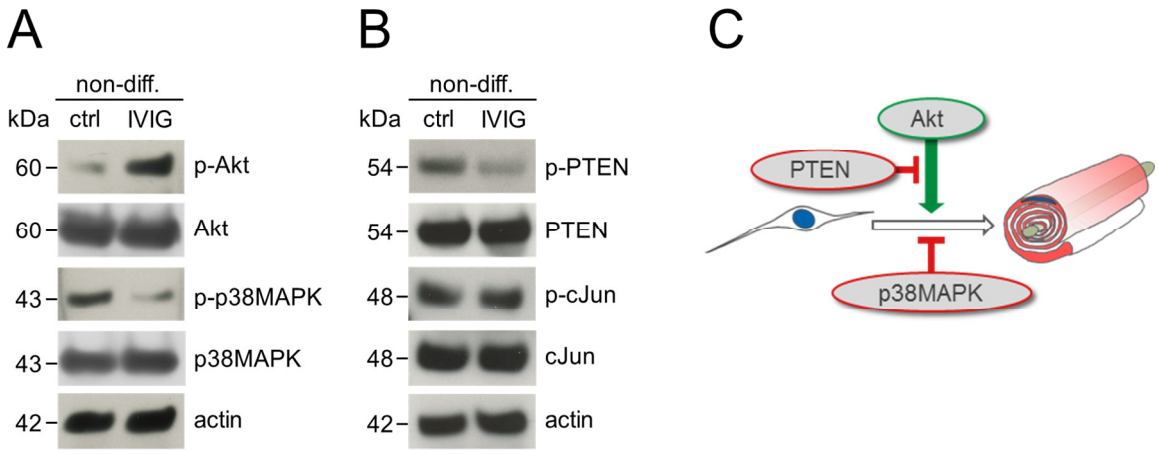

Figure 12. Short-term IVIG effect on signaling molecules. (A, B) Western blot analysis (representative experiments) of signaling pathways related proteins revealed an increase in differentiation associated phospho-Akt (p-Akt) 1 day after IVIG treatment. Differentiation inhibitors such as phosphorylated forms of p38MAPK (p-p38MAPK) (A) or PTEN (p-PTEN) (B) were downregulated upon IVIG stimulation, whereas the protein expression of their unphosphorylated forms remained constant (A, B). Expression of cJun as well as phospho-cJun (p-cJun) (B) was not changed after IVIG incubation. (C) Schematic illustration of the above mentioned signaling molecules that directly or indirectly influence the myelination process. Actin was used for normalization and protein molecular weights are indicated in kDa (kilodalton). Number of experiments: n=2 for (A, B).

4.6 Application of control immunoglobulin preparations[21]

We next investigated whether the gene expression related IVIG effects, most likely initiated by immunoglobulin binding on the Schwann cell surface, are epitope- or Fc receptor dependent. As we could show earlier, both monoclonal IgG1 antibodies (Fig. 6G-I), and $F(ab')_2$ fragments from pepsin digested IVIG (Fig. 6J) specifically bind on the rat Schwann cell surface. Moreover, stimulation of non-differentiating Schwann cell with $F(ab')_2$ fragments led to significant upregulation of prominent myelin genes such as P0, Mbp and Plp1 (Fig. 13A-C). This indicates that Fab-dependent epitope recognition initiates cellular reactions, similar to the ones observed with whole IVIG preparations. Of note, $F(ab')_2$ fragment treatment could be performed only for a duration of 24 hours because they exhibit increased tendency for aggregation and thus high cellular toxicity. As a next step we stimulated the cells with three different humanized monoclonal IgG1 antibodies, Synagis (Palivizumab), Avastin (Bevacizumab), and Herceptin (Trastuzumab), and observed that none of these IgG1 controls increased myelin gene expression (Fig. 13D-I). These results suggest that effects on myelin gene expression are mediated by all IgG components and not solely by the IgG1 fraction of IVIG, and that Fc dependent binding might initiate different effects as the ones induced by the whole IVIG product.

[21] for authorship notice please refer to chapter 9.2

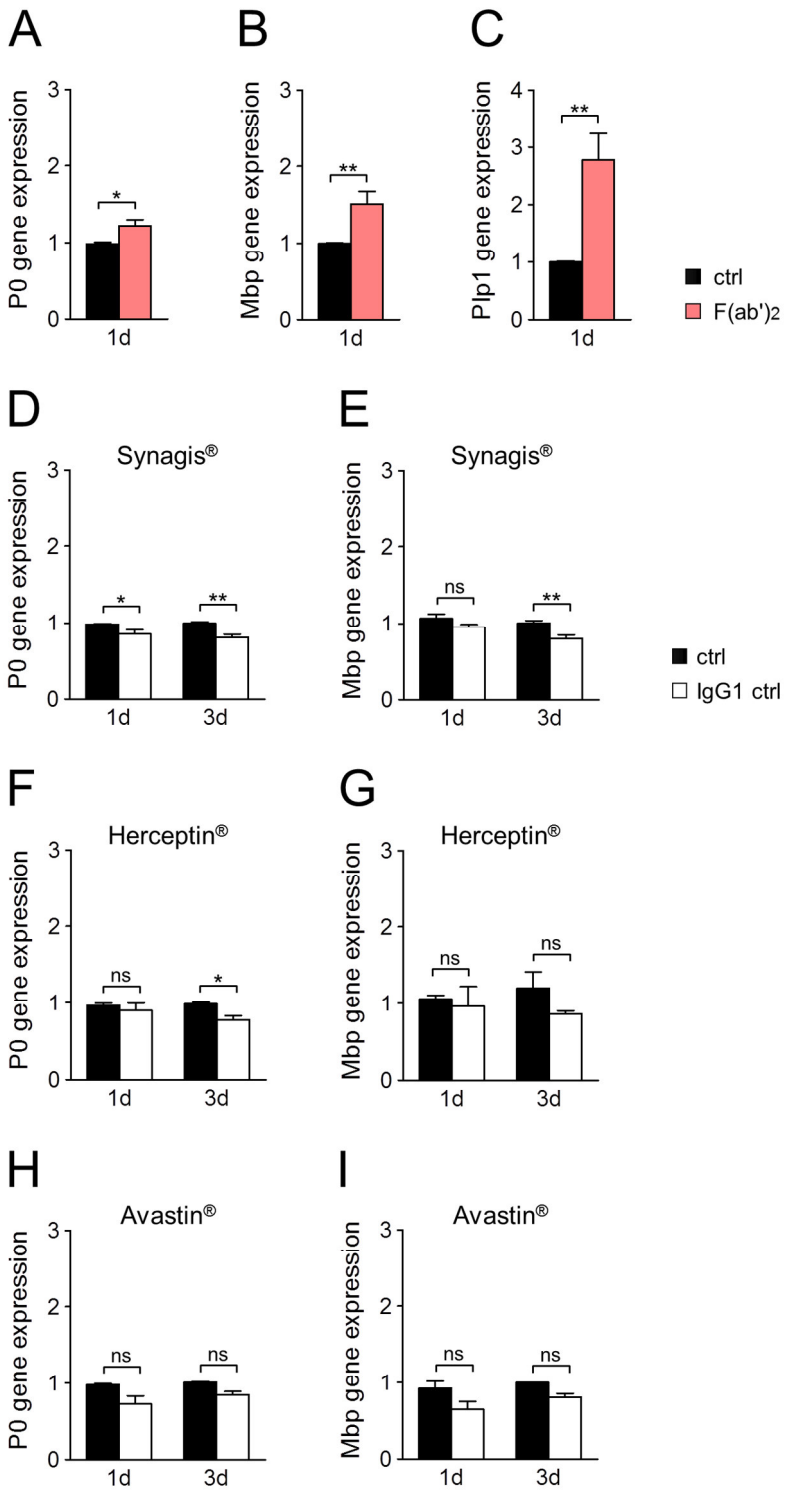

Figure 13. Effects of human F(ab')$_2$ fragments or human monoclonal IgG1 antibodies on Schwann cells. (A-C) Human IVIG3 (lot LE12L341AA) was pepsin-digested, the resulting F(ab')$_2$ fragments (3,65 mg/ml F(ab')$_2$, corresponding to 5 mg/ml IVIG3) were applied to cultured Schwann cells (red bars) for 1 day (1d) and the outcome of the reaction was compared to control buffer treated cells (black bars). Treatment with F(ab')$_2$ fragments led to significant upregulation of myelin genes P0 (A), Mbp (B) and Plp1 (C). (D-I) Application of three different human monoclonal IgG1 control antibodies (white bars) did not induce any upregulation of myelin genes P0 (D, F, H) and Mbp (E, G, I) when compared to control buffer (black bars). Following humanized monoclonal antibodies were used for Schwann cell stimulation for 1d and 3 days (3d) in culture: (D, E) Synagis® (20 mg/ml, dialysed),

Herceptin® (20 mg/ml, dialysed) and Avastin® (20 mg/ml, dialysed). GAPDH was used for normalization. *t*-test (ns, not significant, **p*<0.05, ***p*<0.01). Error bars represent SEM. Number of experiments: n=4 for (A, B), n=2 for (C), n=3 for (D, E), n=2 for (F, G), n=2 for 1d (H, I), n=1 for 3d (H, I).

In order to exclude production dependent effects of IVIG, different IVIG lots were tested. For this purpose we used two additional IVIG preparations, lot LE12L068AB and lot LE12L341AA, respectively termed IVIG2 and IVIG3. Both batches induced myelin gene expression after the first day of treatment, as exemplified by Mbp (Fig. 14B, D, F, H) and P0 (Fig. 14A, C, E, G) gene expression. The different concentrations used for stimulation (5 mg/ml represented in Fig. 14A, B, E, F and 10 mg/ml in Fig. 14C, D, G, H) are based on the fact that both lots revealed a more potent and to some degree negative effect on the Schwann cell morphology in culture, hence further dilutions of the immunoglobulins were undertaken. In particular, P0 gene regulation appeared to depend on higher IVIG concentrations (Fig. 14C, G), since application of low concentrations (Fig. 14A, E) only led to slightly (Fig. 14A) or no upregulation at all (Fig. 14E). The immunoglobulin binding studies revealed very similar staining patterns (Fig. 14I-N) as previously described using the first IVIG batch (Fig. 6A-F). Control buffer treated cells constantly showed no staining signals (Fig. 14I, J), whereas Schwann cell decoration with lots IVIG2 (Fig. 14K, L) and IVIG3 (Fig. 14M, N) revealed the earlier described surface bound immunoglobulin localization (Fig. 6).

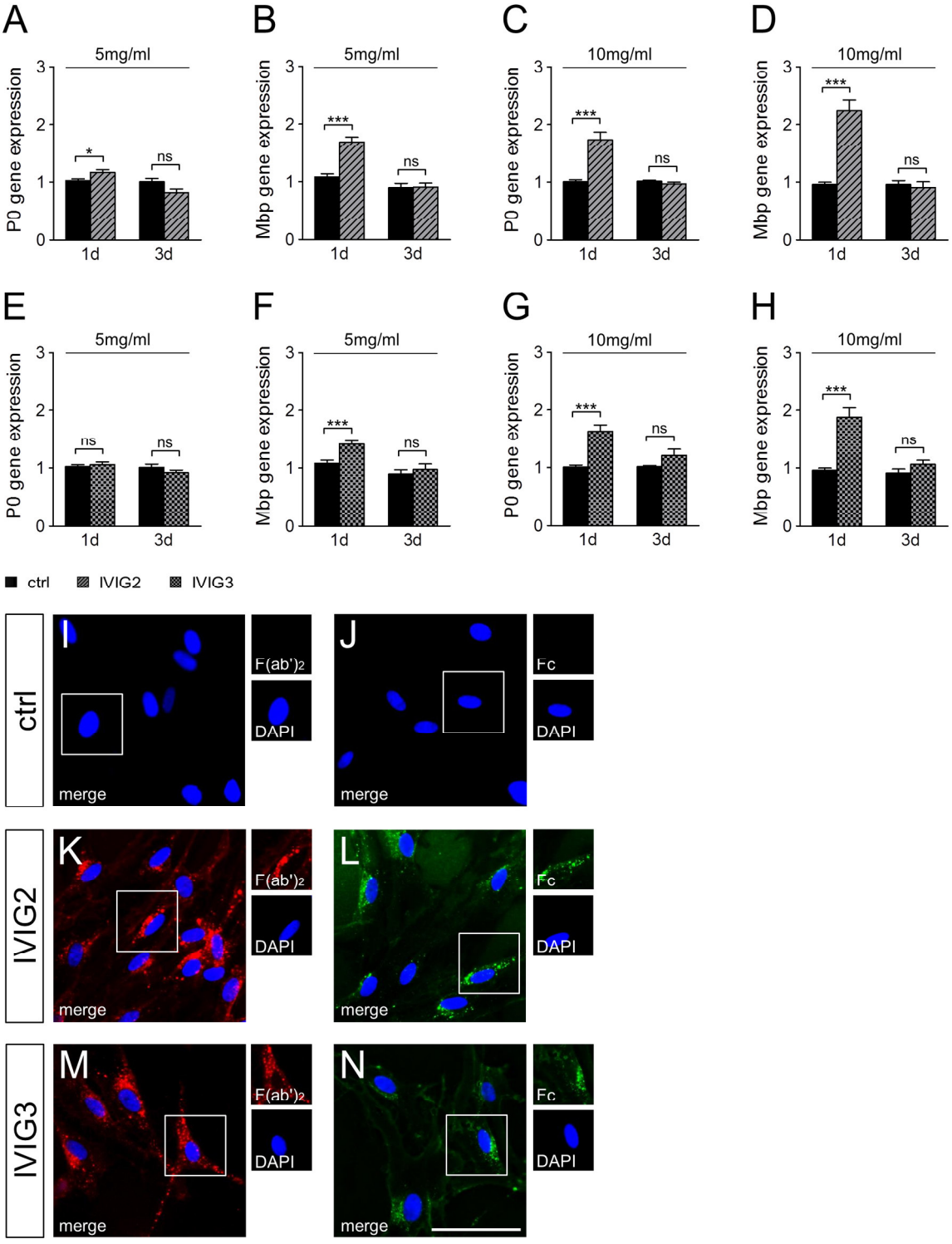

Figure 14. Testing additional IVIG lots on cultured Schwann cells: myelin gene expression and immunoglobulin surface binding studies. (A-H) Quantitative RT-PCR myelin genes expression of cultures Schwann cells was measured after 1 day (1d) and 3 days (3d) of IVIG lot LE12L068AB (IVIG2; grey bars, stripe patterned), IVIG lot LE12L341AA (IVIG3; grey bars, square patterned) and control buffer (ctrl; black bars) treatment, while cells were treated with two different IVIG concentrations: 5 mg/ml of either IVIG2 (A, B) or IVIG3 (E, F) and 10 mg/ml of either IVIG2 (C, D) or IVIG3 (G, H). Mbp consistent and significantly showed upregulation after 1d stimulation with 5 mg/ml (B, F) as well as 10 mg/ml (D, H) dialysed IVIG2/3, as opposed to control buffer application. P0 expression was distinctly increased after 1d stimulation with 10 mg/ml IVIG2/3 (C, G) rather than with

5 mg/ml (A, E), when compared to control buffer treatment. Myelin gene expression after 3d IVIG2 or IVIG3 stimulation was not significant. GAPDH was used for normalization. (I-N) Living Schwann cells were decorated for 24 h either with dialysed control buffer (I, J), 10 mg/ml dialysed IVIG2 (K, L) or 10 mg/ml dialysed IVIG3 (M, N). After fixation the cells were stained against human $F(ab')_2$ (red) and human Fc parts (green), and nuclei were labelled with DAPI (blue). IVIG2 and IVIG3 binding could be detected by means of single staining against human $F(ab')_2$ (I, K, M) or human Fc fragments (J, L, N). Application of dialysed control buffer (I, J) resulted in no staining. *t*-test (ns, not significant, **p*<0.05, ****p*<0.001). Error bars represent SEM. Scale bar: 50 µm. Number of experiments: n=7 for 1d (A-H), n=3 for 3d (A-H), n=2 for (I-N).

4.7 IVIG mediated responses of differentiation competent Schwann cells[22]

Following the observations that non-differentiating Schwann cells transiently benefit from IVIG treatment, we then investigated to what degree such treatment can influence the differentiation process as such. For this purpose, we examined the myelin gene and protein expression of differentiation competent (p57kip2 suppressed) cells upon IVIG treatment (Fig. 15A-L). As previously shown, p57kip2 suppressed Schwann cells exhibit an upregulated myelin gene and protein expression, although they are not engaged in axonal contact (Heinen et al., 2008a). Using quantitative RT-PCR we could show that despite manifold increase after p57kip2 suppression, myelin gene expression was further boosted by IVIG treatment (Fig. 15A-H). Transcript levels of Mbp (Fig. 15B), Prx (Fig. 15C), Plp1 (Fig. 15F), Cx32 (Fig. 15G) and Mag (Fig. 15H) expression levels were strongly induced upon IVIG stimulation, whereas Mpz/P0 and Pmp22 transcript levels (Fig. 15A, D) were rather mildly increased and Pmp2 levels were found to be slightly downregulated (Fig. 15E). Note that myelin gene induction could be observed after a period of 7 days of IVIG treatment and was therefore not limited to early phases, as shown for differentiation incompetent cells (Fig. 11). As an exception, we found that upregulation of Plp1 and Cx32 was not restricted to early periods and could consistently be observed also in non-differentiating cells after 3 and 7 days of stimulation (Fig. 11F, G and Fig. 15F, G). In the case of Pmp2 (Fig. 15E), the expression was slightly downregulated after 3 days IVIG stimulation, similarly to observations in differentiation incompetent cells (Fig. 11E).

In order to confirm the observed induction of myelin gene expression we examined the protein expression levels of P0 and MBP, two of the most abundant proteins of peripheral myelin (Fig. 15I-L). Using Western blot analysis we could demonstrate that in differentiating Schwann cells the P0 (Fig. 15I, J) and to a lesser extent also MBP protein levels (Fig. 15K, L) were elevated after IVIG treatment.

[22] for authorship notice please refer to chapter 9.2

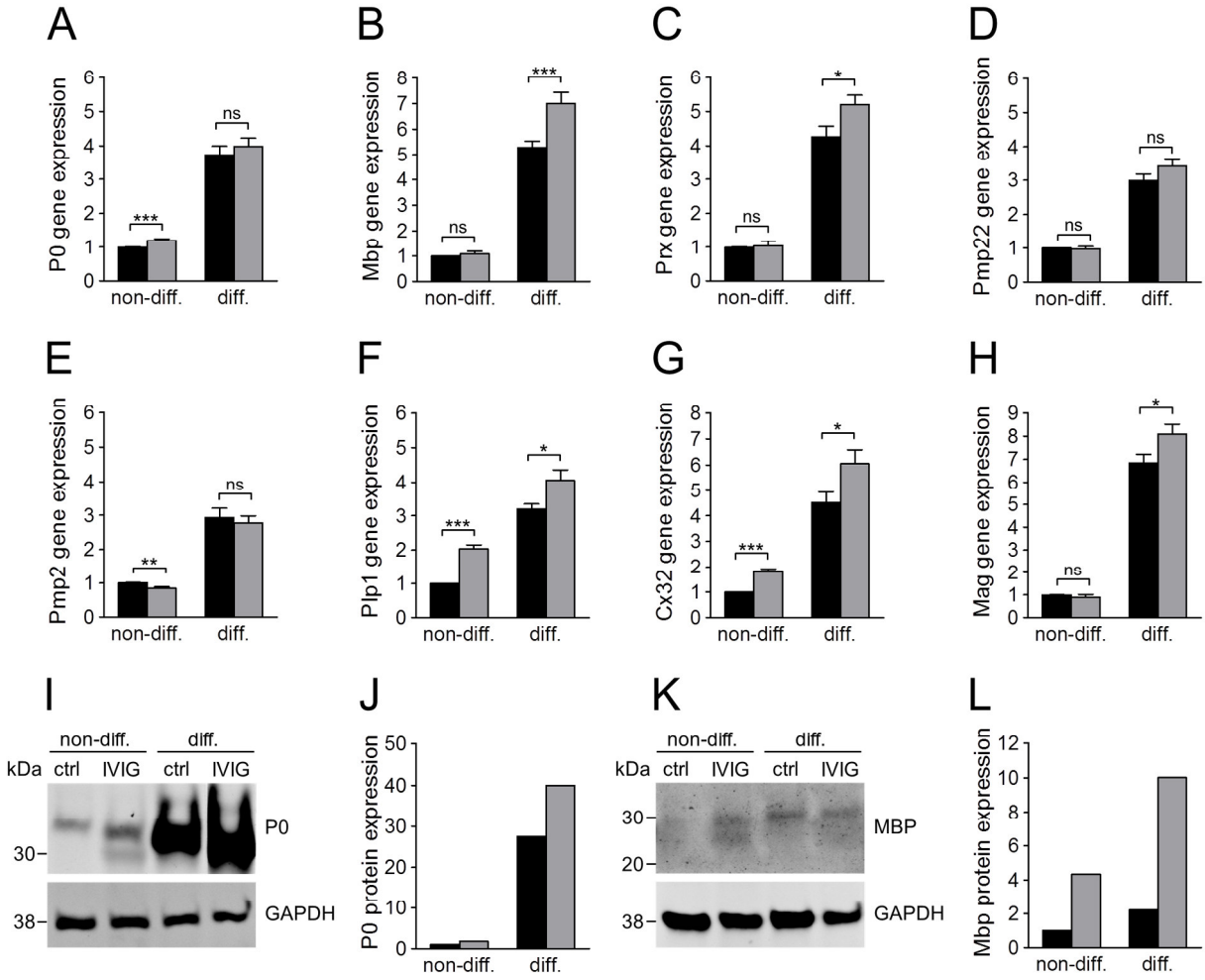

Figure 15. IVIG treatment induces myelin gene and protein expression. Differentiation competent Schwann cells respond to IVIG interaction by increasing their myelin gene (A-H) and protein expression (I-L). 20 mg/ml dialysed IVIG and control buffer (ctrl) were added to the culture medium two days after differentiation was initiated. Treatment of differentiating (diff.) and non-differentiating (non-diff.) cells was pursued for 7 days (7d), with one medium change at day 4. (A-H) Quantitative RT-PCR revealed significant upregulation of most myelin genes after 7d stimulation with IVIG (grey bars) when compared with control buffer (black bars). (I-J) Western blot analysis confirmed increased P0 (I, J) and MBP (K, L) protein expression after 7d stimulation of differentiating and non-differentiating Schwann cells. (I, K) Representative Western blot experiments, (J, L) corresponding Odyssey protein quantifications. Protein molecular weights are indicated in kDa (kilodalton). GAPDH was used as normalization control in all experiments. *t*-test (ns, not significant, **p*<0.05, ***p*<0.01, ****p*<0.001). Error bars represent SEM. Number of experiments: n=10 for (A), n=8 for (B), n=4 for (C), n=7 for (D, E), n=5 for (F, H), n=3 for (G), n=5 for (I-J, K-L).

In order to study the effects of IVIG on axon/Schwann cell interactions we applied an *in vitro* myelination mouse model of dorsal root ganglia (DRG) cultures (Fig. 16A-C). We developed this model based on a previously published protocol using DRG from mouse embryos (Päiväläinen et al., 2008) and modified it correspondingly to our experimental setup (Heinen et al., 2012). Initially, a coculture consisting of precursor Schwann cells and neurons was seeded and after 4 to 5 days of proliferation, the differentiation process was induced by supplying with myelination promoting culture medium (see Materials and Methods, chapter 3.3.6). IVIG stimulation was performed concomitant to the initiation of the myelination process for duration of 7 days. This model represents a dynamic coculture and allows us to study the *in vitro* myelination process in reponse to the applied conditions. In order to evaluate to which extent immunoglobulin treatment can modulate the generation of myelin sheaths (internode formation) neuron/glia cocultures were stained using anti-MBP and anti-ß-tubulin (Fig. 16A-B), and MBP positive internodes were counted (Fig. 16C). This analysis revealed that in IVIG treated myelinating cocultures significantly more internodes were generated as compared to buffer treated cultures (Fig. 16C), indicating that IVIG exert a positive effect on myelin expression as well as on the axonal wrapping process.

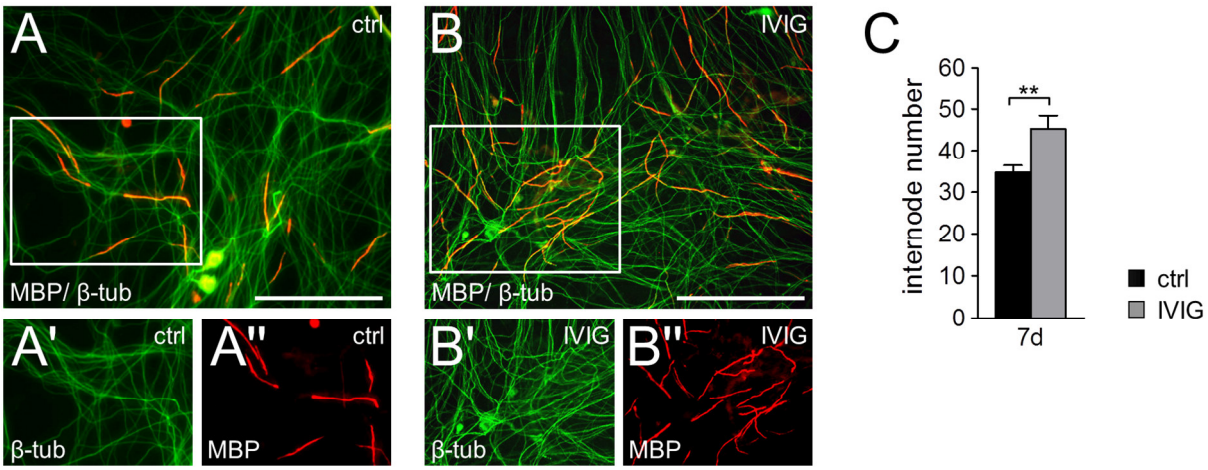

Figure 16. IVIG exhibit a positive effect on *in vitro* myelination. (A-C) Quantification of *in vitro* myelination revealed a significant increase of MBP positive internodes (red) after 7 days IVIG treatment (grey bars; C) when compared to control buffer (ctrl, black bars; C). (A, B) Representative photographs of myelinating neuron/glia cocultures either treated with control buffer (ctrl; A) or IVIG (B); β-tubulin staining (β-tub) is visualized in green and MBP staining in red. *t*-test (**p<0.01). Error bars represent SEM. Scale bar: 200 µm. Number of experiments: n=9 for (A-C).

4.8 GeneChip Array analysis reveals a differentiation related Schwann cell phenotype induced by IVIG

In order to identify additional transcriptional changes induced by IVIG treatment in rat Schwann cells, a GeneChip Array analysis was performed. This study was undertaken on differentiating (p57kip2 suppressed) and non-differentiating (control suppressed) Schwann cells which were stimulated with IVIG or control buffer for 7 days. The RNA samples for the transcriptional analysis were collected from 4 independent experiments, and gene expression analysis of all 16 RNA samples was done by Miltenyi Biotec using Agilent Whole Rat Genome Oligo Microarrays. Following data processing, statistical and functional discriminatory gene analysis (DGA), selected genes, with a fold change ≥ 2 and *p*-values ≥ 0.01, were considered significantly differentially regulated (Fig. 17B, D). Data analysis revealed 21 upregulated and 15 downregulated genes upon IVIG treatment in non-differentiating cells (Fig. 17A, B). On the other hand, in differentiating Schwann cells 6 genes were upregulated and other 5 genes were downregulated (Fig. 17C, D). Many of the identified transcripts were of unknown function. In addition, multiple testing correction was performed in order to adjust the individual p-value for each gene to keep the overall false positive rate to less than or equal to a *p*-value cut-off. Statistically significant changes in expression were considered for genes with adjusted *p*-values of ≤ 0.01. However, upon calculation of the false discovery rate by the method of Benjamini and Hochberg (Benjamini, 1995), none of the adjusted p-values of the selected genes appeared to be significant (Fig. 17B, D illustrates only non-adjusted *p*-values), indicating that, according to the acquired array data, IVIG treatment does not induce high numbers of differences in the expression profile of rat Schwann cells.

In addition, independently of the multiple correction method used, each selection of genes contains some false positives (genes which appear regulated, although there is no true regulation at all), while some false negatives fail to be selected (gene which did not meet the selection criteria, although they are differentially expressed). We therefore decided to further validate the obtained array data for some differentiation related Schwann cell genes (summarized in tables 2 and 3) by means of quantitative RT-PCR.

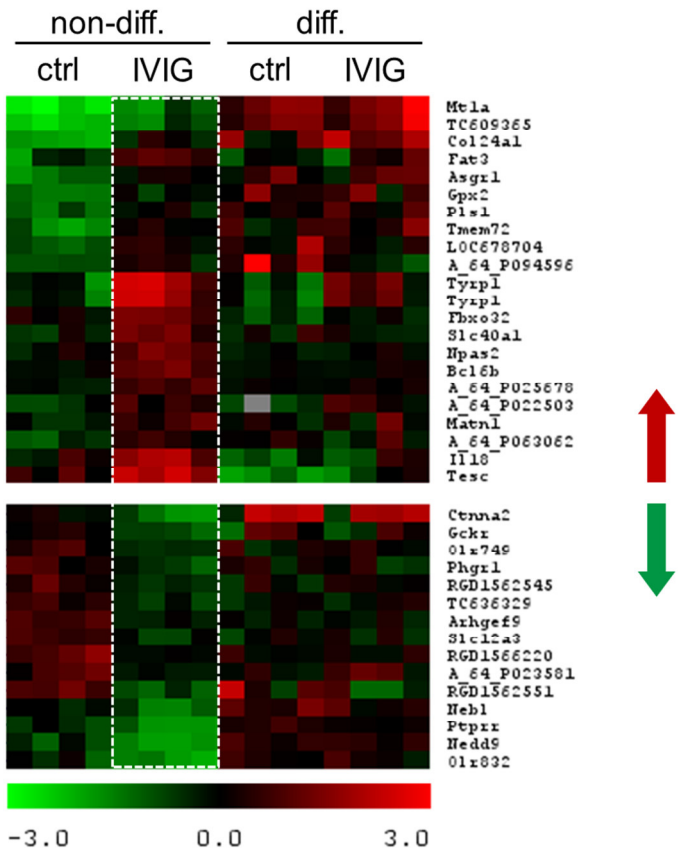

B

non-differentiating cells: IVIG vs ctrl		
gene name	fold change	p-value
Tyrp1	5,693	4,89E-03
Col24a1	3,526	6,70E-04
Fat3	3,176	6,85E-03
Tmem72	3,093	1,32E-03
Tesc	3,079	4,06E-03
Il18	3,054	8,32E-03
Mt1a	2,844	6,96E-03
Slc40a1	2,798	5,09E-03
Asgr1	2,660	7,61E-04
LOC678704	2,364	1,15E-03
TC609365	2,316	7,41E-03
Bcl6b	2,278	4,84E-04
A_64_P063062	2,267	3,47E-03
Npas2	2,238	3,73E-03
Gpx2	2,196	1,68E-03
Matn1	2,156	6,36E-03
A_64_P022503	2,153	9,66E-03
Fbxo32	2,081	6,38E-03
Pls1	2,048	8,66E-03
A_64_P094596	2,047	7,31E-03
A_64_P025678	2,030	2,88E-04

non-differentiating cells: IVIG vs ctrl		
gene name	fold change	p-value
RGD1562551	-3,558	2,05E-04
Ctnna2	-2,678	2,90E-03
Olr832	-2,464	8,52E-03
Phgr1	-2,305	8,80E-03
RGD1566220	-2,231	2,37E-03
Nedd9	-2,141	5,05E-03
Slc12a3	-2,137	4,22E-03
Arhgef9	-2,113	3,57E-04
Gckr	-2,090	8,77E-04
TC636329	-2,090	3,27E-03
A_64_P023581	-2,071	8,32E-03
Ptprr	-2,070	9,24E-03
Olr749	-2,052	3,17E-03
Nebl	-2,017	9,90E-03
RGD1562545	-2,015	6,92E-03

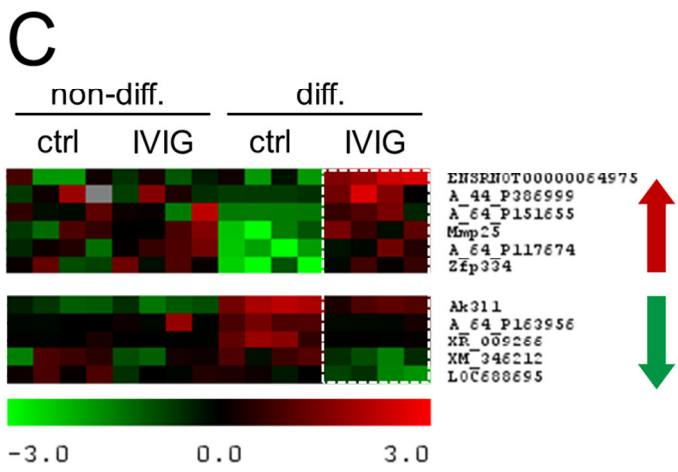

D

differentiating cells: IVIG vs ctrl		
gene name	fold change	p-value
ENSRNOT00000064975	2,832	2,07E-03
Zfp334	2,705	2,84E-03
Mmp25	2,627	4,26E-03
A_64_P117674	2,526	9,78E-04
A_64_P151655	2,072	1,68E-03
A_44_P386999	2,026	9,19E-03

differentiating cells: IVIG vs ctrl		
gene name	fold change	p-value
XM_346212	-2,777	6,67E-03
XR_009266	-2,416	3,65E-03
LOC688695	-2,331	8,35E-03
Ak3l1	-2,100	5,49E-03
A_64_P163956	-2,059	4,69E-04

Figure 17. GeneChip analysis of differentiating and non-differentiating Schwann cells upon IVIG treatment. Differentiation was induced by means of p57kip2 suppression (diff.) for 9 days in culture and control transfected Schwann cells (non-diff.) represented the non-differentiating cell type. IVIG (20 mg/ml, dialysed) or control buffer (ctrl) treatment was pursued for 7 days, starting after the

first 2 days post transfection. RNA samples from 4 independent experiments were collected and all 16 samples (4x non-diff. + ctrl, 4x non-diff. + IVIG, 4x diff. + ctrl, 4x diff. + IVIG) were exposed to Agilent Whole Rat Genome Oligo Microarray analysis. (A-D) The results of the differentially expressed genes after IVIG treatment (enclosed with a white pointed square in A, C) in non-differentiating (A) and differentiating Schwann cells (C) are displayed in heat maps (A, C) and further sorted by decreasing fold change values in tables (B, D); red tables represent the corresponding upregulated and green tables the downregulated genes after IVIG treatment; two types of images of the clustered heat maps, grouped by genes only, were generated: one analysis with all upregulated (red arrow pointing up) and one with all downregulated genes (green arrow pointing down. (B, D) The *p*-values in the tables represent the unadjusted numbers subjected to a Student's *t*-test, but not to a multiple correction, and are therefore indicated by (*). Number of experiments: n=4 (A-D).

Table 2. Selected differentially regulated genes of non-differentiating Schwann cells after IVIG treatment. Represented are the fold change and the corresponding *p*-values* generated by the data processing and statistical analysis of the GeneChip Array study on non-differentiating (control transfected) cells of genes regulated after IVIG versus control buffer (ctrl) treatment. The last column points to the figure number, in which the qRT-PCR validation of the regulated genes is reproduced. (*)The *p*-values in the tables represent the unadjusted numbers subjected to a Student's *t*-test, but not to a multiple correction; red numbers highlight upregulated and green numbers downregulated genes.

non-differentiating cells: IVIG vs ctrl				
gene name	**accession number**	**fold change**	***p*-value***	**result validation**
Tyrp1	NM_001106664	**5,693**	4,89E-03	Figure 18A
IL-18	NM_019165	**3,054**	8,32E-03	Figure 19A
Olig1	NM_021770	**1,986**	2,37E-02	Figure 18B
Plp1	NM_030990	**1,686**	2,40E-02	Figure 15F
Sox10	NM_019193	**1,034**	5,49E-01	Figure 18C
p57kip2 (Cdkn1c)	NM_182735	**-1,334**	1,99E-01	Figure 18D
p57kip2 (Cdkn1c)	NM_001033757	**-1,257**	4,10E-01	Figure 18D

Table 3. Selected differentially regulated genes of differentiating Schwann cells after IVIG treatment. Represented are the fold change and the corresponding *p*-values* generated by the data processing and statistical analysis of the GeneChip Array study on differentiating (p57kip2 suppressed) cells of genes regulated after IVIG versus control buffer (ctrl) treatment. The last column points to the figure number, in which the qRT-PCR validation of the regulated genes is reproduced. (*)The *p*-values in the tables represent the unadjusted numbers subjected to a Student's *t*-test, but not to a multiple correction; red numbers highlight upregulated and green numbers downregulated genes.

differentiating cells: IVIG vs ctrl				
gene name	**accession number**	**fold change**	***p*-value***	**results validation**
Tyrp1	NM_001106664	**2,706**	3,14E-02	Figure 18A
IL-18	NM_019165	**1,566**	2,62E-01	Figure 19A
Olig1	NM_021770	**1,552**	5,49E-02	Figure 18B
Plp1	NM_030990	**1,127**	3,92E-01	Figure 15F
Sox10	NM_019193	**1,083**	2,30E-02	Figure 18C
p57kip2 (Cdkn1c)	NM_182735	**1,155**	1,80E-01	Figure 18D
p57kip2 (Cdkn1c)	NM_001033757	**-1,093**	7,95E-01	Figure 18D

Initially, the regulation of two genes attracted our attention, namely tyrosinase-related protein 1 (Tyrp1) and interleukin-18 (IL-18), two of the most prominently upregulated genes upon IVIG stimulation in non-differentiating Schwann cells (Fig. 17A, B and table 2). IL-18 is a proinflammatory cytokine, belonging to the IL-1 family (Sedimbi et al., 2013) with yet controversial relevance for the peripheral nervous system (Jander and Stoll, 2001, Menge et al., 2001). Additional information regarding the role of IL-18 expression in Schwann cells and their direct environment is described in the following two chapters (4.9 and 4.10). Tyrp1 is considered a functional component and differentiation marker in melanocytes (Ghanem and Fabrice, 2011), but has recently also been shown to be upregulated in Schwann cells that have failed to dedifferentiate upon nerve transection (Arthur-Farraj et al., 2012). The same authors identified oligodendrocyte transcription factor 1 (Olig1), commonly known as lineage transcription factor involved in oligodendroglial differentiation and maturation (Meijer et al., 2012), as a novel (cJun-dependent) activated gene in denervated Schwann cells. We confirmed the differential upregulation of Tyrp1 transcript levels (tables 2 and 3) by means of quantitative RT-PCR in non-differentiating (control transfected) and differentiation competent Schwann cells after 7 days IVIG treatment (Fig. 18A), as well as in non-differentiating cells after 1 and 3 days of stimulation. Surprisingly, we detected that Olig1 was also strongly upregulated after short-term and long-term stimulation of non-differentiating (Fig. 18F, B) and differentiating Schwann cells (Fig. 18B). Similar outcomes resulted also from the array data (tables 2 and 3) though according to the current literature they do not support our present results in total, reflecting an induction of a differentiation-related phenotype in Schwann cells after IVIG stimulation. Furthermore, staining analysis confirmed Olig1 protein expression in Schwann cells, where the transcription factor was found to be localized in the cytoplasm of the cells (Fig. 18G), similarly to previous observations on oligodendroglial cells of the adult mouse brain (Arnett et al., 2004). The observed upregulation upon IVIG stimulation could not be confirmed on protein level.

Concerning the upregulation of the myelin gene Plp1 previously shown in chapter 4.7 (Fig. 15F) by quantitative RT-PCR, we could detect overlapping trends with the results from the array analysis in differentiating as well as non-differentiating cells (tables 2 and 3). Schwann cell transcription factor Sox10 was only mildly induced according to the GeneChip analysis (tables 2 and 3), though we could demonstrate that in non-differentiating cells this upregulation was significant and sustained over a longer period of time (Fig. 18C). We also found that the expression of the p57kip2 gene, found to encode an intrinsic inhibitor of Schwann cell differentiation (Heinen et al., 2008a), was significantly lowered in control transfected (non-differentiating) cells after 7 days of IVIG stimulation (Fig. 18D). IVIG dependent downregulation of the p57kip2 gene appears to start already after 3 days treatment as revealed by short-term stimulation experiments on cultured Schwann cells (Fig.

18H). This is of interest as the array data revaleded no real regulation of p57kip2 transcript levels (tables 2 and 3) and supportes the notion that GeneChip analyses are less sensitive.

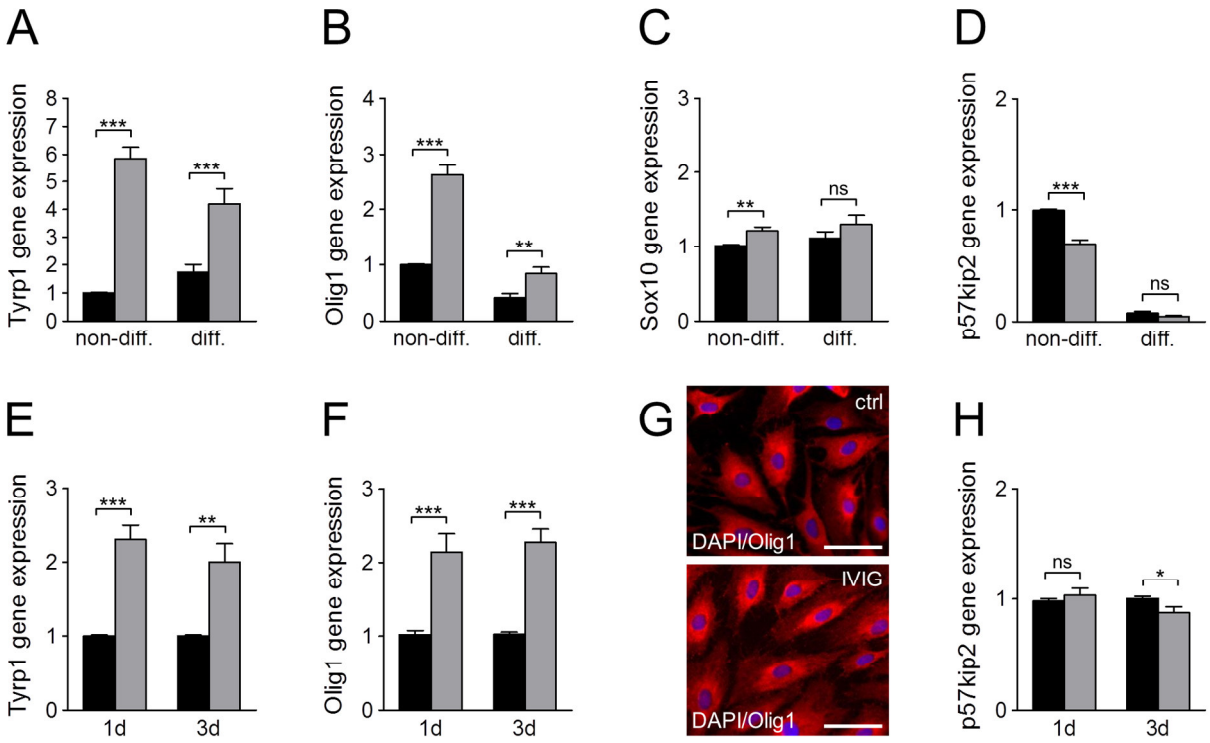

Figure 18. IVIG treatment induces expression of differentiation-related genes. (A-D) Differentiation was induced by p57kip2 suppression (diff. vs control transfected cells (non-diff.)) of cultured Schwann cells and IVIG treatment was performed two days after differentiation was initiated for a total period of 7 days (7d). (E-H) Non-transfected Schwann cells were stimulated with 20 mg/ml dialysed IVIG or ctrl for 1d or 3d in culture. (A, B) Quantitative RT-PCR revealed significant upregulation of Tyrp1 and Olig1 genes upon IVIG stimulation (grey bars, A, B) in both diff. and non-diff. cells when compared to control buffer (black bars). (E, F) Short-term stimulation (1d and 3d) of non-transfected and therefore non-differentiating Schwann cells revealed similar gene upregulation. (C) Sox10 transcriptional levels were upregulated only in non-diff. cells upon IVIG stimulation. (D, H) The expression of the Schwann cell differentiation inhibitor p57kip2 was significantly downregulated not only after 3d but also after a longer period of 7d stimulation with IVIG in non-diff. Schwann cells. (I-J) Staining against Olig1 confirmed the expression of the transcription factor in Schwann cells. GAPDH was used as normalization control in all experiments. *t*-test (ns, not significant, **p*<0.05, ***p*<0.01, ****p*<0.001). Error bars represent SEM. Number of experiments: n=7 for (A-C), n= 12 for (D), n=5 for 1d (E), n=2 for 3d (E), n=8 for 1d (F), n=5 for 3d (F), n=3 for (G), n=13 for 1d (H), n=9 for 3d (H).

4.9 IVIG induce interleukin-18 expression in Schwann cells[23]

One of the most prominently differentially regulated genes upon IVIG stimulation was IL-18, a proinflammatory cytokine, belonging to the IL-1 family (Sedimbi et al., 2013). According to the GeneChip data (table 2 and 3), IL-18 was significantly upregulated in non-differentiating and also slightly increased in differentiating Schwann cells after immunoglobulin treatment. We therefore investigated this finding in greater detail and validated transcript levels by means of quantitative RT-PCR (Fig. 19A). This analysis confirmed the observed strong induction in non-differentiating cells and it could also be shown that IVIG treatment can induce IL-18 expression over a period of at least 9 days (Fig. 19B). These observations could be supported by examination of IL-18 protein levels using ELISA (enzyme-linked immunosorbent assay) (Fig. 19C-E). We could show that cultured Schwann cells consistently produce and secrete elevated IL-18 protein levels at days 1, 4, 7 and 9 upon IVIG stimulation (Fig. 19D). Interestingly, although at late time points differentiating Schwann cells did not show an IVIG dependent increase in IL-18 transcript levels (Fig. 19A), soluble IL-18 protein levels were elevated in both Schwann cell populations after 4 and 7 days (Fig. 19C, E).
In addition, we examined the transcriptional regulation of monocyte attractant protein-1, a further proinflammatory molecule secreted by Schwann cells, involved in both macrophage attraction and activation in the process of Wallerian degeneration (Perrin et al., 2005, Cheepudomwit et al., 2008) as well as in the pathology of genetically induced demyelination (Fischer et al., 2008a). We found Mcp-1 transcript levels to be consistently upregulated at later time points during IVIG stimulation of non-differentiating Schwann cells (Fig. 19F).

[23] for authorship notice please refer to chapter 9.2

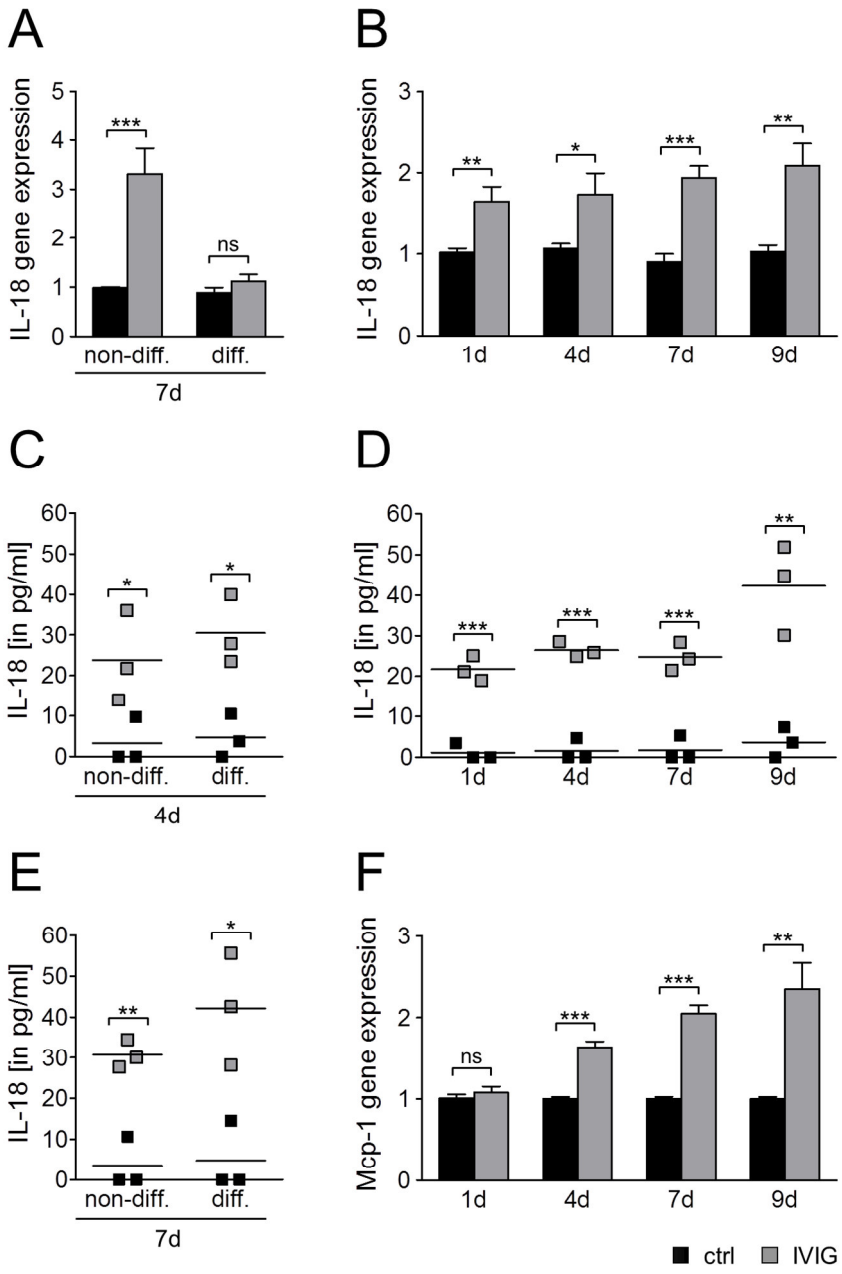

Figure 19. IVIG dependent expression and secretion of IL-18 and Mcp-1. (A, C, E) Two days after transfection differentiating (diff.) and non-differentiating (non-diff.) Schwann cells were stimulated for up to 7 days (7d) with 20 mg/ml dialysed IVIG or control buffer (ctrl) with one medium exchange at 4d. At day 7 quantitative RT-PCR revealed a significant upregulation of IL-18 gene expression in non-differentiating cells (A), but not in differentiating cells. However, ELISA determination revealed elevated secreted IL-18 protein levels at time points, 4d (C) and 7d (E), after IVIG stimulation. (B, D) Similarly induced IL-18 gene and protein expression levels could be observed when naïve (non-transfected and therefore non-differentiating) Schwann cells were IVIG stimulated as shown on time points 1d, 4d, 7d, 9d. Of note, 4d medium was collected before the medium change. (F) Mcp-1 gene expression levels were also upregulated after 4d, 7d and 9d of IVIG stimulation. GAPDH was used as reference gene (A, B, F). *t*-test (ns, not significant, **p*<0.05, ***p*<0.01, ****p*<0.001). Error bars represent SEM. Number of experiments: n=7 for (A), n=3 for (B, F), n=3 for (C, D, E).

4.10 Schwann cell promoted neurite outgrowth is positively influenced by IVIG and IL-18[24]

Considering the previously detected IL-18 expression and secretion (Fig. 19), we investigated whether this cytokine might contribute to the communication between peripheral glial cells and neurons which is among others important for axonal elongation. To this end, we conducted an *in vitro* growth assay using rat DRG explant cultures where we measured axonal outgrowth 24 hours after plating by determination of the relative length of neurofilament-positive neurites, as previously shown (Küry et al., 2002, Heinen et al., 2015). We observed that conditioned medium from Schwann cells treated with IVIG over 3 days could significantly induce neurite outgrowth of sensory neurons (Fig. 20A). Therefore we examined whether IL-18 might contribute to this effect. To test this hypothesis, DRG explants were treated with medium that has been conditioned over a period of 3 days by IL-18 stimulated Schwann cells (Fig. 20B), or supplied with medium freshly supplemented with rat recombinant IL-18 (Fig. 20C). As expected, Schwann cell conditioned medium improved neurite outgrowth (compare levels in Fig. 20A and B vs. C; red dotted line). Importantly, this positive growth effect was further potentiated in a dose-dependent way when medium was conditioned by IL-18 treated Schwann cells (Fig. 20B, D-G). In DRG cultures treated with non-conditioned medium with freshly added IL-18, neurite outgrowth was not affected (Fig. 20C). These results indicate that IL-18 can instruct Schwann cells in order to promote neuritic growth, possibly by means of an enhanced growth factor production.

[24] for authorship notice please refer to chapter 9.2

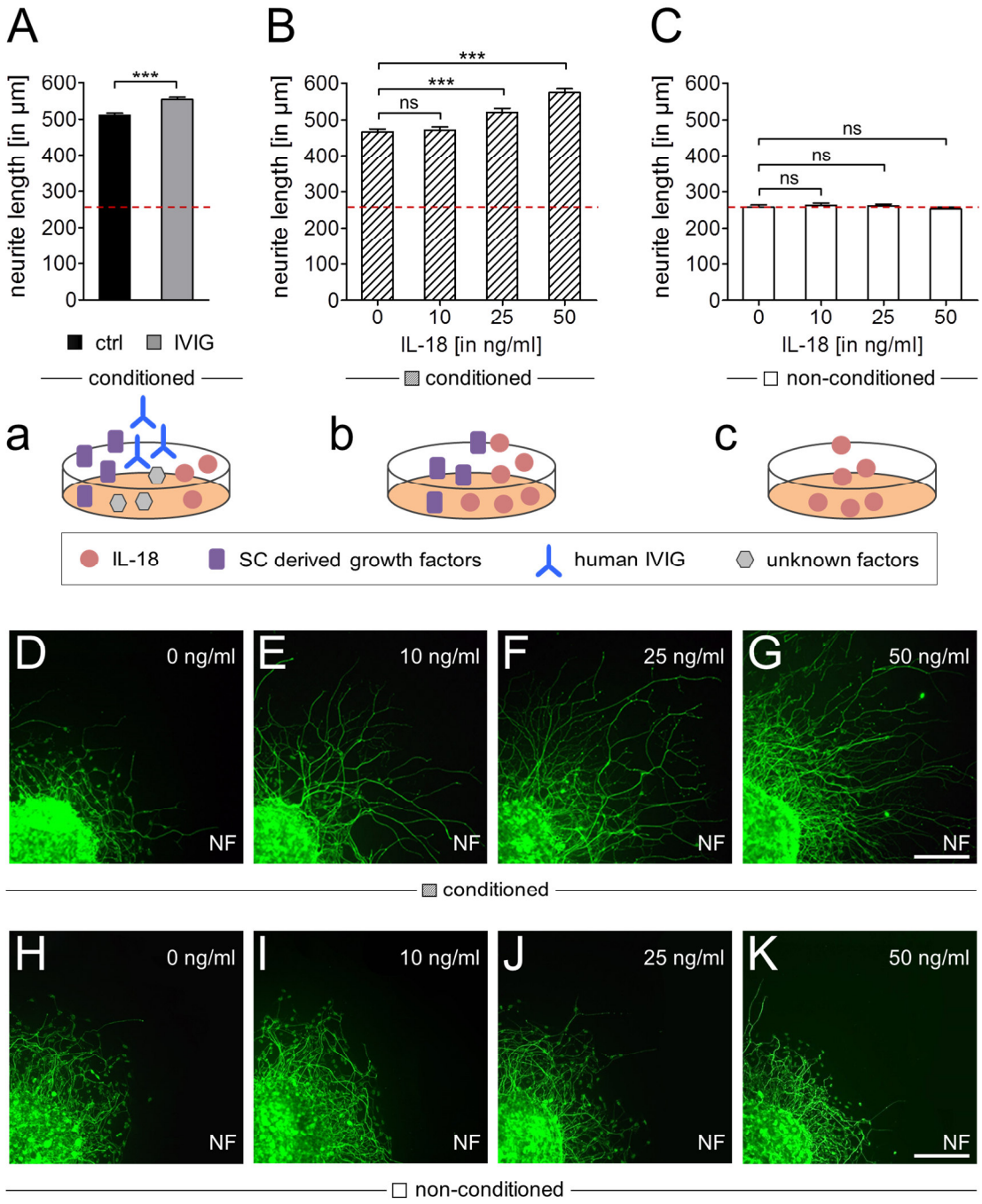

Figure 20. Schwann cell dependent promotion of axonal outgrowth. (A-G) Average neurite growth lengths were determined 24 h after incubation of rat DRG explants in culture medium of Schwann cells treated with control buffer (ctrl), IVIG or different IL-18 concentrations. Three different culture media were used: (A) culture medium conditioned by control buffer treated Schwann cells (black bar) and by cells stimulated with 20 mg/ml dialysed IVIG (grey bar) for 3 days; (B) culture medium conditioned by Schwann cells treated with IL-18 over 3 days and (C) culture medium directly supplemented with IL-18 (non-conditioned). (a-b) Illustrations show the hypothetical medium content used for the 24 h treatment of the corresponding DRG explants: (a) IVIG conditioned medium contains IVIG, Schwann cell (SC) derived IL-18 and growth factors; (b) IL-18 conditioned medium contains IL-18 and SC derived growth factors and (c) non-conditioned medium contains IL-18 only. Quantification of neurite lengths (NF-positive) from the DRG core to the outer rim revealed extensive radial neurite outgrowth in Schwann cell conditioned media (A, B) in comparison to non-conditioned culture media (C). Treatment of Schwann cells with IVIG further increased the neuritic growth (A) and media

conditioned by IL-18 treated Schwann cells also showed a positive, concentration dependent effect on outgrowth (B), whereas direct addition of IL-18 to the culture medium did not exert any effect (C). (D-G) Representative photographs of DRG explants cultured in medium conditioned by Schwann cells, which were stimulated by different IL-18 concentrations (IL-18 conditioned). (H-K) Representative photographs of DRG explants cultured in medium directly supplemented with different IL-18 concentrations (non-conditioned). Neurofilament (NF) staining is visualized in green. *t*-test (ns, not significant, ****p*<0.001). Error bars represent SEM. Scale bar: 200 µm. n=3 for (A), n=5 (B, C), per experiment and condition 6-12 explants were evaluated. Red line marks the average neurite length in response to non-conditioned medium (0 ng/ml IL-18 in C).

5 DISCUSSION[25]

Intravenous immunoglobulins have been used for more than two decades in the treatment of demyelinating immune system disorders, especially inflammatory neuropathies, and their potential immunomodulatory effects have extensively been described (Nimmerjahn and Ravetch, 2008a). However, no direct effect of pooled immunoglobulins on glial cells of the peripheral nervous system, consequently no potential role in modulating the regeneration potential of these cells, has yet been described.

We therefore decided to investigate the possible effect of IVIG on Schwann cells by evaluation of their gene expression, homeostasis, and maturation processes. In the present study a specific binding of human IVIG on the primary rat Schwann cell surface could be demonstrated. In addition, it was revealed that this surface recognition might occur via the variable $F(ab')_2$ domain of the antibody preparation. On the other hand, expression of the high affinity Fc receptor for immunoglobulin binding, CD64, was detected on the cell surface. Treatment with IVIG led to reduced cellular proliferation rates without affecting cell survival. In addition, accelerated growth of cellular processes upon IVIG application resembling early stages of cellular maturation was observed. Furthermore, immature Schwann cells responded to IVIG binding by induction of myelin gene expression and upregulation of signaling cascades positively affecting the myelination process. IVIG treatment resulted in increase of myelin protein expression in differentiating and in myelination competent Schwann cells, as demonstrated by *in vitro* myelinating neuron/glia cocultures. GeneChip array analysis revealed the upregulation of novel Schwann cell lineage factors, including the cytokine IL-18, the melanocyte marker Tyrp1 and the oligodendroglial transcription factor Olig1 upon IVIG stimulation. In addition to enhanced gene expression, our data demonstrated for the first time that Schwann cells secrete IL-18 upon IVIG treatment. In particular, the secretion of this cytokine, but also other putative factors, self-instructs Schwann cells to support axonal growth. It was therefore concluded that IVIG can positively affect Schwann cell differentiation by iduction of maturation related signals.

5.1 Interaction of IVIG with Schwann cells

In our investigations regarding the influence of immunoglobulins on Schwann cells a specific IVIG binding on the cell surface was detected. The underlying mode of action, especially concerning the exact way immunoglobulins interact with Schwann cell surface proteins,

[25] for authorship notice please refer to chapter 9.2

needs to be explored and might include different mechanisms. Currently, we consider two possible ways of surface recognition. The first one is via attachment of the $F(ab')_2$ part of immunoglobulins to Schwann cell epitopes, the second is via binding of the IgG Fc part to corresponding Fc receptors. Detection of CD64 receptor for high affinity IgG binding on Schwann cells, as well as the observation that $F(ab')_2$ fragments, resulting from digested IVIG, specifically interact with the Schwann cell surface, support such dual mode of action. Both surface recognitions might take place either at the same time or separately, depending on the *in vivo* situation. Such a complex mode of action is in line with the current knowledge regarding the IVIG functionality in demyelinating autoimmune diseases where immunoglobulins are thought to interact with the immune system through antigen specific as well as non-specific recognition via $F(ab')_2$- or Fc-mediated immunomodulatory mechanisms respectively (Buttmann et al., 2013).

In this context it is worth mentioning that recent publications suggest that also intrinsic (auto)antibodies, consisting of IgG and IgM molecules, bind to degenerating myelin. This was observed during Wallerian degeneration of peripheral nerves and is thought to accelerate macrophage-mediated phagocytosis (Vargas et al., 2010). Similar immune-related and myelin-labelling mechanisms have been proposed in CMT1 models of inherited neuropathies, where endogenous antibodies might be involved in myelin decoration and thus contribute to macrophage recognition (Martini et al., 2013). Along these observations, IVIG were found to increase the phagocytic activity for myelin debris in macrophages in an *in vitro* model for Wallerian degeneration - a process which involved immune cell Fc receptors (Kuhlmann et al., 2002). Furthermore, in a Theiler's virus-induced animal model of CNS demyelination, monoclonal IgMκ antibodies, raised against spinal cord homogenate, appeared to be polyreactive to intracellular and surface antigens of oligodendrocytes and, as a consequence of binding, they induced remyelination in 20-24 % of the demyelinated area (Asakura et al., 1998). Human IVIG and polyclonal IgM molecules also promoted remyelination in the same animal model, but did not bind on the surface of oligodendrocytes in contrast to human serum-derived monoclonal IgM antibodies (Warrington et al., 2000). The mechanisms of polyclonal antibodies to promote remyelination in the CNS have yet to be revealed and are most likely related to general immunoregulation or neutralization of pathogenic antibodies. In line with the study of Vargas and colleagues (Vargas et al., 2010), the authors of this study hypothesized that the enhanced CNS remyelination capacity of monoclonal antibodies could be due to direct targeting of the monoclonal IgM molecules to damaged CNS myelin (injured oligodendrocytes) and recruitment of microglial cells for faster myelin clearance (Warrington et al., 2000). Nevertheless, these investigations suggest that the way these two antibody classes induce remyelination in the CNS might be different, given

the fact that IVIG also exhibit an immunomodulatory activity via Fc receptors on immune cells (Nagelkerke and Kuijpers, 2014).

Of note, binding of monoclonal human IgG1 molecules (Herceptin and Avastin) was also detected on the Schwann cell surface. This can be considered as an indirect proof of IgG binding via Fc receptors, as Avastin should not be able to recognize any rat Schwann cell epitopes. However, Herceptin recognizes and binds human epidermal growth factor receptor 2 (Her2/ErbB2), which is expressed on the surface of human breast cancer but also on Schwann cells (Slamon et al., 1987, Jin et al., 1993). Hence, it is conceivable but not shown that Herceptin could exhibit xenoreactive effects via binding to the rat ErbB2 receptor. This antibody has already been applied as an ErbB2 receptor blocker in a rat model for peripheral nerve injury, however the authors of this study did not comment on the specificity of the binding to the rat receptor (Placheta et al., 2014). We therefore conclude that immunoglobulin binding via Fc receptors is also likely to occur on Schwann cell surfaces. In order to investigate such Fc dependent functions, future studies should involve fractionation of IVIG preparations and binding assays using isolated Fc fragments.

So far it can be concluded that IVIG most likely exhibit a dual surface recognition pattern on Schwann cells. Binding via the $F(ab')_2$ part of immunoglobulins could be responsible for faster removal of myelin debris by targeting it to peripheral macrophages, as previously shown in WD models (Vargas et al., 2010). According to our gene expression data (Fig. 13), epitope recognition might also be involved in induction of maturation signals in Schwann cells. Such a hypothesis is supported by a number of previous observations documenting that IVIG exhibit reactivity to a number of human self-proteins (Miescher et al., 2005, Schaub et al., 2007, Bussone et al., 2009). The study of Schaub and colleagues (Schaub et al., 2007) showed the self-reactivity of IVIG to be mainly directed against nuclei and the perinuclear cytoplasm of human Hep-2 (larynx carcinoma epithelial) cells. IVIG recognized proteins of different functions and origins from the cytoplasmic extract of Hep-2 cells including actin, tubulin, heat-shock proteins, some enzymes, nuclear components and other proteins, many of which have already been mentioned in the context of autoimmune and/or inflammatory diseases (Schaub et al., 2007). A different study, investigating the IVIG autoantibody reactivity to cytoplasmic extracts of HUVEC (human umbilical vein endothelial cells) and nuclear proteins enriched extracts of Hep-2 cells, identified 96 different proteins 14 of which were common to both extracts (Bussone et al., 2009). These comprised glycolysis, RNA processing and cytoskeletal proteins, but no membrane proteins, since the applied isolation procedure did not allow their determination (Bussone et al., 2009). An identification of the Schwann cell epitopes recognized by IVIG would constitute a major step towards understanding of the contribution of glial-reactive IgG antibodies to therapeutic effects of the IVIG preparations. Such investigations will be reserved for future experiments and will imply

state of the art biochemical analyses of Schwann cell membrane proteins. Moreover, currently it can not be excluded that other immunoglobulin classes such as IgM, already shown to be effective in oligodendoglial differentiation, or IgA, present in trace amounts in IVIG, also bind to the Schwann cell surface. Their potential influence on the glial cells of the PNS also needs to be addressed in future studies.

5.2 Immunoglobulin receptor expression on Schwann cells

In the present study it could be demonstrated that the CD64 receptor for high affinity IgG binding is expressed on the rat Schwann cell surface. Previous studies using nerve sections revealed that human Schwann cells express an Fc gamma receptor (Vedeler et al., 1989), later designated as FcγR3, the low affinity immunoglobulin binding receptor CD16 (Vedeler and Fitzpatrick-Klove, 1990, Vedeler et al., 1991). Nevertheless, human Schwann cells appeared to lose the receptor expression when kept in culture, suggesting expression of FcγR3 is dependent on axonal contact (Vedeler et al., 1990). Furthermore, the FcγR3 expression in cultured rat Schwann cells was confirmed, however, to a much lesser extent as compared to macrophages (Vedeler et al., 1992). This is in line with our data showing that differentiation competent Schwann cells, which have exited the cell cycle and have initiated maturation (Heinen et al., 2008a), show a significant upregulation of the CD64 receptor when compared to cultured non-differentiating Schwann cells. Consequently, an involvement of the CD64 receptor in Schwann cell maturation can be suggested. Again this hypothesis will require future confirmation, including an examination of receptor expression during nerve development or after nerve injury.

As already described earlier, Fc receptors are also expressed on cells of the CNS such as microglia, astrocytes, oligodendrocytes and neurons (Okun et al., 2010). For more details please refer to chapter 2.6.3 in the introduction. Oligodendrocytes were shown to express an Fc receptor for IgM as well as FcR gamma chain, the common gamma chain of immunoglobulin Fc receptors. The latter is most likely involved in OPC differentiation (Nakahara et al., 2003a, Nakahara et al., 2003b). FcγRs on microglia were shown to be responsible for activation of these immune-like cells and consequent aggravation of pathological processes in CNS demyelinating diseases or ischemic stroke (Ulvestad et al., 1994, Komine-Kobayashi et al., 2004). Neuronal FcγR expression was brought in connection to pain and inflammatory signaling in sensory DRG neurons. Furthermore, a possible developmental role in cerebellar neurons was suggested (Andoh and Kuraishi, 2004a, Nakamura et al., 2007).

CD64 expression on Schwann cells suggests that this receptor exerts a certain immune-modulatory function and might be involved in binding immune complexes, induction of phagocytosis or local (immuno)regulation. Our observations revealed a downregulation of the CD64 receptor expression in non-differentiating Schwann cells after IVIG treatment, probably due to a receptor blockade via IVIG. Similar IVIG mechanisms of action have been proposed for macrophages, where activating Fc receptors are blocked but inhibitory ones are upregulated leading to a diminished immune competence and thus to an anti-inflammatory mode of action (Schwab and Nimmerjahn, 2013). Further to this, by applying human monoclonal IgG1 antibodies, which most likely bind to Fc receptors on the Schwann cell surface, none of the observed maturation effects induced by the polyclonal IVIG product could be observed. The role of CD64 in Schwann cells, whether responsible for immunoglobulin binding or a different not yet known function will be addressed in future experiments.

CD64 is an activating receptor and as such contains an immunoreceptor tyrosine-based activation motif (ITAM) in its Fc receptor common gamma chain. Phosphorylation of ITAM is performed by activated intracellular Src-family protein tyrosine kinases, such as Fyn, Src and Lyn. Subsequent downstream signaling events in immune cells involve SYK kinase activation (Takai, 2002). Of note, it has already been proposed that the FcγR-Fyn-MBP signaling cascade is crucial for OPC differentiation and CNS myelination processes (Nakahara et al., 2003b). However, SYK expression could not be detected in rat Schwann cells on protein or transcript levels, indicating that different pathways are employed in glial cells.

Another interesting function of Fc receptors is the internalization of bound antigen-antibody immune complexes and the consequent antigen presentation to MHC class I or class II antigen-presenting molecules (Takai, 2002). As recently reviewed, Schwann cells are well-known for their immune cell-like properties and indeed express MHC class molecules on their surface and are therefore considered accessory antigen presenting cells (Tzekova et al., 2014). Future investigations will address the question whether there is a connection between Fc receptor expression and antigen presentation in Schwann cells.

Another vague possibility implies that CD64 expression in Schwann cells might not necessarily be connected to immunoglobulin binding. Fc receptors were shown to possess the ability to bind non-immunoglobulin ligands on the surface of other cell types. In this regard Galon and colleagues have shown that a soluble form of the extracellular domain of CD16 receptor, present in blood plasma, bound to complement receptor (CR) 3 and 4 on leukocytes (Galon et al., 1996). This binding resulted in proinflammatory cytokine secretion by monocytes and dendritic cells (Galon et al., 1996). We have recently summarized a number of immune mediator molecules secreted by Schwann cells and pointed out that these cells also express components of the complement system (Tzekova et al., 2014). It

can therefore not be excluded that the CD64 receptor on Schwann cells is involved in a different immunomodulatory role such as interacting with complement molecules.
Future experiments with IVIG derived Fc fragments will be an important step toward the elucidation of antibody binding modes on the Schwann cell surface as well as the cellular reactions issued by this surface interaction. Additional experiments are needed to determine the function of the CD64 receptor in PNS glial cells. CD64 knockout mice exist already and it has been revealed that the deletion of this receptor leads to profound alterations in immunomodulatory cell responses (Barnes et al., 2002). Nevertheless, these mice can not be considered as a suitable *in vivo* model for functional studies on the CD64 receptor role in Schwann cells. Notably, a lot of cells express FcγR1, including immune cells such as macrophages, monocytes and dendritic cells, along with various neural cells (Okun et al., 2010, van der Poel et al., 2011). An interesting aspect for future investigations would thus comprise the generation of a Schwann cell specific FcγR1 deficiency. This conditional knockout could be achieved by crossing mice expressing the FcγR1 gene targeted with loxP sites (34-base pair palindromic sequences) with mice expressing the Cre recombinase as transgene under the control of a Schwann cell-specific promoter, for instance P0/Mpz.

5.3 IVIG promote Schwann cells differentiation signals

Differentiation and functional maturation of Schwann cells is highly dependent on the expression of myelin proteins. We found that expression levels of the most prominent myelin genes and major Schwann cell differentiation related transcription factors, such as Krox20, Sox10 and Oct-6 (Jessen and Mirsky, 2002), were transiently induced in non-differentiating Schwann cells after short-term IVIG stimulation. This was corroborated by the observation that signaling molecules, prominently involved in regulating Schwann cell differentiation, such as Akt (Ogata et al., 2004), depicted significant upregulation on protein level. On the other hand, PTEN, a molecule acting upstream of the Akt signaling pathway and thereby responsible for Akt inhibition (Cotter et al., 2010, Goebbels et al., 2010), was downregulated after IVIG stimulation. The observed transient myelin gene upregulation in non-differentiating Schwann cells can be explained with the fact that cells used in our model were cultured in presence of 2 µM forskolin, enabling the cells to divide faster while differentiation does not take place (Küry et al., 2002).
Notably, IVIG managed to sustain not only myelin gene but also protein upregulation for much longer periods of time in differentiation competent Schwann cells. These findings were then supported by the observation that IVIG stimulation also significantly increased numbers of myelin internodes in the applied *in vitro* myelination culture system providing strong

evidence that in differentiation competent cells (as induced following suppression of the p57kip2 gene; (Heinen et al., 2008a)) or in presence of axons glial maturation is clearly promoted by IVIG. There are already several publications reporting a beneficial effect of polyvalent immunoglobulins on CNS and PNS remyelination (Rodriguez and Lennon, 1990, van Engelen et al., 1994, Gabriel et al., 1997, Warrington et al., 2000, Lin et al., 2007a). Although polyclonal IgM molecules turned out to be more potent inducers of oligodendrocyte differentiation and remyelination in different CNS *in vivo* demyelination models, human IVIG can also promote this process (Bieber et al., 2000, Warrington et al., 2000, Bieber et al., 2002). On the other hand, treatment of rats with induced experimental autoimmune neuritis (EAN), an animal model of GBS, using human IVIG induced recovery and amelioration of disease course and showed more extensive remyelination in their nerves upon histological analysis (Gabriel et al., 1997, Lin et al., 2007a). In a follow up study, the authors demonstrated that this effect was due to the Fc rather than the $F(ab')_2$ portion in IVIG, though IVIG still turned out to be superior (Lin et al., 2007b). It is debatable whether the above-mentioned IVIG effects are due to regulation of the immune related processes, to myelin opsonisation allowing faster myelin repair or due to a direct IVIG effect on oligodendrocytes and Schwann cells. The latter of which has so far not been studied and reported. It is only here, in the present study where first direct evidence that IVIG interact and instruct Schwann cells is provided. Since IVIG also reduced glial proliferation rates and myelin synthesis by Schwann cells starts when cell proliferation is arrested, this was considered an additional evidence for initiation of the glial differentiation process. Of note, in a paper focusing on the IVIG effect on immune cells, similar results regarding proliferation control have been obtained in cultured human Schwann cells from nerve biopsies and fibroblasts. IVIG were shown to inhibit cell growth in concentrations (15 mg/ml) similar to those used in our study (van Schaik et al., 1997). Moreover, using our model of differentiation competent Schwann cells (Heinen et al., 2008a), we found that IVIG induced also an accelerated growth of cellular processes in early stages of the differentiation process. Thus, IVIG seem to positively influence the morphology of cells towards differentiation.

As discussed above it can be speculated whether this maturation promoting effect is either due to epitope or Fc receptor binding, or results from both interactions together. Using digested $F(ab')_2$ fragments from IVIG for cell stimulation, we not only detected binding to the Schwann cell surface but also induction of myelin genes. Since for technical reasons it was not possible to use IVIG derived Fc fragments, monoclonal IgG1 antibodies were applied instead. Importantly, while they bound to the Schwann cell surface, they clearly failed in promoting glial maturation. This important experiment indicated that the cellular reaction is not induced by the IgG1 content of the pooled immunoglobulins alone, but by IVIG as a whole product. Despite the fact that IVIG mostly contain IgG1 molecules, future stimulation

experiments with IgG2, IgG3 and IgG4 subclasses should be conducted in order to determine whether they might be involved in the induction of cellular differentiation. Of note, expression of the corresponding FcγRs for IgG2 and IgG4, FcγR2 and FcγR2 or FcγR3, respectively, was not detected on the rat Schwann cell surface. IgG1 and IgG3 bind to all receptors. On the other hand, it has also to be considered that as human monoclonal antibodies, the used IgG1s should not be able to recognize rat epitopes and are therefore more likely to bind via Fc receptors. Of note, the Avastin IgG1 which binds selectively human soluble vascular endothelial growth factor (VEGF) and the Synagis IgG1 which binds to an A epitope of a fusion protein of the human Respiratory Syncytial Virus (RSV) cannot bind to epitopes on the Schwann cell surface. Herceptin, on the other hand, could eventually bind to Schwann cell epitopes, as the target protein ErbB2 is naturally expressed in this lineage. Moreover, we could then show that this binding does not induce the same reactions as IVIG, supporting the conclusion that neither the IgG1 fraction nor binding to ErbB2 was responsible for the effect alone.

Of note, in a recent research article Herceptin has been used as ErbB2 receptor inhibitor in a rat model for nerve regeneration (Placheta et al., 2014). The authors paid attention to the direct effect on nerve recovery and observed increased outgrowth of axons upon Herceptin treatment, although this effect was apparently independent of neuregulin-ErbB2 signaling and hence in contrast to the expected results. Subsequently, Akt phosphorylation in the nerve tissue was significantly diminished despite the positive effect on regenerating nerves (Placheta et al., 2014). IVIG stimulation of non-differentiating cultured Schwann cells, on the other hand, led to induction of Akt phosphorylation, indicating that IVIG possibly activate different pathways from Herceptin, independently from the way they bind on the Schwann cell surface. Nevertheless, the control experiments conducted with either $F(ab')_2$ fragments or IgG1 point to a potential mechanism of action where for IVIG both binding possibilities could take place either at the same time or at different time points depending on the *in vivo* situation and the availability of the Fc receptor or epitope expression. As we could not detect mRNA and protein expression of SYK, a kinase, which is involved in the downstream signal transduction of activating Fc receptors in immune cells (Mocsai et al., 2010), it can be suggested that the initiation of Schwann cell differentiation signals might take place through the variable region of the immunoglobulins. The initiation of yet to be defined signal transduction pathways in Schwann cells, stimulated via Fc receptor or $F(ab')_2$ binding, will be addressed in follow up studies. Furthermore, it can not be excluded that Fc signaling in Schwann cells might not be SYK-dependent.

IVIG also induced additional reactions in Schwann cells such as upregulation of Olig1 and Tyrp1 genes or downregulation of the glial differentiation inhibitor p57kip2 as revealed by GeneChip array analysis. Olig1 was among the most upregulated transcripts upon IVIG

stimulation in non-differentiating as well as differentiating Schwann cells. Olig1 is a basic helix-loop-helix transcription factor, known to be expressed predominantly in the CNS and in both developing and mature oligodendrocytes (Ligon et al., 2006). It promotes differentiation of oligodendrocyte precursor cells into mature oligodendrocytes, is needed for postnatal myelination (Xin et al., 2005) and has a role in remyelination (Arnett et al., 2004). However, little is known about Olig1 functions in the PNS. In a recent study Olig1 has been mentioned for the first time in the context of peripheral glial cells and as a gene which shows strong cJun dependent induction in denervated Schwann cells of injured sciatic nerves, suggesting a role in the regeneration process (Arthur-Farraj et al., 2012). In line with this observation, another group detected Olig1 expression in myelinating and non-myelinating mouse nerve tissue and showed remarkable Olig1 transcript downregulation after high-dose forskolin-induced differentiation in cultured Schwann cells. (Schmid et al., 2014). The authors concluded that Olig1 is a newly discovered transcription factor for the Schwann cell lineage, exerting a certain role in these cell's differentiation processes (Schmid et al., 2014). As these authors defined induced Schwann cell differentiation solely by a significant upregulation of Mpz/P0 transcripts, whereas crucial Schwann cell transcription factors such as Sox10 and Krox20 were not regulated by forskolin treatment, and myelin genes such as Mbp and plasmolipin (Pllp) were even downregulated (Schmid et al., 2014), the conclusions drawn in this paper are probably premature and need to be re-addressed. Even more so, since in contrast to the decreased Olig1 expression in differentiating cells, the authors detected gradually increased Olig1 expression levels during peripheral nerve development (Schmid et al., 2014). In the present work, the observed upregulation of Olig1 after IVIG stimulation did not correlate with cJun regulation, as cJun protein expression remained constant upon treatment. It was therefore concluded that Olig1 upregulation by IVIG is cJun independent and hence rather supports the differentiation potential of Schwann cells, which is in line with the above mentioned upregulation of Olig1 in sciatic nerve development (Schmid et al., 2014). Nevertheless, a role for Olig1 in regeneration of peripheral nerves cannot be excluded.

In our study Olig1 was detected exclusively in the cytoplasm, whereas Schmid and colleagues (Schmid et al., 2014) noticed Olig1 mainly in the cytoplasm but also weakly expressed in nuclei. In the CNS, the cellular sublocalization of Olig1 changes depending on the developmental stage of oligodendrocytes (reviewed in (Göttle and Küry, 2015)). Nuclear localization can be observed in early development and with proceeding maturation this transcription factor becomes redistributed to the cytosol, where it remains in cells of the adult white matter (Arnett et al., 2004). The function of Olig1 was further elucidated showing that the nuclear form facilitates MBP expression, but the cytoplasmic one is responsible for membrane extension (Niu et al., 2012). In response to injury Olig1 again translocates into

nuclei and is thus necessary in the remyelination process (Arnett et al., 2004). One interesting aspect for future studies would be to determine whether Olig1 subcellular localization in Schwann cells also plays an important role for its activity and function. Using the established model of myelinating neuron/glia cocultures its subcellular localization during the maturation and *in vitro* myelination process could be examined. Furthermore, genetic manipulation of participating Schwann cells by means of Olig1 overexpression or RNA interference dependent suppression (similarly to experiments performed in (Heinen et al., 2012)) could shed light on its functional impact.

In the present study the myelinating glial cell specific transcription factor Sox10 was upregulated after short- and long-term IVIG stimulation experiments. Interestingly, it has recently been shown that Sox10 is involved in induction of Mbp transcription in the CNS by binding to Olig1 in oligodendrocytes (Li et al., 2007). Moreover, Sox10 can regulate the expression of Tyrp1, one of the essential proteins required for melanin synthesis in melanocytes (Harris et al., 2010). It can therefore be assumed that Sox10 is active upstream of Tyrp1 in Schwann cells and might consequently be responsible for their induction upon IVIG stimulation.

To date, Tyrp1 has only been mentioned once in context of PNS regeneration. This gene was identified as one of the most significantly upregulated genes in Schwann cells that fail to dedifferentiate in injured nerves upon depletion of the cJun gene (Arthur-Farraj et al., 2012). This could be interpreted as involvement in the glial differentiation process and would be in line with our findings, where Tyrp1 expression was highly increased after IVIG stimulation (Fig. 17 and Fig. 18). Remarkably, it was also found to be decreased in Schwann cells, which adapt to a repair cell phenotype (Heinen et al., 2015). Although the exact function of Tyrp1 in Schwann cells is not clear yet, numerous publications exist which point to a direct connection between melanocytes and Schwann cells. This is even more intriguing, given the fact that both cell types originate from the same progenitors, the neural crest cells (Le Douarin et al., 1991, Erickson, 1993). There are observations showing that melanocytes develop from peripheral nerve cells after severe nerve injury and that this process is most likely induced by the presence of certain cytokines of the injured environment (Rizvi et al., 2002). It has also been demonstrated that melanocytes do not exclusively arise from neural crest cells but also from Schwann cell precursors on extending spinal nerve ends below the skin (Adameyko et al., 2009) and that this process is strictly regulated by an interplay of lineage-specific transcription factors (Adameyko et al., 2012). A further description of the Tyrp1 protein and its interactions and roles in Schwann cells would therefore be of considerable interest for future studies. Nevertheless, the regulation of most of the above mentioned transcripts upon IVIG stimulation, along with the downregulation of the glial differentiation inhibitor p57kip2, support the observed tendency for an initiation of differentiation signals in Schwann cells.

Future studies should then also try to reveal to what degree glial reactions depend on IgG monomers, dimers, or oligomers. The presence of monomeric and dimeric IgG fractions in IVIG is well documented (Gronski et al., 1988a, Gronski et al., 1988b) and it has been shown that pooling of the immunoglobulins and to a reduced extent the preparation method are responsible for dimer formation, as immunoglobulins in single donor plasma are usually monomeric (Tankersley et al., 1988, Roux and Tankersley, 1990). IVIG tolerability in patients is thought to be dependent on the dimer content of IgG preparations, as it can induce inconvenient side effects in humans, and is therefore kept minimal in the formulated IVIG products (Miescher et al., 2005). All three components, monomers, dimers, or oligomers, occur in non-dialysed and dialysed IVIG solutions (87-89 % monomers and 10-13 % dimers), but the amount of oligomers/polymers is considered non-significant (less than 1 %; see Materials and methods section, SEC data; (Teeling et al., 2001)). According to our SEC data, IgG dimers are present but their fraction did not substantially change upon dialysis over time. It has already been shown that dimers most likely result from idiotype-anti-idiotype reactions, which occur between the immunoglobulins of different donors (Roux and Tankersley, 1990, Tankersley, 1994). This fact makes them less likely to bind on Schwann cell epitopes, but one should be aware that these dimers could induce additional cellular reactions via Fc receptors. A biochemical separation of monomeric and dimeric fractions could thus be of interest for the future investigations aiming at the description of the underlying mode of action.

5.4 IL-18 cytokine expression in the PNS

In the present work, it could be shown for the first time that Schwann cells express and secrete the cytokine IL-18 and that expression levels were induced upon stimulation with IVIG. IL-18 is considered a proinflammatory cytokine, belonging to the IL-1 family. Its expression is not only restricted to immune competent cells such as T lymphocytes and macrophages, but also described for neural cells such as microglia and astrocytes and other non-immune cells like keratinocytes and osteoblasts (Nakanishi et al., 2001). This cytokine plays multiple roles in protection against intracellular host infections by inducing IFNγ production in type 1 T helper cells (Th1), NK and CD8+ cells. It is also involved in allergic responses by initiating Th2 cell maturation, and is considered an important link between the immune system and other tissues of the body due to its expression by various cell types (Nakanishi et al., 2001). IL-18 has also been detected in the peripheral nervous system. In particular, in inflamed nerve roots of EAN rats, the animal model of experimental autoimmune neuritis, as well as in serum and cerebrospinal fluid of GBS patients, elevated

levels of IL-18 were found, and corresponding immunostainings co-localized with activated macrophages (Jander and Stoll, 2001). Furthermore, IL-18 was induced after peripheral injury in the first week after nerve crush, but the upregulated expression was again attributed to macrophages and their role in myelin recognition and uptake in the initial phases after axonal injury (Menge et al., 2001).

Besides IL-18, another proinflammatory molecule to be regulated in response to immunoglobulin stimulation was identified. In cultured Schwann cells, IVIG induced transcript levels of the chemokine Mcp-1, known to attract macrophages to the site of injury in Wallerian degeneration and models of CMT (Martini et al., 2013). While Mcp-1 expression can be beneficial for the inflammation process after nerve injury it exerts a negative impact on inherited demyelination diseases. In such conditions the nerve regeneration process is impaired and proinflammatory mediators lead to enhanced inflammation and even more severe myelin damage (Martini et al., 2013). In order to learn more about the role of these cytokines, IL-18 secretion and Mcp-1 expression should therefore be examined in suitable *in vivo* models of peripheral nerve injury, possibly upon IVIG stimulation.

The secretion of IL-18 by Schwann cells is an indirect evidence for inflammasome activation in peripheral glial cells by IVIG, since inflammasome activation is needed for the cleavage of immature IL-18. Inflammasomes are intracellular nucleotide-binding oligomerization domain (NOD)-like receptors (short NLRs), a kind of pattern recognition receptors, which converge into large multi-protein complexes, activating proinflammatory caspase-1 as a consequence (Schroder and Tschopp, 2010). Caspase-1 is involved in the cleavage, hence in the maturation of interleukins such as IL-1 beta and IL-18, two potent proinflammatory cytokines playing a role in infection at the sites of injury (Schroder and Tschopp, 2010). Schwann cells also express the P2X7 receptor, shown to be involved in the inflammasome cascade activation and production of active IL-1β and IL-18 (Perregaux et al., 2000), underlining the importance of these cells as immune competent cells in the peripheral nervous system (Colomar et al., 2003). On the other hand, it has recently been demonstrated that IVIG protect neurons in an animal model for ischemic stroke, by quenching the NLR pyrin domain-containing (NLRP) NLRP1 and NLRP3 inflammasome-mediated neuronal death which consequently downregulates the maturation of both pro-inflammatory cytokines IL-1 beta and IL-18 (Fann et al., 2013). Although this regulation is the other way around it should be considered relevant in future studies since cortical neurons also seem to respond to IVIG and express IL-18 (Fann et al., 2013). Most of the literature emphasizes the proinflammatory character of IL-18; nevertheless, some different aspects of its function could be revealed in our study. Notably, IL-18 seems to instruct Schwann cells in order to induce axonal outgrowth more efficiently. Whether this positive response is due to an auto- or paracrine effect on Schwann cells or due to a beneficial cross-interaction between IL-18 and other yet

unknown glial cell secreted neurotrophic factors is yet unknown. It would therefore be interesting to see if Schwann cells express the IL-18 receptor in order to detect auto- or paracrine signals from their environment or whether the related IL-1 receptor can adopt this role.

5.5 Biomedical relevance of IVIG effect on Schwann cells

For more than two decades intravenous immunoglobulins have successfully been used as first-line therapy in the treatment of inflammatory demyelinating neuropathies of the PNS, such as GBS, CIDP and MMN (Dalakas, 2004, Gold et al., 2007). Moreover, they are occasionally also applied for the treatment of demyelinating disorders of the CNS, such as some cases of Multiple sclerosis (Buttmann et al., 2013). Their immunomodulatory effects which include binding to pathogenic antibodies/anti-idiotype interactions, inhibition of complement binding and thus prevention of lytic attack, suppression of proinflammatory cytokines, modulation of cells of the immune system and their receptors, as well as possible modes of action have extensively been described (Dalakas, 2004, Nimmerjahn and Ravetch, 2008a, Buttmann et al., 2013, Schwab and Nimmerjahn, 2013). Nevertheless, there are still many pathological nerve conditions where urgent treatment is needed. One such case is nerve regeneration after acute injury. Vargas and colleagues (Vargas et al., 2010) showed that endogenous antibodies are necessary for faster regeneration after peripheral nerve injury, as they attract macrophages to subsequently clear myelin debris by phagocytosis. The application of the human monoclonal antibody Herceptin has also been shown to stimulate axonal outgrowth after nerve transection (Placheta et al., 2014). Nonetheless, up to this moment there are no studies revealing a direct positive effect of pooled immunoglobulins on the peripheral nerve regeneration capacity after injury. In the CNS, IVIG are now being considered a potential pharmacological treatment of spinal cord injury (Tzekou and Fehlings, 2014), as a single low dose of human IgG shortly after injury reduced inflammation in the scar and was sufficient to enhance functional recovery (Nguyen et al., 2012). In the study presented here, it could be demonstrated that the cytokine IL-18, induced by IVIG stimulation, positively influenced Schwann cells to promote axonal growth. It would be therefore of interest to address in future investigations the application and possible effect of immunoglobulins in the regeneration capacity of peripheral nerves after acute injury. For this purpose we propose an *in vivo* model where IVIG can be administered upon axotomy of rat sciatic nerves. The degeneration phase of the nerves can be kept very short by applying immediate surgical repair or it can be prolonged from several days up to four weeks, thus prompting more severe nerve damage and inflammation processes. In order to prevent

spontaneous relegation, hence nerve regeneration in the second paradigm, both detached nerve ends can be sutured. This setup results in chronically injured and denervated nerve segments. After a defined degeneration period (short- or long-term), an end-to-end nerve anastomosis can be performed to enable again axonal repair. During this regeneration phase IVIG and a corresponding buffer control can be administered to the animals. Using different parameters such as histological analysis, electrophysiological measurements of nerve conduction and functional evaluation tests, the potential immunoglobulin impact on nerve repair can be undertaken. This *in vivo* paradigm would give us the opportunity, on the one hand to observe the IVIG effect on immediate regeneration phases of Wallerian degeneration. On the other hand, IVIG impact on long-term chronic denervated nerves can be evaluated. Such investigations are of high biomedical relevance and would eventually answer the question whether pooled immunoglobulins also exert a regenerative role *in vivo*. Upon delivering such a proof of connect, subsequent studies should then focus on the function of the FcγR in Schwann cells as these receptors may provide novel targets for therapeutic intervention in peripheral neuropathies or in acute nerve injury.

5.6 Conclusions

Taken together, this study shows for the first time that human immunoglobulins specifically bind to Schwann cell surfaces, resulting in induction of the glial differentiation process, which is of importance for promotion of regeneration. According to our results, two possible ways of surface recognition can be considered, via the F(ab') or the Fc domain of immunoglobulins. IVIG binding on certain Schwann cell epitopes can be of importance for activation of maturation-related factors by triggering yet unknown cellular signaling pathways. The identification of these glial epitopes would be a challenge for future experiments. Nevertheless, possible IVIG recognition via Fc receptors on the cell surface cannot be excluded, as we demonstrated that Schwann cells express the CD64 receptor for immunoglobulin binding. Our results confirm the well-known fact that Schwann cells are not only essential as glial cells and support for the peripheral nerve, but also possess important immunomodulatory functions. IVIG promoted the upregulation of a novel transcription factor, known to be involved in oligodendrocyte maturation. It also induced the expression of melanocyte-related marker, which, according to the current literature, can be connected to Schwann cell differentiation. The regulation of these novel genes for the Schwann cell lineage was accompanied by a significant induction of myelin gene and protein expression, along with activation of Schwann cell differentiation associated signaling molecules and transcription factors. Furthermore, increased expression as well as secretion of

proinflammatory molecules by Schwann cells was detected upon IVIG stimulation. This led to a positive effect on the neuronal compartment, by instructing the glial cells to promote axonal outgrowth. Treatment with IVIG reduced cellular proliferation rates and accelerated growth of Schwann cell processes, resembling early maturation stages. These results indicate a direct positive IVIG effect on the glial cells of the PNS and point out an important role for immunoglobulins in the plasticity of the Schwann cell differentiation process. Additional *in vitro* studies are needed in order to understand the underlying molecular pathways by which the IVIG effect is mediated in Schwann cells. Further to this, *in vivo* nerve injury models can be used to elaborate the potential IVIG influence on nerve regeneration and remyelination.

6 REFERENCES[26]

Abbott NJ, Ronnback L, Hansson E (2006) Astrocyte-endothelial interactions at the blood-brain barrier. Nature reviews Neuroscience 7:41-53.

Adameyko I, Lallemend F, Aquino JB, Pereira JA, Topilko P, Müller T, Fritz N, Beljajeva A, Mochii M, Liste I, Usoskin D, Suter U, Birchmeier C, Ernfors P (2009) Schwann cell precursors from nerve innervation are a cellular origin of melanocytes in skin. Cell 139:366-379.

Adameyko I, Lallemend F, Furlan A, Zinin N, Aranda S, Kitambi SS, Blanchart A, Favaro R, Nicolis S, Lubke M, Müller T, Birchmeier C, Suter U, Zaitoun I, Takahashi Y, Ernfors P (2012) Sox2 and Mitf cross-regulatory interactions consolidate progenitor and melanocyte lineages in the cranial neural crest. Development 139:397-410.

Ahn M, Moon C, Jeong C, Matsumoto Y, Koh CS, Shin T (2010) Upregulation of erythropoietin in rat peripheral nervous system with experimental autoimmune neuritis. Brain research 1333:82-90.

Andoh T, Kuraishi Y (2004a) Direct action of immunoglobulin G on primary sensory neurons through Fc gamma receptor I. FASEB journal : official publication of the Federation of American Societies for Experimental Biology 18:182-184.

Andoh T, Kuraishi Y (2004b) Expression of Fc epsilon receptor I on primary sensory neurons in mice. Neuroreport 15:2029-2031.

Anthony RM, Wermeling F, Karlsson MC, Ravetch JV (2008) Identification of a receptor required for the anti-inflammatory activity of IVIG. Proceedings of the National Academy of Sciences of the United States of America 105:19571-19578.

Archelos JJ, Roggenbuck K, Schneider-Schaulies J, Linington C, Toyka KV, Hartung HP (1993) Production and characterization of monoclonal antibodies to the extracellular domain of P0. Journal of neuroscience research 35:46-53.

Armati PJ, Pollard JD, Gatenby P (1990) Rat and human Schwann cells in vitro can synthesize and express MHC molecules. Muscle & nerve 13:106-116.

Arnett HA, Fancy SP, Alberta JA, Zhao C, Plant SR, Kaing S, Raine CS, Rowitch DH, Franklin RJ, Stiles CD (2004) bHLH transcription factor Olig1 is required to repair demyelinated lesions in the CNS. Science 306:2111-2115.

Arthur-Farraj PJ, Latouche M, Wilton DK, Quintes S, Chabrol E, Banerjee A, Woodhoo A, Jenkins B, Rahman M, Turmaine M, Wicher GK, Mitter R, Greensmith L, Behrens A, Raivich G, Mirsky R, Jessen KR (2012) c-Jun reprograms Schwann cells of injured nerves to generate a repair cell essential for regeneration. Neuron 75:633-647.

[26] for authorship notice please refer to chapters 9.1 and 9.2

Asakura K, Miller DJ, Pease LR, Rodriguez M (1998) Targeting of IgMkappa antibodies to oligodendrocytes promotes CNS remyelination. The Journal of neuroscience : the official journal of the Society for Neuroscience 18:7700-7708.

Asakura K, Pogulis RJ, Pease LR, Rodriguez M (1996) A monoclonal autoantibody which promotes central nervous system remyelination is highly polyreactive to multiple known and novel antigens. Journal of neuroimmunology 65:11-19.

Aschermann S, Lux A, Baerenwaldt A, Biburger M, Nimmerjahn F (2010) The other side of immunoglobulin G: suppressor of inflammation. Clinical and experimental immunology 160:161-167.

Auld DS, Robitaille R (2003) Perisynaptic Schwann cells at the neuromuscular junction: nerve- and activity-dependent contributions to synaptic efficacy, plasticity, and reinnervation. The Neuroscientist : a review journal bringing neurobiology, neurology and psychiatry 9:144-157.

Barnes N, Gavin AL, Tan PS, Mottram P, Koentgen F, Hogarth PM (2002) FcgammaRI-deficient mice show multiple alterations to inflammatory and immune responses. Immunity 16:379-389.

Be'eri H, Reichert F, Saada A, Rotshenker S (1998) The cytokine network of wallerian degeneration: IL-10 and GM-CSF. Eur J Neurosci 10:2707-2713.

Benjamini YH, Y. (1995) Controlling the false discovery rate: a practical and powerful approach to multiple testin. Journal of the Royal Statistical Society Series B (Methodological) 57:289-300.

Bieber A, Asakura K, Warrington A, Kaveri SV, Rodriguez M (2000) Antibody-mediated remyelination: relevance to multiple sclerosis. Multiple sclerosis 6 Suppl 2:S1-5; discussion S33.

Bieber AJ, Warrington A, Asakura K, Ciric B, Kaveri SV, Pease LR, Rodriguez M (2002) Human antibodies accelerate the rate of remyelination following lysolecithin-induced demyelination in mice. Glia 37:241-249.

Blasczyk R, Westhoff U, Grosse-Wilde H (1993) Soluble CD4, CD8, and HLA molecules in commercial immunoglobulin preparations. Lancet 341:789-790.

Boggs JM (2006) Myelin basic protein: a multifunctional protein. Cellular and molecular life sciences : CMLS 63:1945-1961.

Bolin LM, Verity AN, Silver JE, Shooter EM, Abrams JS (1995) Interleukin-6 production by Schwann cells and induction in sciatic nerve injury. Journal of neurochemistry 64:850-858.

Bonetti B, Valdo P, Ossi G, De Toni L, Masotto B, Marconi S, Rizzuto N, Nardelli E, Moretto G (2003) T-cell cytotoxicity of human Schwann cells: TNFalpha promotes fasL-mediated apoptosis and IFN gamma perforin-mediated lysis. Glia 43:141-148.

Bonetti B, Valdo P, Stegagno C, Tanel R, Zanusso GL, Ramarli D, Fiorini E, Turazzi S, Carner M, Moretto G (2000) Tumor necrosis factor alpha and human Schwann cells: signalling and phenotype modulation without cell death. Journal of neuropathology and experimental neurology 59:74-84.

Brockes JP, Fields KL, Raff MC (1979) Studies on cultured rat Schwann cells. I. Establishment of purified populations from cultures of peripheral nerve. Brain research 165:105-118.

Bussone G, Dib H, Dimitrov JD, Camoin L, Broussard C, Tamas N, Guillevin L, Kaveri SV, Mouthon L (2009) Identification of target antigens of self-reactive IgG in intravenous immunoglobulin preparations. Proteomics 9:2253-2262.

Buttmann M, Kaveri S, Hartung HP (2013) Polyclonal immunoglobulin G for autoimmune demyelinating nervous system disorders. Trends in pharmacological sciences 34:445-457.

Cheepudomwit T, Guzelsu E, Zhou C, Griffin JW, Hoke A (2008) Comparison of cytokine expression profile during Wallerian degeneration of myelinated and unmyelinated peripheral axons. Neuroscience letters 430:230-235.

Colomar A, Marty V, Medina C, Combe C, Parnet P, Amedee T (2003) Maturation and release of interleukin-1beta by lipopolysaccharide-primed mouse Schwann cells require the stimulation of P2X7 receptors. The Journal of biological chemistry 278:30732-30740.

Cotter L, Ozcelik M, Jacob C, Pereira JA, Locher V, Baumann R, Relvas JB, Suter U, Tricaud N (2010) Dlg1-PTEN interaction regulates myelin thickness to prevent damaging peripheral nerve overmyelination. Science 328:1415-1418.

Dace DS, Khan AA, Stark JL, Kelly J, Cross AH, Apte RS (2009) Interleukin-10 overexpression promotes Fas-ligand-dependent chronic macrophage-mediated demyelinating polyneuropathy. PloS one 4:e7121.

Dailey AT, Avellino AM, Benthem L, Silver J, Kliot M (1998) Complement depletion reduces macrophage infiltration and activation during Wallerian degeneration and axonal regeneration. The Journal of neuroscience : the official journal of the Society for Neuroscience 18:6713-6722.

Dalakas MC (2004) The use of intravenous immunoglobulin in the treatment of autoimmune neuromuscular diseases: evidence-based indications and safety profile. Pharmacology & therapeutics 102:177-193.

Dalakas MC (2015) Pathogenesis of immune-mediated neuropathies. Biochimica et biophysica acta 1852:658-666.

Dale Purves GJA, David Fitzpatrick, William C. Hall, Anthony-Samuel LaMantia, James O. McNamara, Leonard E. White (2008) Neuroscience. Sunderland, MA U.S.A.: Sinauer Associates, Inc.

Dashiell SM, Vanguri P, Koski CL (1997) Dibutyryl cyclic AMP and inflammatory cytokines mediate C3 expression in Schwann cells. Glia 20:308-321.

de Jonge RR, Vreijling JP, Meintjes A, Kwa MS, van Kampen AH, van Schaik IN, Baas F (2003) Transcriptional profile of the human peripheral nervous system by serial analysis of gene expression. Genomics 82:97-108.

Debré M, Bonnet MC, Fridman WH, Carosella E, Philippe N, Reinert P, Vilmer E, Kaplan C, Teillaud JL, Griscelli C (1993) Infusion of Fc gamma fragments for treatment of children with acute immune thrombocytopenic purpura. Lancet 342:945-949.

Diezi M, Buclin T, Kuntzer T (2013) Toxic and drug-induced peripheral neuropathies: updates on causes, mechanisms and management. Current opinion in neurology 26:481-488.

Duan RS, Jin T, Yang X, Mix E, Adem A, Zhu J (2007) Apolipoprotein E deficiency enhances the antigen-presenting capacity of Schwann cells. Glia 55:772-776.

Dyachuk V, Furlan A, Shahidi MK, Giovenco M, Kaukua N, Konstantinidou C, Pachnis V, Memic F, Marklund U, Müller T, Birchmeier C, Fried K, Ernfors P, Adameyko I (2014) Neurodevelopment. Parasympathetic neurons originate from nerve-associated peripheral glial progenitors. Science 345:82-87.

Erickson CA (1993) From the crest to the periphery: control of pigment cell migration and lineage segregation. Pigment cell research / sponsored by the European Society for Pigment Cell Research and the International Pigment Cell Society 6:336-347.

Espinosa-Medina I, Outin E, Picard CA, Chettouh Z, Dymecki S, Consalez GG, Coppola E, Brunet JF (2014) Neurodevelopment. Parasympathetic ganglia derive from Schwann cell precursors. Science 345:87-90.

Fann DY, Lee SY, Manzanero S, Tang SC, Gelderblom M, Chunduri P, Bernreuther C, Glatzel M, Cheng YL, Thundyil J, Widiapradja A, Lok KZ, Foo SL, Wang YC, Li YI, Drummond GR, Basta M, Magnus T, Jo DG, Mattson MP, Sobey CG, Arumugam TV (2013) Intravenous immunoglobulin suppresses NLRP1 and NLRP3 inflammasome-mediated neuronal death in ischemic stroke. Cell death & disease 4:e790.

Fernandez-Valle C, Gorman D, Gomez AM, Bunge MB (1997) Actin plays a role in both changes in cell shape and gene-expression associated with Schwann cell myelination. The Journal of neuroscience : the official journal of the Society for Neuroscience 17:241-250.

Fields RD, Stevens-Graham B (2002) New insights into neuron-glia communication. Science 298:556-562.

Figlewicz DA, Quarles RH, Johnson D, Barbarash GR, Sternberger NH (1981) Biochemical demonstration of the myelin-associated glycoprotein in the peripheral nervous system. Journal of neurochemistry 37:749-758.

Filbin MT, Walsh FS, Trapp BD, Pizzey JA, Tennekoon GI (1990) Role of myelin P0 protein as a homophilic adhesion molecule. Nature 344:871-872.

Fischbeck KH, Abel A, Lin GS, Scherer SS (1999) X-linked Charcot-Marie-Tooth disease and connexin32. Annals of the New York Academy of Sciences 883:36-41.

Fischer S, Kleinschnitz C, Müller M, Kobsar I, Ip CW, Rollins B, Martini R (2008a) Monocyte chemoattractant protein-1 is a pathogenic component in a model for a hereditary peripheral neuropathy. Molecular and cellular neurosciences 37:359-366.

Fischer S, Weishaupt A, Troppmair J, Martini R (2008b) Increase of MCP-1 (CCL2) in myelin mutant Schwann cells is mediated by MEK-ERK signaling pathway. Glia 56:836-843.

Funabashi K, Okada N, Matsuo S, Yamamoto T, Morgan BP, Okada H (1994) Tissue distribution of complement regulatory membrane proteins in rats. Immunology 81:444-451.

Gabriel CM, Gregson NA, Redford EJ, Davies M, Smith KJ, Hughes RA (1997) Human immunoglobulin ameliorates rat experimental autoimmune neuritis. Brain : a journal of neurology 120 (Pt 9):1533-1540.

Galon J, Gauchat JF, Mazieres N, Spagnoli R, Storkus W, Lotze M, Bonnefoy JY, Fridman WH, Sautes C (1996) Soluble Fcgamma receptor type III (FcgammaRIII, CD16) triggers cell activation through interaction with complement receptors. Journal of immunology 157:1184-1192.

Gaudet AD, Popovich PG, Ramer MS (2011) Wallerian degeneration: gaining perspective on inflammatory events after peripheral nerve injury. Journal of neuroinflammation 8:110.

Ghanem G, Fabrice J (2011) Tyrosinase related protein 1 (TYRP1/gp75) in human cutaneous melanoma. Molecular oncology 5:150-155.

Giese KP, Martini R, Lemke G, Soriano P, Schachner M (1992) Mouse P0 gene disruption leads to hypomyelination, abnormal expression of recognition molecules, and degeneration of myelin and axons. Cell 71:565-576.

Glenn TD, Talbot WS (2013) Signals regulating myelination in peripheral nerves and the Schwann cell response to injury. Current opinion in neurobiology 23:1041-1048.

Goebbels S, Oltrogge JH, Kemper R, Heilmann I, Bormuth I, Wolfer S, Wichert SP, Möbius W, Liu X, Lappe-Siefke C, Rossner MJ, Groszer M, Suter U, Frahm J, Boretius S, Nave KA (2010) Elevated phosphatidylinositol 3,4,5-trisphosphate in glia triggers cell-autonomous membrane wrapping and myelination. The Journal of neuroscience : the official journal of the Society for Neuroscience 30:8953-8964.

Gold R, Stangel M, Dalakas MC (2007) Drug Insight: the use of intravenous immunoglobulin in neurology--therapeutic considerations and practical issues. Nature clinical practice Neurology 3:36-44.

Göttle P, Küry P (2015) Intracellular Protein Shuttling: A Mechanism Relevant for Myelin Repair in Multiple Sclerosis? International journal of molecular sciences 16:15057-15085.

Göttle P, Sabo JK, Heinen A, Venables G, Torres K, Tzekova N, Parras CM, Kremer D, Hartung HP, Cate HS, Küry P (2015) Oligodendroglial maturation is dependent on intracellular protein shuttling. The Journal of neuroscience : the official journal of the Society for Neuroscience 35:906-919.

Gould RM, Byrd AL, Barbarese E (1995) The number of Schmidt-Lanterman incisures is more than doubled in shiverer PNS myelin sheaths. Journal of neurocytology 24:85-98.

Greenfield S, Brostoff S, Eylar EH, Morell P (1973) Protein composition of myelin of the peripheral nervous system. Journal of neurochemistry 20:1207-1216.

Griffin JW, Thompson WJ (2008) Biology and pathology of nonmyelinating Schwann cells. Glia 56:1518-1531.

Groh J, Heinl K, Kohl B, Wessig C, Greeske J, Fischer S, Martini R (2010) Attenuation of MCP-1/CCL2 expression ameliorates neuropathy in a mouse model for Charcot-Marie-Tooth 1X. Hum Mol Genet 19:3530-3543.

Gronski P, Bauer R, Bodenbender L, Boland P, Diderrich G, Harthus HP, Kanzy EJ, Kuhn K, Schmidt KH, Walter G, et al. (1988a) On the nature of IgG dimers. II. Idiotype--anti-idiotype complexes of polyclonal and monoclonal origin: size distribution patterns and molecular geometries. Behring Institute Mitteilungen 144-153.

Gronski P, Bauer R, Bodenbender L, Kanzy EJ, Schmidt KH, Zilg H, Seiler FR (1988b) On the nature of IgG dimers. I. Dimers in human polyclonal IgG preparations: kinetic studies. Behring Institute Mitteilungen 127-143.

Hagedorn L, Suter U, Sommer L (1999) P0 and PMP22 mark a multipotent neural crest-derived cell type that displays community effects in response to TGF-beta family factors. Development 126:3781-3794.

Hanani M (2005) Satellite glial cells in sensory ganglia: from form to function. Brain research Brain research reviews 48:457-476.

Hanani M (2010) Satellite glial cells in sympathetic and parasympathetic ganglia: in search of function. Brain research reviews 64:304-327.

Harris ML, Baxter LL, Loftus SK, Pavan WJ (2010) Sox proteins in melanocyte development and melanoma. Pigment cell & melanoma research 23:496-513.

Heinen A, Beyer F, Tzekova N, Hartung HP, Küry P (2015) Fingolimod induces the transition to a nerve regeneration promoting Schwann cell phenotype. Experimental neurology 271:25-35.

Heinen A, Kremer D, Göttle P, Kruse F, Hasse B, Lehmann H, Hartung HP, Küry P (2008a) The cyclin-dependent kinase inhibitor p57kip2 is a negative regulator of Schwann cell differentiation and in vitro myelination. Proceedings of the National Academy of Sciences of the United States of America 105:8748-8753.

Heinen A, Kremer D, Hartung HP, Küry P (2008b) p57 kip2's role beyond Schwann cell cycle control. Cell Cycle 7:2781-2786.

Heinen A, Lehmann HC, Küry P (2013) Negative regulators of schwann cell differentiation-novel targets for peripheral nerve therapies? Journal of clinical immunology 33 Suppl 1:S18-26.

Heinen A, Tzekova N, Graffmann N, Torres KJ, Uhrberg M, Hartung HP, Küry P (2012) Histone methyltransferase enhancer of zeste homolog 2 regulates Schwann cell differentiation. Glia 60:1696-1708.

Hirota H, Kiyama H, Kishimoto T, Taga T (1996) Accelerated Nerve Regeneration in Mice by upregulated expression of interleukin (IL) 6 and IL-6 receptor after trauma. J Exp Med 183:2627-2634.

Imbach P, Barandun S, d'Apuzzo V, Baumgartner C, Hirt A, Morell A, Rossi E, Schoni M, Vest M, Wagner HP (1981) High-dose intravenous gammaglobulin for idiopathic thrombocytopenic purpura in childhood. Lancet 1:1228-1231.

Inoue G, Gaultier A, Li X, Mantuano E, Richardson G, Takahashi K, Campana WM (2010) Erythropoietin promotes Schwann cell migration and assembly of the provisional extracellular matrix by recruiting beta1 integrin to the cell surface. Glia 58:399-409.

Inouye H, Kirschner DA (2015) Evolution of myelin ultrastructure and the major structural myelin proteins. Brain research.

Jadasz JJ, Rivera FJ, Taubert A, Kandasamy M, Sandner B, Weidner N, Aktas O, Hartung HP, Aigner L, Küry P (2012) p57kip2 regulates glial fate decision in adult neural stem cells. Development 139:3306-3315.

Jander S, Pohl J, Gillen C, Stoll G (1996) Differential expression of interleukin-10 mRNA in Wallerian degeneration and immune-mediated inflammation of the rat peripheral nervous system. Journal of neuroscience research 43:254-259.

Jander S, Stoll G (2001) Interleukin-18 is induced in acute inflammatory demyelinating polyneuropathy. Journal of neuroimmunology 114:253-258.

Jerath NU, Shy ME (2015) Hereditary motor and sensory neuropathies: Understanding molecular pathogenesis could lead to future treatment strategies. Biochimica et biophysica acta 1852:667-678.

Jessen KR, Mirsky R (1999) Schwann cells and their precursors emerge as major regulators of nerve development. Trends in neurosciences 22:402-410.

Jessen KR, Mirsky R (2002) Signals that determine Schwann cell identity. Journal of anatomy 200:367-376.

Jessen KR, Mirsky R (2005) The origin and development of glial cells in peripheral nerves. Nature reviews Neuroscience 6:671-682.

Jessen KR, Mirsky R (2008) Negative regulation of myelination: relevance for development, injury, and demyelinating disease. Glia 56:1552-1565.

Jin JJ, Nikitin A, Rajewsky MF (1993) Schwann cell lineage-specific neu (erbB-2) gene expression in the developing rat nervous system. Cell growth & differentiation : the molecular biology journal of the American Association for Cancer Research 4:227-237.

Joseph NM, Mukouyama YS, Mosher JT, Jaegle M, Crone SA, Dormand EL, Lee KF, Meijer D, Anderson DJ, Morrison SJ (2004) Neural crest stem cells undergo multilineage differentiation in developing peripheral nerves to generate endoneurial fibroblasts in addition to Schwann cells. Development 131:5599-5612.

Kadlubowski M, Hughes RA, Gregson NA (1980) Experimental allergic neuritis in the Lewis rat: characterization of the activity of peripheral myelin and its major basic protein,P2. Brain research 184:439-454.

Kaneko Y, Nimmerjahn F, Ravetch JV (2006) Anti-inflammatory activity of immunoglobulin G resulting from Fc sialylation. Science 313:670-673.

Kazatchkine MD, Kaveri SV (2001) Immunomodulation of autoimmune and inflammatory diseases with intravenous immune globulin. The New England journal of medicine 345:747-755.

Keswani SC, Leitz GJ, Hoke A (2004) Erythropoietin is neuroprotective in models of HIV sensory neuropathy. Neuroscience letters 371:102-105.

Kieseier BC, Tani M, Mahad D, Oka N, Ho T, Woodroofe N, Griffin JW, Toyka KV, Ransohoff RM, Hartung HP (2002) Chemokines and chemokine receptors in inflammatory demyelinating neuropathies: a central role for IP-10. Brain : a journal of neurology 125:823-834.

Kiguchi N, Maeda T, Kobayashi Y, Fukazawa Y, Kishioka S (2010) Macrophage inflammatory protein-1alpha mediates the development of neuropathic pain following peripheral nerve injury through interleukin-1beta up-regulation. Pain 149:305-315.

Kim MK, Pan XQ, Huang ZY, Hunter S, Hwang PH, Indik ZK, Schreiber AD (2001) Fc gamma receptors differ in their structural requirements for interaction with the tyrosine kinase Syk in the initial steps of signaling for phagocytosis. Clinical immunology 98:125-132.

Kingston AE, Bergsteinsdottir K, Jessen KR, Van der Meide PH, Colston MJ, Mirsky R (1989) Schwann cells co-cultured with stimulated T cells and antigen express major histocompatibility complex (MHC) class II determinants without interferon-gamma pretreatment: synergistic effects of interferon-gamma and tumor necrosis factor on MHC class II induction. European journal of immunology 19:177-183.

Kitamura H, Kamon H, Sawa S, Park SJ, Katunuma N, Ishihara K, Murakami M, Hirano T (2005) IL-6-STAT3 controls intracellular MHC class II alphabeta dimer level through cathepsin S activity in dendritic cells. Immunity 23:491-502.

Klein D, Groh J, Wettmarshausen J, Martini R (2014) Nonuniform molecular features of myelinating Schwann cells in models for CMT1: distinct disease patterns are associated with NCAM and c-Jun upregulation. Glia 62:736-750.

Kohl B, Fischer S, Groh J, Wessig C, Martini R (2010) MCP-1/CCL2 modifies axon properties in a PMP22-overexpressing mouse model for Charcot-Marie-tooth 1A neuropathy. The American journal of pathology 176:1390-1399.

Komine-Kobayashi M, Chou N, Mochizuki H, Nakao A, Mizuno Y, Urabe T (2004) Dual role of Fcgamma receptor in transient focal cerebral ischemia in mice. Stroke; a journal of cerebral circulation 35:958-963.

Koski CL, Estep AE, Sawant-Mane S, Shin ML, Highbarger L, Hansch GM (1996) Complement regulatory molecules on human myelin and glial cells: differential expression affects the deposition of activated complement proteins. Journal of neurochemistry 66:303-312.

Kremer D, Heinen A, Jadasz J, Göttle P, Zimmermann K, Zickler P, Jander S, Hartung HP, Küry P (2009) p57kip2 is dynamically regulated in experimental autoimmune encephalomyelitis and interferes with oligodendroglial maturation. Proceedings of the National Academy of Sciences of the United States of America 106:9087-9092.

Kuhlmann T, Wendling U, Nolte C, Zipp F, Maruschak B, Stadelmann C, Siebert H, Bruck W (2002) Differential regulation of myelin phagocytosis by macrophages/microglia, involvement of target myelin, Fc receptors and activation by intravenous immunoglobulins. Journal of neuroscience research 67:185-190.

Küry P, Greiner-Petter R, Cornely C, Jurgens T, Müller HW (2002) Mammalian achaete scute homolog 2 is expressed in the adult sciatic nerve and regulates the expression of Krox24, Mob-1, CXCR4, and p57kip2 in Schwann cells. The Journal of neuroscience : the official journal of the Society for Neuroscience 22:7586-7595.

Lara-Ramirez R, Segura-Anaya E, Martinez-Gomez A, Dent MA (2008) Expression of interleukin-6 receptor alpha in normal and injured rat sciatic nerve. Neuroscience 152:601-608.

Le Douarin N, Dulac C, Dupin E, Cameron-Curry P (1991) Glial cell lineages in the neural crest. Glia 4:175-184.

Le N, Nagarajan R, Wang JY, Araki T, Schmidt RE, Milbrandt J (2005) Analysis of congenital hypomyelinating Egr2Lo/Lo nerves identifies Sox2 as an inhibitor of Schwann cell differentiation and myelination. Proceedings of the National Academy of Sciences of the United States of America 102:2596-2601.

Lee M, Brennan A, Blanchard A, Zoidl G, Dong Z, Tabernero A, Zoidl C, Dent MA, Jessen KR, Mirsky R (1997) P0 is constitutively expressed in the rat neural crest and embryonic nerves and is negatively and positively regulated by axons to generate non-myelin-forming and myelin-forming Schwann cells, respectively. Molecular and cellular neurosciences 8:336-350.

Li H, Lu Y, Smith HK, Richardson WD (2007) Olig1 and Sox10 interact synergistically to drive myelin basic protein transcription in oligodendrocytes. The Journal of neuroscience : the official journal of the Society for Neuroscience 27:14375-14382.

Li X, Gonias SL, Campana WM (2005) Schwann cells express erythropoietin receptor and represent a major target for Epo in peripheral nerve injury. Glia 51:254-265.

Li YN, Qin XJ, Kuang F, Wu R, Duan XL, Ju G, Wang BR (2008) Alterations of Fc gamma receptor I and Toll-like receptor 4 mediate the antiinflammatory actions of microglia and astrocytes after adrenaline-induced blood-brain barrier opening in rats. Journal of neuroscience research 86:3556-3565.

Ligon KL, Fancy SP, Franklin RJ, Rowitch DH (2006) Olig gene function in CNS development and disease. Glia 54:1-10.

Lilje O, Armati PJ (1997) The distribution and abundance of MHC and ICAM-1 on Schwann cells in vitro. Journal of neuroimmunology 77:75-84.

Lin HH, Spies JM, Lu JL, Pollard JD (2007a) Effective treatment of experimental autoimmune neuritis with human immunoglobulin. Journal of the neurological sciences 256:61-67.

Lin HH, Wang MX, Spies JM, Pollard JD (2007b) Effective treatment of experimental autoimmune neuritis with Fc fragment of human immunoglobulin. Journal of neuroimmunology 186:133-140.

Lisak RP, Bealmear B (1994) Antibodies to interleukin-6 inhibit Schwann cell proliferation induced by unfractionated cytokines. Journal of neuroimmunology 50:127-132.

Lisak RP, Bealmear B, Ragheb S (1994) Interleukin-1 alpha, but not interleukin-1 beta, is a co-mitogen for neonatal rat Schwann cells in vitro and acts via interleukin-1 receptors. Journal of neuroimmunology 55:171-177.

Lünemann JD, Quast I, Dalakas MC (2015) Efficacy of Intravenous Immunoglobulin in Neurological Diseases. Neurotherapeutics : the journal of the American Society for Experimental NeuroTherapeutics.

Luo B, Jiang M, Yang X, Zhang Z, Xiong J, Schluesener HJ, Zhang Z, Wu Y (2013) Erythropoietin is a hypoxia inducible factor-induced protective molecule in experimental autoimmune neuritis. Biochimica et biophysica acta 1832:1260-1270.

Mancardi GL, Cadoni A, Zicca A, Schenone A, Tabaton M, De Martini I, Zaccheo D (1988) HLA-DR Schwann cell reactivity in peripheral neuropathies of different origins. Neurology 38:848-851.

Martini R, Klein D, Groh J (2013) Similarities between inherited demyelinating neuropathies and Wallerian degeneration: an old repair program may cause myelin and axon perturbation under nonlesion conditions. The American journal of pathology 183:655-660.

Maurel P, Salzer JL (2000) Axonal regulation of Schwann cell proliferation and survival and the initial events of myelination requires PI 3-kinase activity. The Journal of neuroscience : the official journal of the Society for Neuroscience 20:4635-4645.

Meijer DH, Kane MF, Mehta S, Liu H, Harrington E, Taylor CM, Stiles CD, Rowitch DH (2012) Separated at birth? The functional and molecular divergence of OLIG1 and OLIG2. Nature reviews Neuroscience 13:819-831.

Menge T, Jander S, Stoll G (2001) Induction of the proinflammatory cytokine interleukin-18 by axonal injury. Journal of neuroscience research 65:332-339.

Meyer Zu Horste G, Heidenreich H, Lehmann HC, Ferrone S, Hartung HP, Wiendl H, Kieseier BC (2010) Expression of antigen processing and presenting molecules by Schwann cells in inflammatory neuropathies. Glia 58:80-92.

Miescher SM, Schaub A, Ghielmetti M, Baumann M, Vogel M, Bolli R, Stadler B (2005) Comparative analysis of antigen specificities in the monomeric and dimeric fractions of intravenous immunoglobulin. Annals of the New York Academy of Sciences 1051:582-590.

Miller DJ, Sanborn KS, Katzmann JA, Rodriguez M (1994) Monoclonal autoantibodies promote central nervous system repair in an animal model of multiple sclerosis. The Journal of neuroscience : the official journal of the Society for Neuroscience 14:6230-6238.

Mirsky R, Woodhoo A, Parkinson DB, Arthur-Farraj P, Bhaskaran A, Jessen KR (2008) Novel signals controlling embryonic Schwann cell development, myelination and dedifferentiation. Journal of the peripheral nervous system : JPNS 13:122-135.

Mitchell GW, Williams GS, Bosch EP, Hart MN (1991) Class II antigen expression in peripheral neuropathies. Journal of the neurological sciences 102:170-176.

Mocsai A, Ruland J, Tybulewicz VL (2010) The SYK tyrosine kinase: a crucial player in diverse biological functions. Nature reviews Immunology 10:387-402.

Motohashi T, Kunisada T (2015) Extended multipotency of neural crest cells and neural crest-derived cells. Current topics in developmental biology 111:69-95.

Müller HW (2000) Tetraspan myelin protein PMP22 and demyelinating peripheral neuropathies: new facts and hypotheses. Glia 29:182-185.

Murata K, Dalakas MC (2000) Expression of the co-stimulatory molecule BB-1, the ligands CTLA-4 and CD28 and their mRNAs in chronic inflammatory demyelinating polyneuropathy. Brain : a journal of neurology 123 (Pt 8):1660-1666.

Murwani R, Armati P (1998) Peripheral nerve fibroblasts as a source of IL-6, TNFalpha and IL-1 and their modulation by IFNgamma. Journal of the neurological sciences 161:99-109.

Myers RR, Sekiguchi Y, Kikuchi S, Scott B, Medicherla S, Protter A, Campana WM (2003) Inhibition of p38 MAP kinase activity enhances axonal regeneration. Experimental neurology 184:606-614.

Nagelkerke SQ, Kuijpers TW (2014) Immunomodulation by IVIg and the Role of Fc-Gamma Receptors: Classic Mechanisms of Action after all? Frontiers in immunology 5:674.

Nakahara J, Seiwa C, Shibuya A, Aiso S, Asou H (2003a) Expression of Fc receptor for immunoglobulin M in oligodendrocytes and myelin of mouse central nervous system. Neuroscience letters 337:73-76.

Nakahara J, Tan-Takeuchi K, Seiwa C, Gotoh M, Kaifu T, Ujike A, Inui M, Yagi T, Ogawa M, Aiso S, Takai T, Asou H (2003b) Signaling via immunoglobulin Fc receptors induces oligodendrocyte precursor cell differentiation. Developmental cell 4:841-852.

Nakamura K, Hirai H, Torashima T, Miyazaki T, Tsurui H, Xiu Y, Ohtsuji M, Lin QS, Tsukamoto K, Nishimura H, Ono M, Watanabe M, Hirose S (2007) CD3 and immunoglobulin G Fc receptor regulate cerebellar functions. Molecular and cellular biology 27:5128-5134.

Nakanishi K, Yoshimoto T, Tsutsui H, Okamura H (2001) Interleukin-18 is a unique cytokine that stimulates both Th1 and Th2 responses depending on its cytokine milieu. Cytokine & growth factor reviews 12:53-72.

Nave KA (2010) Myelination and support of axonal integrity by glia. Nature 468:244-252.

Nave KA, Schwab MH (2005) Glial cells under remote control. Nature neuroscience 8:1420-1422.

Newbern JM (2015) Molecular control of the neural crest and peripheral nervous system development. Current topics in developmental biology 111:201-231.

Nguyen DH, Cho N, Satkunendrarajah K, Austin JW, Wang J, Fehlings MG (2012) Immunoglobulin G (IgG) attenuates neuroinflammation and improves neurobehavioral recovery after cervical spinal cord injury. Journal of neuroinflammation 9:224.

Nimmerjahn F, Ravetch JV (2008a) Anti-inflammatory actions of intravenous immunoglobulin. Annual review of immunology 26:513-533.

Nimmerjahn F, Ravetch JV (2008b) Fcgamma receptors as regulators of immune responses. Nature reviews Immunology 8:34-47.

Niu J, Mei F, Wang L, Liu S, Tian Y, Mo W, Li H, Lu QR, Xiao L (2012) Phosphorylated olig1 localizes to the cytosol of oligodendrocytes and promotes membrane expansion and maturation. Glia 60:1427-1436.

Nose M, Katoh M, Okada N, Kyogoku M, Okada H (1990) Tissue distribution of HRF20, a novel factor preventing the membrane attack of homologous complement, and its predominant expression on endothelial cells in vivo. Immunology 70:145-149.

Ogata T, Iijima S, Hoshikawa S, Miura T, Yamamoto S, Oda H, Nakamura K, Tanaka S (2004) Opposing extracellular signal-regulated kinase and Akt pathways control Schwann cell myelination. The Journal of neuroscience : the official journal of the Society for Neuroscience 24:6724-6732.

Ohara PT, Vit JP, Bhargava A, Romero M, Sundberg C, Charles AC, Jasmin L (2009) Gliopathic pain: when satellite glial cells go bad. The Neuroscientist : a review journal bringing neurobiology, neurology and psychiatry 15:450-463.

Okun E, Mattson MP, Arumugam TV (2010) Involvement of Fc receptors in disorders of the central nervous system. Neuromolecular medicine 12:164-178.

Orlikowski D, Chazaud B, Plonquet A, Poron F, Sharshar T, Maison P, Raphael JC, Gherardi RK, Creange A (2003) Monocyte chemoattractant protein 1 and chemokine receptor CCR2 productions in Guillain-Barré syndrome and experimental autoimmune neuritis. Journal of neuroimmunology 134:118-127.

Ozaki A, Nagai A, Lee YB, Myong NH, Kim SU (2008) Expression of cytokines and cytokine receptors in human Schwann cells. Neuroreport 19:31-35.

Päiväläinen S, Nissinen M, Honkanen H, Lahti O, Kangas SM, Peltonen J, Peltonen S, Heape AM (2008) Myelination in mouse dorsal root ganglion/Schwann cell cocultures. Molecular and cellular neurosciences 37:568-578.

Parkinson DB, Bhaskaran A, Arthur-Farraj P, Noon LA, Woodhoo A, Lloyd AC, Feltri ML, Wrabetz L, Behrens A, Mirsky R, Jessen KR (2008) c-Jun is a negative regulator of myelination. The Journal of cell biology 181:625-637.

Patzig J, Jahn O, Tenzer S, Wichert SP, de Monasterio-Schrader P, Rosfa S, Kuharev J, Yan K, Bormuth I, Bremer J, Aguzzi A, Orfaniotou F, Hesse D, Schwab MH, Möbius W, Nave KA, Werner HB (2011) Quantitative and integrative proteome analysis of peripheral nerve myelin identifies novel myelin proteins and candidate neuropathy loci. The Journal of neuroscience : the official journal of the Society for Neuroscience 31:16369-16386.

Pereira JA, Lebrun-Julien F, Suter U (2012) Molecular mechanisms regulating myelination in the peripheral nervous system. Trends in neurosciences 35:123-134.

Perregaux DG, McNiff P, Laliberte R, Conklyn M, Gabel CA (2000) ATP acts as an agonist to promote stimulus-induced secretion of IL-1 beta and IL-18 in human blood. Journal of immunology 165:4615-4623.

Perrin FE, Lacroix S, Aviles-Trigueros M, David S (2005) Involvement of monocyte chemoattractant protein-1, macrophage inflammatory protein-1alpha and interleukin-1beta in Wallerian degeneration. Brain : a journal of neurology 128:854-866.

Placheta E, Hendry JM, Wood MD, Lafontaine CW, Liu EH, Cecilia Alvarez Veronesi M, Frey M, Gordon T, Borschel GH (2014) The ErbB2 inhibitor Herceptin (Trastuzumab) promotes axonal outgrowth four weeks after acute nerve transection and repair. Neuroscience letters 582:81-86.

Pollard JD, Baverstock J, McLeod JG (1987) Class II antigen expression and inflammatory cells in the Guillain-Barré syndrome. Annals of neurology 21:337-341.

Pollard JD, McCombe PA, Baverstock J, Gatenby PA, McLeod JG (1986) Class II antigen expression and T lymphocyte subsets in chronic inflammatory demyelinating polyneuropathy. Journal of neuroimmunology 13:123-134.

Press R, Pashenkov M, Jin JP, Link H (2003) Aberrated levels of cerebrospinal fluid chemokines in Guillain-Barré syndrome and chronic inflammatory demyelinating polyradiculoneuropathy. Journal of clinical immunology 23:259-267.

Putzu GA, Figarella-Branger D, Bouvier-Labit C, Liprandi A, Bianco N, Pellissier JF (2000) Immunohistochemical localization of cytokines, C5b-9 and ICAM-1 in peripheral nerve of Guillain-Barré syndrome. Journal of the neurological sciences 174:16-21.

Qin Y, Cheng C, Wang H, Shao X, Gao Y, Shen A (2008) TNF-alpha as an autocrine mediator and its role in the activation of Schwann cells. Neurochemical research 33:1077-1084.

Quast I, Cueni F, Nimmerjahn F, Tackenberg B, Lünemann JD (2015) Deregulated Fcgamma receptor expression in patients with CIDP. Neurology(R) neuroimmunology & neuroinflammation 2:e148.

Radosevich M, Burnouf T (2010) Intravenous immunoglobulin G: trends in production methods, quality control and quality assurance. Vox sanguinis 98:12-28.

Raghavan M, Bjorkman PJ (1996) Fc receptors and their interactions with immunoglobulins. Annual review of cell and developmental biology 12:181-220.

Ramaglia V, King RH, Nourallah M, Wolterman R, de Jonge R, Ramkema M, Vigar MA, van der Wetering S, Morgan BP, Troost D, Baas F (2007) The membrane attack complex of the complement system is essential for rapid Wallerian degeneration. The Journal of neuroscience : the official journal of the Society for Neuroscience 27:7663-7672.

Readhead C, Hood L (1990) The dysmyelinating mouse mutations shiverer (shi) and myelin deficient (shimld). Behavior genetics 20:213-234.

Ressot C, Bruzzone R (2000) Connexin channels in Schwann cells and the development of the X-linked form of Charcot-Marie-Tooth disease. Brain research Brain research reviews 32:192-202.

Reuben S, Sumi MG, Mathai A, Nair MD, Radhakrishnan VV (2003) Intravenous immunoglobulin reduces serum tumor necrosis factor alpha in patients with Guillain-Barré syndrome. Neurology India 51:487-489.

Rizvi TA, Huang Y, Sidani A, Atit R, Largaespada DA, Boissy RE, Ratner N (2002) A novel cytokine pathway suppresses glial cell melanogenesis after injury to adult nerve. The Journal of neuroscience : the official journal of the Society for Neuroscience 22:9831-9840.

Rodriguez M, Lennon VA (1990) Immunoglobulins promote remyelination in the central nervous system. Annals of neurology 27:12-17.

Rostami A, Brown MJ, Lisak RP, Sumner AJ, Zweiman B, Pleasure DE (1984) The role of myelin P2 protein in the production of experimental allergic neuritis. Annals of neurology 16:680-685.

Rotshenker S (2011) Wallerian degeneration: the innate-immune response to traumatic nerve injury. Journal of neuroinflammation 8:109.

Roux KH, Tankersley DL (1990) A view of the human idiotypic repertoire. Electron microscopic and immunologic analyses of spontaneous idiotype-anti-idiotype dimers in pooled human IgG. Journal of immunology 144:1387-1395.

Rutkowski JL, Tuite GF, Lincoln PM, Boyer PJ, Tennekoon GI, Kunkel SL (1999) Signals for proinflammatory cytokine secretion by human Schwann cells. Journal of neuroimmunology 101:47-60.

Salzer JL (2012) Axonal regulation of Schwann cell ensheathment and myelination. Journal of the peripheral nervous system : JPNS 17 Suppl 3:14-19.

Salzer JL (2015) Schwann cell myelination. Cold Spring Harbor perspectives in biology 7:a020529.

Salzer JL, Brophy PJ, Peles E (2008) Molecular domains of myelinated axons in the peripheral nervous system. Glia 56:1532-1540.

Samuel NM, Jessen KR, Grange JM, Mirsky R (1987) Gamma interferon, but not Mycobacterium leprae, induces major histocompatibility class II antigens on cultured rat Schwann cells. Journal of neurocytology 16:281-287.

Samuelsson A, Towers TL, Ravetch JV (2001) Anti-inflammatory activity of IVIG mediated through the inhibitory Fc receptor. Science 291:484-486.

Schachner M, Bartsch U (2000) Multiple functions of the myelin-associated glycoprotein MAG (siglec-4a) in formation and maintenance of myelin. Glia 29:154-165.

Schaub A, Wymann S, Heller M, Ghielmetti M, Beleznay Z, Stadler BM, Bolli R, Miescher S (2007) Self-reactivity in the dimeric intravenous immunoglobulin fraction. Annals of the New York Academy of Sciences 1110:681-693.

Scherer SS (1999) Nodes, paranodes, and incisures: from form to function. Annals of the New York Academy of Sciences 883:131-142.

Scherer SS, Arroyo EJ (2002) Recent progress on the molecular organization of myelinated axons. Journal of the peripheral nervous system : JPNS 7:1-12.

Schmid D, Zeis T, Schaeren-Wiemers N (2014) Transcriptional regulation induced by cAMP elevation in mouse Schwann cells. ASN neuro 6:137-157.

Schroder K, Tschopp J (2010) The inflammasomes. Cell 140:821-832.

Schroeder HW, Jr., Cavacini L (2010) Structure and function of immunoglobulins. The Journal of allergy and clinical immunology 125:S41-52.

Schwab I, Nimmerjahn F (2013) Intravenous immunoglobulin therapy: how does IgG modulate the immune system? Nature reviews Immunology 13:176-189.

Sedimbi SK, Hagglof T, Karlsson MC (2013) IL-18 in inflammatory and autoimmune disease. Cellular and molecular life sciences : CMLS 70:4795-4808.

Shamash S, Reichert F, Rotshenker S (2002) The cytokine network of Wallerian degeneration: tumor necrosis factor-alpha, interleukin-1alpha, and interleukin-1beta. The Journal of neuroscience : the official journal of the Society for Neuroscience 22:3052-3060.

Sharief MK, Ingram DA, Swash M, Thompson EJ (1999) I.v. immunoglobulin reduces circulating proinflammatory cytokines in Guillain-Barré syndrome. Neurology 52:1833-1838.

Sherman DL, Wu LM, Grove M, Gillespie CS, Brophy PJ (2012) Drp2 and periaxin form Cajal bands with dystroglycan but have distinct roles in Schwann cell growth. The Journal of neuroscience : the official journal of the Society for Neuroscience 32:9419-9428.

Siberil S, Elluru S, Negi VS, Ephrem A, Misra N, Delignat S, Bayary J, Lacroix-Desmazes S, Kazatchkine MD, Kaveri SV (2007) Intravenous immunoglobulin in autoimmune and inflammatory diseases: more than mere transfer of antibodies. Transfusion and apheresis science : official journal of the World Apheresis Association : official journal of the European Society for Haemapheresis 37:103-107.

Sindic CJ (2013) Infectious neuropathies. Current opinion in neurology 26:510-515.

Skundric DS, Lisak RP, Rouhi M, Kieseier BC, Jung S, Hartung HP (2001) Schwann cell-specific regulation of IL-1 and IL-1Ra during EAN: possible relevance for immune regulation at paranodal regions. Journal of neuroimmunology 116:74-82.

Slamon DJ, Clark GM, Wong SG, Levin WJ, Ullrich A, McGuire WL (1987) Human breast cancer: correlation of relapse and survival with amplification of the HER-2/neu oncogene. Science 235:177-182.

Spierings E, de Boer T, Wieles B, Adams LB, Marani E, Ottenhoff TH (2001) Mycobacterium leprae-specific, HLA class II-restricted killing of human Schwann cells by CD4+ Th1 cells: a novel immunopathogenic mechanism of nerve damage in leprosy. Journal of immunology 166:5883-5888.

Stoll G, Jander S, Myers RR (2002) Degeneration and regeneration of the peripheral nervous system: from Augustus Waller's observations to neuroinflammation. Journal of the peripheral nervous system : JPNS 7:13-27.

Stoll G, Schmidt B, Jander S, Toyka KV, Hartung HP (1991) Presence of the terminal complement complex (C5b-9) precedes myelin degradation in immune-mediated demyelination of the rat peripheral nervous system. Annals of neurology 30:147-155.

Stolt CC, Wegner M (2015) Schwann cells and their transcriptional network: Evolution of key regulators of peripheral myelination. Brain research.

Suter U, Snipes GJ (1995) Biology and genetics of hereditary motor and sensory neuropathies. Annual review of neuroscience 18:45-75.

Svaren J, Meijer D (2008) The molecular machinery of myelin gene transcription in Schwann cells. Glia 56:1541-1551.

Tackenberg B, Jelcic I, Baerenwaldt A, Oertel WH, Sommer N, Nimmerjahn F, Lünemann JD (2009) Impaired inhibitory Fcgamma receptor IIB expression on B cells in chronic inflammatory demyelinating polyneuropathy. Proceedings of the National Academy of Sciences of the United States of America 106:4788-4792.

Takai T (2002) Roles of Fc receptors in autoimmunity. Nature reviews Immunology 2:580-592.

Tang W, Lv Q, Chen XF, Zou JJ, Liu ZM, Shi YQ (2013) CD8(+) T cell-mediated cytotoxicity toward Schwann cells promotes diabetic peripheral neuropathy. Cellular physiology and biochemistry : international journal of experimental cellular physiology, biochemistry, and pharmacology 32:827-837.

Tankersley DL (1994) Dimer formation in immunoglobulin preparations and speculations on the mechanism of action of intravenous immune globulin in autoimmune diseases. Immunological reviews 139:159-172.

Tankersley DL, Preston MS, Finlayson JS (1988) Immunoglobulin G dimer: an idiotype-anti-idiotype complex. Molecular immunology 25:41-48.

Taskinen HS, Roytta M (2000) Increased expression of chemokines (MCP-1, MIP-1alpha, RANTES) after peripheral nerve transection. Journal of the peripheral nervous system : JPNS 5:75-81.

Taveggia C, Zanazzi G, Petrylak A, Yano H, Rosenbluth J, Einheber S, Xu X, Esper RM, Loeb JA, Shrager P, Chao MV, Falls DL, Role L, Salzer JL (2005) Neuregulin-1 type III determines the ensheathment fate of axons. Neuron 47:681-694.

Teeling JL, Jansen-Hendriks T, Kuijpers TW, de Haas M, van de Winkel JG, Hack CE, Bleeker WK (2001) Therapeutic efficacy of intravenous immunoglobulin preparations depends on the immunoglobulin G dimers: studies in experimental immune thrombocytopenia. Blood 98:1095-1099.

Toews AD, Barrett C, Morell P (1998) Monocyte chemoattractant protein 1 is responsible for macrophage recruitment following injury to sciatic nerve. Journal of neuroscience research 53:260-267.

Trapp BD, Dubois-Dalcq M, Quarles RH (1984) Ultrastructural localization of P2 protein in actively myelinating rat Schwann cells. Journal of neurochemistry 43:944-948.

Turner M, Schweighoffer E, Colucci F, Di Santo JP, Tybulewicz VL (2000) Tyrosine kinase SYK: essential functions for immunoreceptor signalling. Immunology today 21:148-154.

Tzekou A, Fehlings MG (2014) Treatment of spinal cord injury with intravenous immunoglobulin G: preliminary evidence and future perspectives. Journal of clinical immunology 34 Suppl 1:S132-138.

Tzekova N, Heinen A, Bunk S, Hermann C, Hartung HP, Reipert B, Küry P (2015) Immunoglobulins stimulate cultured Schwann cell maturation and promote their potential to induce axonal outgrowth. Journal of neuroinflammation 12:107.

Tzekova N, Heinen A, Küry P (2014) Molecules involved in the crosstalk between immune- and peripheral nerve Schwann cells. Journal of clinical immunology 34 Suppl 1:S86-104.

Ulvestad E, Williams K, Vedeler C, Antel J, Nyland H, Mork S, Matre R (1994) Reactive microglia in multiple sclerosis lesions have an increased expression of receptors for the Fc part of IgG. Journal of the neurological sciences 121:125-131.

Vaegter CB (2014) Neurotrophins and their receptors in satellite glial cells following nerve injury. Neural regeneration research 9:2038-2039.

van der Poel CE, Spaapen RM, van de Winkel JG, Leusen JH (2011) Functional characteristics of the high affinity IgG receptor, FcgammaRI. Journal of immunology 186:2699-2704.

van Engelen BG, Miller DJ, Pavelko KD, Hommes OR, Rodriguez M (1994) Promotion of remyelination by polyclonal immunoglobulin in Theiler's virus-induced demyelination and in multiple sclerosis. Journal of neurology, neurosurgery, and psychiatry 57 Suppl:65-68.

van Schaik IN, Vermeulen M, Brand A (1997) Immunomodulation and remyelination: two aspects of human polyclonal immunoglobulin treatment in immune mediated neuropathies? Multiple sclerosis 3:98-104.

Vargas ME, Barres BA (2007) Why is Wallerian degeneration in the CNS so slow? Annual review of neuroscience 30:153-179.

Vargas ME, Watanabe J, Singh SJ, Robinson WH, Barres BA (2010) Endogenous antibodies promote rapid myelin clearance and effective axon regeneration after nerve injury. Proceedings of the National Academy of Sciences of the United States of America 107:11993-11998.

Vedeler CA (1987) Demonstration of Fc gamma receptors on human peripheral nerve fibres. Journal of neuroimmunology 15:207-216.

Vedeler CA, Conti G, Bannerman P, Pleasure D (1992) Expression of genes encoding receptors for IgG (FcRIII) and for C3b/C4b (Crry) in rat sciatic nerve during development and Wallerian degeneration. Journal of neuroscience research 31:654-661.

Vedeler CA, Fitzpatrick-Klove L (1990) Receptors for immunoglobulin G demonstrated on human peripheral nerve fibres by electron microscopy. Neuroscience letters 115:167-170.

Vedeler CA, Matre R (1988) Complement receptors CR1 on human peripheral nerve fibres. Journal of neuroimmunology 17:315-322.

Vedeler CA, Matre R, Kristoffersen EK, Ulvestad E (1991) IgG Fc receptor heterogeneity in human peripheral nerves. Acta neurologica Scandinavica 84:177-180.

Vedeler CA, Nilsen R, Matre R (1989) Localization of Fc gamma receptors and complement receptors CR1 on human peripheral nerve fibres by immunoelectron microscopy. Journal of neuroimmunology 23:29-33.

Vedeler CA, Scarpini E, Beretta S, Doronzo R, Matre R (1990) The ontogenesis of Fc gamma receptors and complement receptors CR1 in human peripheral nerve. Acta neuropathologica 80:35-40.

Vincent AM, Calabek B, Roberts L, Feldman EL (2013) Biology of diabetic neuropathy. Handbook of clinical neurology 115:591-606.

Vincent AM, Callaghan BC, Smith AL, Feldman EL (2011) Diabetic neuropathy: cellular mechanisms as therapeutic targets. Nature reviews Neurology 7:573-583.

Waller A (1850) Experiments on the Section of the Glossopharyngeal and Hypoglossal Nerves of the Frog, and Observations of the Alterations Produced Thereby in the Structure of Their Primitive Fibres. Philosophical Transactions of the Royal Society of London 140:423-429.

Warrington AE, Asakura K, Bieber AJ, Ciric B, Van Keulen V, Kaveri SV, Kyle RA, Pease LR, Rodriguez M (2000) Human monoclonal antibodies reactive to oligodendrocytes promote remyelination in a model of multiple sclerosis. Proceedings of the National Academy of Sciences of the United States of America 97:6820-6825.

Warrington AE, Bieber AJ, Ciric B, Pease LR, Van Keulen V, Rodriguez M (2007) A recombinant human IgM promotes myelin repair after a single, very low dose. Journal of neuroscience research 85:967-976.

Weider M, Reiprich S, Wegner M (2013) Sox appeal - Sox10 attracts epigenetic and transcriptional regulators in myelinating glia. Biological chemistry 394:1583-1593.

Wohlleben G, Ibrahim SM, Schmidt J, Toyka KV, Hartung HP, Gold R (2000) Regulation of Fas and FasL expression on rat Schwann cells. Glia 30:373-381.

Wrabetz L, Feltri ML, Quattrini A, Imperiale D, Previtali S, D'Antonio M, Martini R, Yin X, Trapp BD, Zhou L, Chiu SY, Messing A (2000) P(0) glycoprotein overexpression causes congenital hypomyelination of peripheral nerves. The Journal of cell biology 148:1021-1034.

Xin M, Yue T, Ma Z, Wu FF, Gow A, Lu QR (2005) Myelinogenesis and axonal recognition by oligodendrocytes in brain are uncoupled in Olig1-null mice. The Journal of neuroscience : the official journal of the Society for Neuroscience 25:1354-1365.

Xu X, Warrington AE, Wright BR, Bieber AJ, Van Keulen V, Pease LR, Rodriguez M (2011) A human IgM signals axon outgrowth: coupling lipid raft to microtubules. Journal of neurochemistry 119:100-112.

Yan WX, Archelos JJ, Hartung HP, Pollard JD (2001) P0 protein is a target antigen in chronic inflammatory demyelinating polyradiculoneuropathy. Annals of neurology 50:286-292.

Yanagi S, Inatome R, Takano T, Yamamura H (2001) Syk expression and novel function in a wide variety of tissues. Biochemical and biophysical research communications 288:495-498.

Yang DP, Kim J, Syed N, Tung YJ, Bhaskaran A, Mindos T, Mirsky R, Jessen KR, Maurel P, Parkinson DB, Kim HA (2012) p38 MAPK activation promotes denervated Schwann cell phenotype and functions as a negative regulator of Schwann cell differentiation and myelination. The Journal of neuroscience : the official journal of the Society for Neuroscience 32:7158-7168.

Yuki N, Hartung HP (2012) Guillain-Barré syndrome. The New England journal of medicine 366:2294-2304.

Zenker J, Stettner M, Ruskamo S, Domenech-Estevez E, Baloui H, Medard JJ, Verheijen MH, Brouwers JF, Kursula P, Kieseier BC, Chrast R (2014) A role of peripheral myelin protein 2 in lipid homeostasis of myelinating Schwann cells. Glia 62:1502-1512.

Zhu J, Bai XF, Mix E, Link H (1997) Cytokine dichotomy in peripheral nervous system influences the outcome of experimental allergic neuritis: dynamics of mRNA expression for IL-1 beta, IL-6, IL-10, IL-12, TNF-alpha, TNF-beta, and cytolysin. Clin Immunol Immunopathol 84:85-94.

7 ABBREVIATIONS

AIDP	acute inflammatory demyelinating polyneuropathy
Akt	serine-threonine kinase
AMAN	acute motor axonal neuropathy
ATP	adenosine triphosphate
B19	parvovirus B19
BBB	blood-brain barrier
BrdU	5-Bromo-2'-deoxyuridine
BSA	bovine serum albumin
C. jejuni	*Campylobacter jejuni*
C57BL/6 mouse	C57 black 6 mouse (laboratory strain)
CDKI	cyclin-dependent kinase inhibitor
cDNA	copy DNA
CIDP	Chronic inflammatory demyelinating polyneuropathy
CMT(1)	Charcot-Marie-Tooth disease (type 1)
CMV	Cytomegalovirus
CNS	central nervous system
CR(1)	complement receptor (1)
ctrl	control buffer
Cx32	connexin-32
d	day/days
DAF	decay accelerating factor
DAPI	4´,6-diamidino-2-phenylindole
ddH_2O	double-distilled water
DGA	functional discriminatory gene analysis
diff.	differentiating
DNA	desoxyribonucleic acid
DNase	deoxyribonuclease
DRG(s)	dorsal root ganglion(-lia)
E	embryonic day
E. coli	*Escherichia coli*
EAN	experimental autoimmune neuritis
EBV	Epstein-Barr virus
EDTA	ethylenediaminetetraacetic acid
Epo	erythropoietin
EpoR	Epo receptor
$F(ab')_2$	Fragment, antigen-binding, including hinge region (both arms)
Fab	Fragment, antigen-binding

Fas/CD95	apoptosis receptor
FasL/CD95L	Fas ligand
Fc	Fragment crystallisable
Fcgr1a/CD64 (gene name *R. norvegicus*)	Fc fragment of IgG, high affinity 1a, receptor
Fcgr2a/CD32a (gene name *R. norvegicus*)	Fc fragment of IgG, low affinity 2a, receptor
Fcgr2b/CD32b (gene name *R. norvegicus*)	Fc fragment of IgG, low affinity 2b, receptor
Fcgr3a/CD16 (gene name *R. norvegicus*)	Fc fragment of IgG, low affinity 3a, receptor
FcR(s)	Fc receptor(s)
FcRn	neonatal FcR
FCS	foetal calf serum
FcγR(s)	Fc gamma receptor(s)
Fig.	figure
g	gram
GAPDH	glyceraldehyde-3-phosphate dehydrogenase
GBS	Guillain-Barré Syndrome
h	hour/hours
H_2O	water
HAV	hepatitis A virus
HBsAg	hepatitis B surface antigen
HBV	hepatitis B virus
HCV	hepatitis C virus
Her-2 cells	larynx carcinoma epithelial cells
Her2/ErbB2	human epidermal growth factor receptor 2
HIV	human immunodeficiency virus
HMSN	hereditary motor and sensory neuropathy
HRP	horse-radish-peroxidase
HS	horse serum
HUVEC	human umbilical vein endothelial cells
ICAM-3	intercellular adhesion molecule 3
IFNγ	interferon gamma
Ig(s)	immunoglobulin(s)
IgA	immunoglobulin A
IgD	immunoglobulin D
IgE	immunoglobulin E
IgG	immunoglobulin G
IgM	immunoglobulin M
IL	interleukin
IL-10	interleukin-10
IL-18	interleukin-18
IL-1R	IL-1 receptor
IL-1α	interleukin-1 alpha

IL-1β	interleukin-1 beta
IL-6	interleukin-6
IL-6R	IL-6 receptor
ITAM	immunoreceptor tyrosine-based activation motif
ITIM	immunoreceptor tyrosine-based inhibitory motif
ITP	Idiopathic thrombocytopenic purpura
IVIG	intravenous immunoglobulins
JNK	jun N-terminal kinase
K+	potassium
kDa	kilodalton
kg	kilogram
Krox20/Egr2	Krüppel box protein 20/early growth response protein-2
L	liter
LB agar/medium	Luria-Bertani agar/medium
LPS	lipopolysaccharide
mA	milliampere
MAC	membrane attack complex
Mag	myelin-associated glycoprotein
MAPK	mitogen-activated protein kinase
Mbp	myelin basic protein
Mcp-1/CCL2	monocyte chemoattractant protein-1
Mfn2	mitofusin 2
MG	Myasthenia gravis
mg	milligram
MHC (I and II)	major histocompatibility complex (I and II)
min	minute
MIP	macrophage inflammatory protein
ml	milliliter
mm	millimeter
MMN	Multifocal motor neuropathy
Mpz/P0	myelin protein zero
mRNA	messenger RNA
MS	Multiple Sclerosis
MWCO	molecular weight cut-off
n	number of experiments
Na+	sodium
NF	neurofilament
ng	nanogram
NGF	nerve growth factor
NGS	normal goat serum

NK cells	naturl killer cells
NLR(s)	nucleotide-binding oligomerization domain (NOD)-like receptor(s)
NLRP	NLR pyrin domain-containing
NMJ	neuromuscular junction
non-diff.	non-differentiating
NRS	normal rabbit serum
NSC(s)	neural stem cell(s)
ø	diameter
Oct6/Pou3f1	octamer-binding transcription factor-6
ODC	ornithine decarboxylase
Olig1	oligodendrocyte transcription factor 1
OPC(s)	oligodendroglial precursor cell(s)
P	postnatal day
p38MAPK	p38 mitogen-activated protein kinase
PBS	phosphate-buffered saline
PCR	polymerase chain reaction
PDL	poly-D-lysine
PE	plasma exchange/plasmapheresis
PFA	paraformaldehyde
phalloidin-TRITC	phalloidin-tetramethylrhodamine B isothiocyanate
PI3K	phosphatidylinositol-3-kinase
PIP2	phosphatidylinositol-(4,5)-bisphosphate
PIP3	phosphatidylinositol-(3,4,5)-trisphosphate
Pllp	plasmolipin
Plp1/DM20	proteolipid protein 1
Pmp2/P2/Fabp8	peripheral myelin protein 2
Pmp22	peripheral myelin protein-22
PNS	peripheral nervous system
PRR	pattern recognition receptors
Prx	periaxin
PTEN	phosphatase and tensin homolog
qRT-PCR	quantitative real time PCR
R. norvegicus	*Rattus norvegicus*
RNA	ribonucleic acid
RNase	ribonuclease
rpm	rounds per minute
rrIL-18	rat recombinant interleukin-18
RSV	Respiratory Syncytial Virus
RT	room temperature
SCP(s)	Schwann cell precursor(s)

SDS	sodium dodecyl sulphate
SDS PAGE	sodium dodecyl sulfate polyacrylamide gel electrophoresis
sec	second
SEC-HPLC	size exclusion chromatography
SEM	standard error of the mean
SIGN-R1	specific ICAM-3 grabbing non-integrin-related 1
Sox10	SRY-related HMGbox-10
SYK	spleen thyrosine kinase
TAE buffer	tris-acetate-EDTA buffer
TGF-β	transforming growth factor beta
Th1 cells	type 1 T helper cells
Th2 cells	type 2 T helper cells
TLR	toll-like receptor
TMEV	Theiler's murine encephalomyelitis virus
TNFα	necrosis factor alpha
Tyrp1	tyrosinase-related protein 1
UV	ultraviolet
V	volt
v/v	volume per volume
VCAM	vascular cell adhesion protein
VEGF	vascular endothelial growth factor
w/v	weight per volume
WD	Wallerian degeneration
α	alpha (Greek)
β	beta (Greek)
β-tub	β-III-tubulin
γ	gamma (Greek)
δ/Δ	delta (Greek)
ε	epsilon (Greek)
κ	kappa (Greek)
µ	mu (Greek)
µl	microliter

8 AKNOWLEDGEMENTS/DANKSAGUNG

An erster Stelle möchte ich mich bei meinem Betreuer, Herrn Prof. Patrick Küry, bedanken, dass er es mir ermöglicht hat, in der Arbeitsgruppe Translationale Gliazellforschung zu promovieren, für die unzähligen, stets produktiven und von schweizerischer Gelassenheit geprägten Projektabstimmungen, und allgemein für seine fachliche und moralische Unterstützung meiner Forschungsarbeit. Hervorheben möchte ich auch die unvergesslichen Glia-Retreats, die wir mit der Arbeitsgruppe im Berner Oberland verbringen durften.

Ich danke Herrn Prof. Thomas Klein für seine Bereitschaft, meine Arbeit als Zweitgutachter zu betreuen.

Ein ganz besonderer Dank gilt Dr. Peter Göttle für seine stetige Hilfsbereitschaft, seine enorm positive Ausstrahlung und Witzigkeit und die außergewöhnliche Freundschaft, die mich durch die Zeit meiner Doktorarbeit begleitet haben.

Ich danke Dr. André Heinen für seine anfängliche Betreuung meiner Arbeit und Unterstützung, für die ausgiebigen und interessanten Diskussionsrunden und die treue Freundschaft.

Herzlich danken möchte ich auch unseren technischen Assitentinnen Brigida Ziegler, Julia Domke und Birgit Blomenkamp, deren hervorragende Unterstützung ich sehr zu schätzen gelernt habe.

Bei allen Arbeitskolleg/innen und Freunden bedanke ich mich für die tollen Momente während meiner gesamten Doktorarbeit, für echte Hilfsbereitschaft, Motivation und allgemein für Eure Unterstützung! Ganz besonders bedanke ich mich bei Carola Dröge für das unglaublich zügige und akkurate Korrekturlesen meiner Arbeit.

Zu guter Letzt möchte ich mich bei meiner Familie bedanken für deren liebevolle Unterstützung und ganz besonders bei meinem Freund Christian Förster für alles, was er für mich getan hat.

9 ANNEX

Teile dieser Dissertation orientieren sich an publizierten Manuskripten. Unter Bezugnahme auf § 6 Abs. 3) der Promotionsordnung der Heinrch-Heine Universität in der Fassung vom 20.03.2015 sind alle übernommenen oder angepassten Teile mit Fussnoten kenntlich gemacht worden.

9.1 Publizierter Review-Artikel

Vollständige Referenz des Manuskriptes:
Tzekova N, Heinen A, Küry P (2014) Molecules involved in the crosstalk between immune- and peripheral nerve Schwann cells. Journal of clinical immunology 34 Suppl 1:S86-104. doi: 10.1007/s10875-014-0015-6. Epub 2014 Apr 17.

Liste aller am Manuskript beteiligten Autoren:
Nevena Tzekova (Doktorandin), Dr. André Heinen, Prof. Dr. Patrick Küry

Inhaltlicher Anteil der Verfasserin dieser Dissertation am Manuskript: ca. 50 %
Nevena Tzekova hat folgende Kapitel des Manuskriptes selbständig verfasst:
„Major Histocompatibility Complex and Antigen Presentation“ and „Molecules Involved in Cell-Cell Interactions“. Das Kapitel „Surface Molecules/Receptors Expressed by Schwann Cells“ wurde überwiegend von Nevena Tzekova verfasst. Die Abbildungen wurden mit Unterstützung von Dr. André Heinen erstellt.

9.2 Publizierter wissenschaftlicher Artikel

Vollständige Referenz des Manuskriptes:
Tzekova N, Heinen A, Bunk S, Hermann C, Hartung HP, Reipert B, Küry P (2015) Immunoglobulins stimulate cultured Schwann cell maturation and promote their potential to induce axonal outgrowth. Journal of neuroinflammation 12:107. doi: 10.1186/s12974-015-0331-7.

Liste aller am Manuskript beteiligten Autoren:

Nevena Tzekova (Doktorandin), Dr. André Heinen, Dr. Sebastian Bunk, Dr. Birgit Reipert, Univ.-Prof. Dr. Hans-Peter Hartung, Dr. Corinna Hermann, Prof. Dr. Patrick Küry

Inhaltlicher Anteil der Verfasserin dieser Dissertation am Manuskript: ca. 75 %

Nevena Tzekova hat eigenverantwortlich sämtliche in die Bewertung einbezogenen Experimente durchgeführt. Sie wurde operativ unterstützt durch technische Assistenten der Arbeitsgruppe. Die Verfasserin zeichnet ferner verantwortlich für die Datenerhebung, -analyse und -interpretation für diese Arbeit. Der Erstentwurf des Manuskripts sowie alle Abbildungen wurden von Nevena Tzekova erarbeitet.

Hiermit bestätige ich, dass die vorgenannten Angaben korrekt sind.

Düsseldorf,.. ....

Prof. Dr. Patrick Küry

10 ERKLÄRUNG

Ich versichere an Eides Statt, dass die Dissertation von mir selbständig und ohne unzulässige fremde Hilfe unter Beachtung der „Grundsätze zur Sicherung guter wissenschaftlicher Praxis an der Heinrich-Heine- Universität Düsseldorf“ erstellt worden ist.

Düsseldorf,.. ....

Nevena Tzekova